Oceanography of the Sargasso Sea
An Update Concerning the Scientific Case for Protection of the Sargasso Sea

Nicholas R. Bates[a,b,c,d], Leocadio Blanco-Bercial[a,b,e], Ruth Curry[a], Damian S. Grundle [a,b,c], Rodney J. Johnson[a,b], and Sheryl Murdock[a,b]

[a] Bermuda Institute of Ocean Sciences (BIOS), 17 Biological Lane, Ferry Reach Bermuda;

[b] The School of Ocean Futures, Julie Ann K. Wrigley Global Futures Laboratory at Arizona State University, Tempe, Arizona, USA

[c] The School of Earth and Space Exploration, Arizona State University, Tempe, Arizona, USA

[d] School of Earth and Ocean Sciences, University of Southampton, Southampton, UK (note: former affiliation during much of the work contained in this report)

[e] The School of Life Sciences, Arizona State University, Tempe, Arizona, USA

BIOS

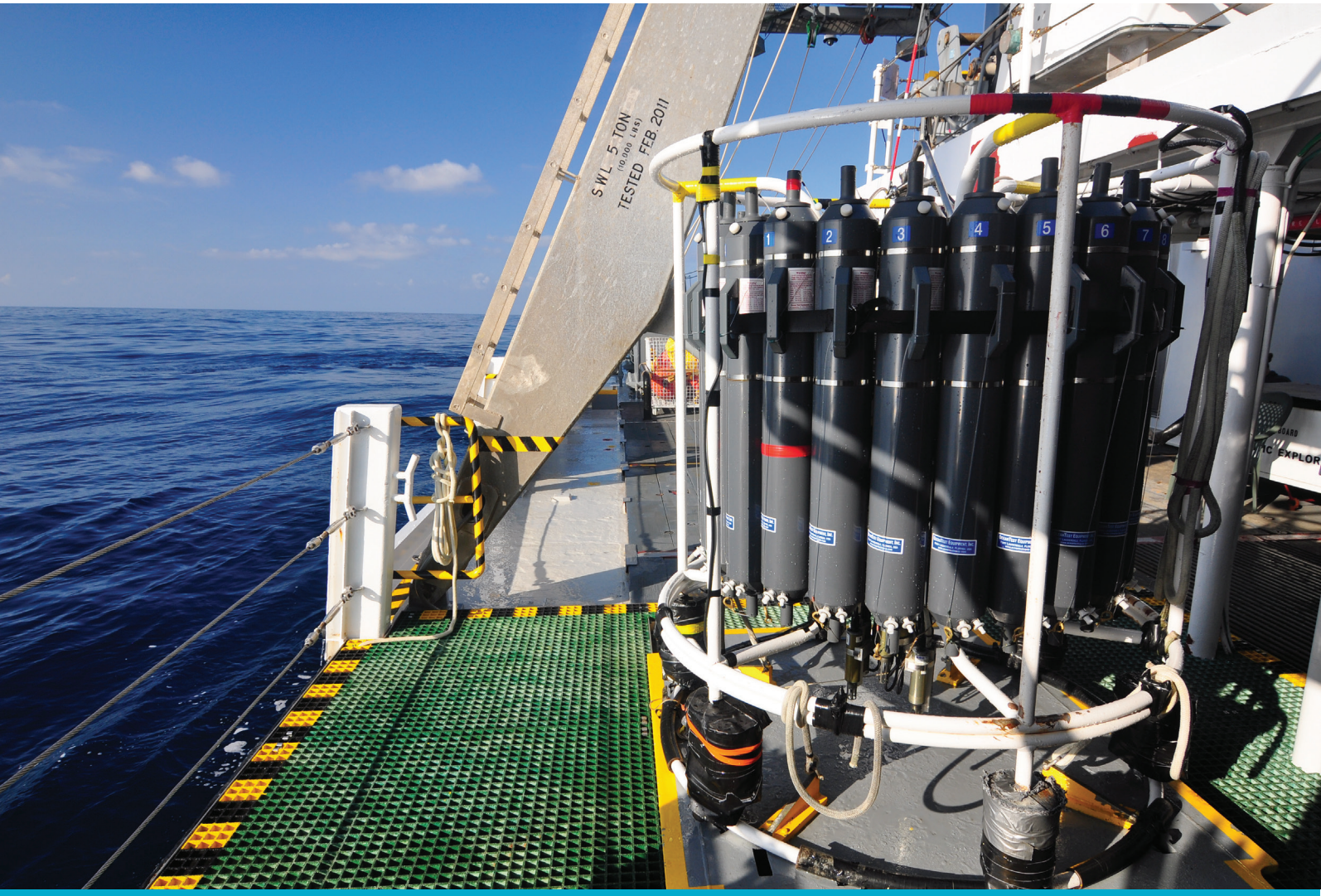

A Report Submitted to Sargasso Sea Commission

SARGASSO SEA COMMISSION

Bermuda Institute of Ocean Sciences

ASU Julie Ann Wrigley Global Futures Laboratory Arizona State University

SARGADOM

FFEM FONDS FRANÇAIS POUR L'ENVIRONNEMENT MONDIAL

Oceanography of the Sargasso Sea

An Update Concerning the Scientific Case for Protection of the Sargasso Sea

A Report Submitted to Sargasso Sea Commission

The Sargasso Sea Commission works to "encourage and facilitate voluntary collaboration toward the conservation of the Sargasso Sea." The Hamilton Declaration on Collaboration for the Conservation of the Sargasso Sea, established in 2014, provides a framework for voluntary collaboration between ten signatory governments and a Commission of scientific experts operating in their independent capacities for the conservation of the Sargasso Sea.

This work is an underlying report to the Socio-Ecosystem Diagnostic Analysis (SEDA) for the Sargasso Sea—the first analysis of its kind of a high seas ecosystem.

This work was funded under two separate but complementary projects of the Sargasso Sea Commission, the Global Environment Facility funded Sargasso Sea project (GEF-UNDP-IOC-SSC), a child project of the Common Oceans Program, implemented by UNDP and executed by IOC-UNESCO, and the French Facility for Global Environment funded 'SARGADOM' project in partnership with the University of Western Brittany and Mar Viva.

Further details: The Secretariat of the Sargasso Sea Commission is hosted by the Washington D.C. Office of the International Union for the Conservation of Nature (IUCN), Suite 300, 1630 Connecticut Avenue NW, Washington D.C., 2009, USA.

A full version of this report and of the reports commissioned by the SSC are available for download on the website at www.sargassoseacommission.org

For further details contact:
Dr David Freestone (Executive Secretary) at dfreestone@sargassoseacommission.org or
Fae Sapsford (Communications Officer) at fsapsford@sargassoseacommission.org

Table of Contents

List of Figures

Acknowledgements

We thank the numerous scientists who have worked in the Sargasso Sea and whose research is cited within this report. The future knowledge about the Sargasso Sea relies on the efforts and legacy of these scientists whose research spans nearly seven decades. We would like to thank the Fonds Français pour l'Environnement Mondial (FFEM) for their funding support of this project through the Sargasso Sea Commission, and our thanks and appreciation to David Freestone. We extend out thanks to the staff of the Bermuda Institute of Ocean Sciences (BIOS) and in particular, Dr. William Curry, President and CEO of BIOS. Finally to Dylan Simons for editing support.

CHAPTER 1

Overview of the Oceanographic Importance of the Sargasso Sea

N.R. Bates

1.1 Preamble

This report updates the scientific understanding of the Sargasso Sea, first compiled by Lomas *et al.* (2011) as scientific support for the management and protection of this region of the North Atlantic Ocean (Laloffey *et al.*, 2011). Twelve years have passed since the publication of the Lomas *et al.* (2011) and Laloffey *et al.* (2011) reports that were commissioned by the Sargasso Sea Commission (SSC). A deeper understanding of this region has been garnered by a broad and diverse range of scientific publications. This report is intended to provide a research update about the oceanography of the Sargasso Sea and, importantly, observed environmental changes. Furthermore, it is a complementary and supportive framework for other Sargasso Sea Commission (SSC) reports on regional fisheries.

The Sargasso Sea is part of the central North Atlantic Ocean, with Europe and Africa to the east, North America to the west and the Caribbean to the south (Figure 1.1). The island of Bermuda constitutes the only landmass, and the Sargasso Sea has abyssal depths of 4,000 meters or more, with notable eroded seamounts (Figure 1.2). The Sargasso Sea is an anticyclonic gyre with the surface currents of the North Atlantic Current to the north, the Canaries Current to the east, the North Equatorial Current and Antilles Current to the south, and the western boundary current Gulf Stream to the west. As such, it is one of five oceanic gyres that cover about 60% of the global ocean (the others are the South Atlantic, North Pacific, South Pacific and Indian Ocean gyres).

The upper ocean of the Sargasso Sea has distinct seasons with winter to summertime variabilities such as temperature differences of ~8-10°C, and mixed layer depth deeper in the wintertime (typically ~150-300 m)

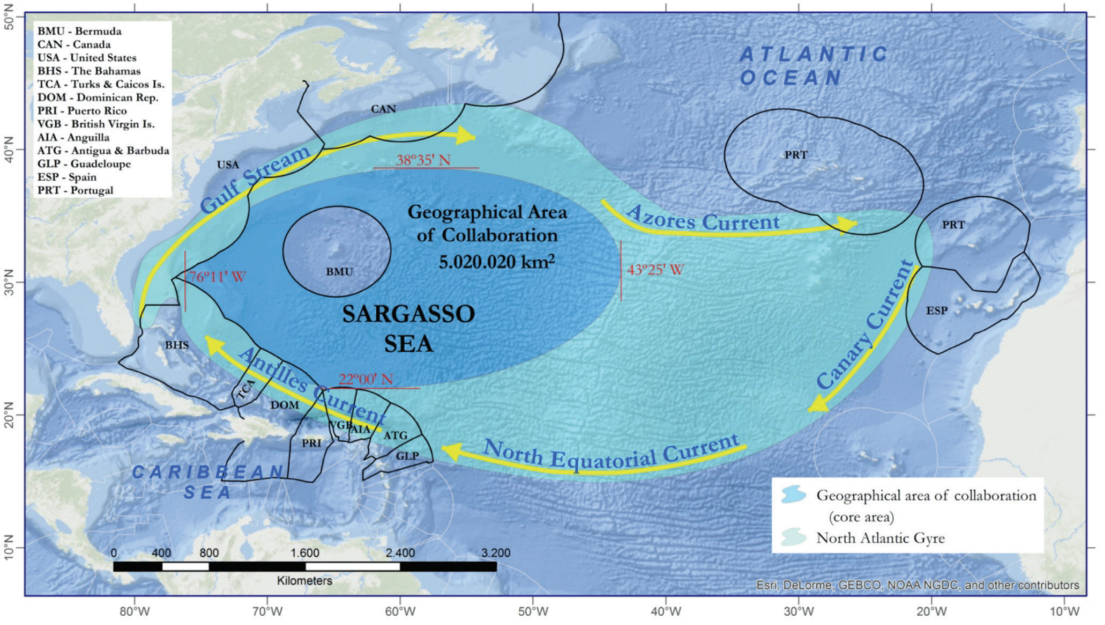

FIGURE 1.1 **Geographic location of the Sargasso Sea and its major surface currents (yellow arrows). Black lines delimit the EEZs of international stakeholders listed in the legend. Credit: Marine Geospatial Ecology Lab, Duke University, and MarViva) and SARGADOM FFEM, http://www.sargassoseacommission.org/our-work/projects/ffem.**

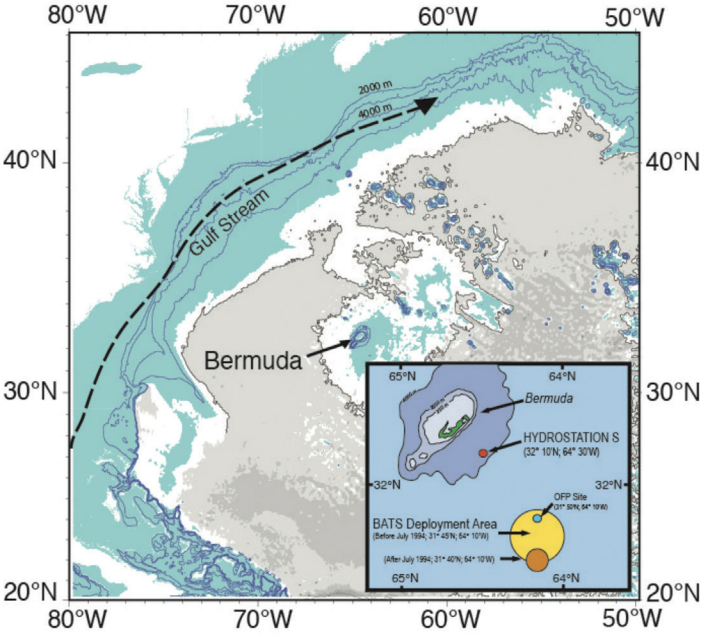

FIGURE 1.2. **Location map of the island of Bermuda and two ocean time-series (Hydrostation S, 1954 to present; and the Bermuda Atlantic Time-series, BATS, 1988-present) site. The position of the Ocean Flux Program (OFP, 1978 to present; deep ocean sediment trap program) is also shown. Credit, Bates and Johnson, 2023.**

and shallower in the summer (typically ~20-30 m; Michaels and Knap, 1996; Lomas *et al.*, 2013). The northern part of the Sargasso Sea is strongly affected by seasonality, whereas the southern part of the gyre is warmer and permanently stratified. The Gulf Stream and physical circulation of the gyre produce numerous mesoscale eddies in the Sargasso Sea (e.g., McGillicuddy *et al.*, 2007). In wintertime, eighteen-degree or subtropical mode water forms south of the Gulf Stream and ventilates the Sargasso Sea subtropical gyre at depths of ~250 to 400 m deep (Stevens *et al.*, 2020). In the southern part of the gyre, the North Atlantic subtropical underwater is found beneath the mixed layer (Montes *et al.*, 2016). In the deeper waters of the Sargasso Sea, other water masses are found from intermediate to deep, including Mediterranean Water, Labrador Sea Water, North Atlantic Deep Water and Antarctic Bottom Water.

An important oceanographic feature of the Sargasso Sea is that it is an oligotrophic gyre that, despite low inorganic nutrient levels, supports a "spring bloom" of marine phytoplankton photosynthesis and biomass growth. This, in turn, supports a rich microbial community of ocean bacteria and viruses and higher trophic level communities of zooplankton, fish, marine mammals and pelagic seabirds, for example.

A unique ecological community in the Caribbean Sea, the Gulf of Mexico and the Sargasso Sea is the free-floating pelagic plant Sargassum and the mats it forms (Laloffey *et al.*, 2011). The Sargassum provides an essential ecological niche for glass shrimps Sargassum fish, and protection for juvenile turtles, shade protection for young fish, and resting places for pelagic seabirds.

The first oceanographic expeditions of the Sargasso Sea were associated with the *HMS Challenger* (1873) and *SMS Gazelle* (1874-1876) voyages (Gould, 2022). Many of these organisms were described by William Beebe, who first described pelagic and mid and deep water organisms of the Atlantic Ocean in his record bathyscape dives off the island of Bermuda in 1932. The first sustained ocean measurements were started by the late Henry Stommel in 1954 at Hydrostation S, providing the world's longest insight into changing conditions of the deep ocean (Figure 2). The Bermuda Atlantic Time-series Study (BATS) project began in 1988 (Michaels and Knap, 1996; Steinberg *et al.*, 2001; Lomas *et al.*, 2013; Lopez *et al.*, 2023) and continues to the present day (Bates and Johnson, 2020, 2022, 2023). These ocean time series and a wide range of research projects and studies across the Sargasso Sea have provided a broad and diverse scope of knowledge about the ocean function of this oligotrophic gyre.

The critical ecological features of the Sargasso Sea include the Sargassum community, the yearly eel migration/spawning activity (e.g., American eel, *Anguilla rostrata*, and the European eel, *Anguilla anguilla*, Righton *et al.*, 2016; Hanel *et al.*, 2014; Rypina *et al.*, 2014), the deep-sea fisheries occurring beyond the economic exclusion zones (EEZs) of nation-states (Figure 1), and the migration of marine mammals past the island of Bermuda each year. Notably, the last forty years have seen significant surface ocean warming of ~1.2°C, lengthening of

summertime and shortening of wintertime conditions, slow-down of subtropical mode water formation, salinification due to reorganization of the global water cycle, and uptake of anthropogenic carbon dioxide such that the pH and chemical conditions (i.e., ocean acidification) in the 2020s of the Sargasso Sea are outside the range observed in the 1980s and before (e,g., Bates and Johnson, 2020, 2023; Stevens *et al.,* 2020). Marine photosynthesis has also changed (Lomas *et al.,* 2022) with profound implications for the higher trophic level ecology of the Sargasso Sea.

The outline of this report is as follows with the primary authors listed and will focus on the physics, chemistry, biology, biogeochemistry and carbon cycle of the Sargasso Sea.

1.2 References

Bates, N.R., and Johnson, R.J., 2020. Acceleration of ocean warming, salinification, deoxygenation, and acidification in the surface subtropical North Atlantic Ocean. *Nature Communications in Earth and Environment*, **1**, 1-12.

Bates, N.R., and Johnson, R.J., 2022. Ocean observing in the North Atlantic subtropical gyre. *Oceanography*, **34**(4), 32-33.

Bates, N.R., and Johnson, R.J., 2023. Forty years of ocean acidification observations (1983- 2023) in the Sargasso Sea at the Bermuda Atlantic Time-series Study (BATS) site. *Frontiers in Marine Science.*

Gould, W. J., 2022. HMS *Challenger* and SMS *Gazelle* – their 19th century voyages compared, Hist. Geo Space. Sci., 13, 171–204, https://doi.org/10.5194/hgss-13-171-2022. Hanel, R., Stepputtis, D., Bonhommeau, S., Castonguay, M., Schaber, M., Wysujack, K., Vobach, M., and Miller, M.J., 2014. *Naturewissenschaften*, **101**, 1041-1054. Laffoley, D. d'A., Roe, H.S.J., Angel, M.V., Ardron, J., Bates, N.R., Boyd, I.L., Brooke, S., Buck, K.N., Carlson, C.A., Causey, B., Conte, M.H., Christiansen, S., Cleary, J., Donnelly, J., Earle, S.A., Edwards, R., Gjerde, K.M., Giovannoni, S.J., Gulick, S., Gollock, M., Hallet, J., Halpin, P., Hanel, R., Hemphill, A., Johnson, R.J., Knap, A.H., Lomas, M.W., McKenna, S.A., Miller, M.J., Miller, P., Ming, F.W., Moffitt, R., Nelson, N.B., Parson, L., Peters, A.J., Pitt, J., Rouja, P., Roberts, J., Roberts, J., Seigel, D.A., Siuda, A., Steinberg, D.K., Stevenson, A., Sumaila, V.R., Swartz, W., Trott, T.M., and Vats. V., 2011. *The protection and management of the Sargasso Sea: The golden floating rainforest of the Atlantic Ocean: Summary Science and Supporting Evidence Case.* Sargasso Sea Alliance, 44 pp. Lomas, M.W., Bates, N.R., Buck, K.R., and Knap, A.H., 2011. Oceanography of the Sargasso Sea Overview of Scientific Studies. Sargasso Sea Commission, 94 pp.

Lomas, M.W., Bates, N.R., Johnson, R.J., Knap, A.H, Steinberg, D.K., Carlson, C.A., 2013. Two decades and counting: 23–years of sustained open ocean biogeochemical measurements in the Sargasso Sea. *Deep–Sea Research II,* 93, 16–32, doi: 10.1016/j.dsr2.2013.01.008.

Lomas, M.W., Bates, N.R., Johnson, R.J., Steinberg, D.K., and Tanioka, T., 2022. Adaptive carbon response to warming in the Sargasso Sea. *Nature Communications*, **13** (1), 1211. Lopez, P.Z., Johnson, R.J., Medley, C.M., Davey, E.L., Hayden, M.G., Anderson, Z.T., Montgomery, Q., Pacheco, F., Lethaby, P.J., Parsons, R., Garley, R., Lomas, M.W., and Bates, N.R., 2023. Protocols for the Bermuda Atlantic Time-series Study (BATS) core measurements. ASU-Bermuda Institute of Ocean Sciences, 142 pp.

McGillicuddy, D.J., Anderson, L.A., Bates, N.R., Bibby, T., Buesseler, K.O., Carlson, C.A., Davis, C.S., Ewart, C., Falkowski, P.G., Goldthwait, S.A., Hansell, D.A., Jenkins, W.J., Johnson, R., Kosnyrev, V.K., Ledwell, J.R., Li, Q.P., Siegel, D.A., and Steinberg, D.K., 2007. Eddy/wind interactions stimulate extraordinary mid-ocean plankton blooms. *Science, 316* (5827), 1016-1021, doi:10.1126/science.1136256.

Michaels, A.F., and Knap, A.H., 1996. Overview of the U.S. JGOFS Bermuda Atlantic Time series Study and the Hydrostation S program. *Deep-Sea Research II*, **43**, 2-3, 157-198. Montes, E., Muller-Karger, F.E., Cianca, A., Lomas, M.W., Lorenzoni, L., and Habtes, S., 2016. Decadal variability in the oxygen inventory of North Atlantic subtropical underwater captured by sustained, long-term oceanographic time series observations. *Global Biogeochemical Cycles*, **30** (3), 460-478.

Righton, D., Westerberg, H., Feunteun, E., Økland, F., Gargan, P., Amilhat, E., Metcalfe, J., Lobon-Cervia, J., Sjöberg, N., Simon, J., Acou, A., Vedor, M., Walker, A., Trancart, T., Brämcart, U., and Aarestrup, K., 2016. Empirical observations of the spawning migration of European eels: The long and dangerous road to the Sargasso Sea. *Science Advances*, **2** (10).

Rypina, I.I., Llopiz, J.K., Pratt, L.J., and Lozier, M.S., 2014. Dispersal pathways of American eel larvae from the Sargasso Sea. *Limnology and Oceanography*, **59** (5), 1704-1714. Stevens, S.W., Johnson, R.J., Maze, G., and Bates, N.R. 2020. A recent decline in North Atlantic subtropical mode water formation. *Nature Climate Change*, **10** (4), 335-341.

CHAPTER 2

Physical characteristics of the oceanography of the Sargasso Sea

R. Curry, R.J., Johnson and N.R. Bates

2.1 Physical oceanography of the Sargasso Sea

R. Curry and R.J. Johnson

Our present understanding of the physical state and dynamical underpinnings of the Sargasso Sea was built from painstaking measurements acquired over decades extending well back into the 20th century. These observational efforts have encompassed a variety of programs, platforms and sensors spanning a technological spectrum, beginning with primarily mechanical instrumentation in the mid-1950s, giving way to digital sensors in the 1980s, the development of satellite remote sensing in the 1990s, and autonomous systems in the 21st century. By 2011, when the last Sargasso Sea report was published (Lomas *et al.*, 2011), the major components of the region's circulation and property distributions had been reasonably well-described on a variety of spatial scales ranging from the ocean gyre (1000s of kilometres) to eddies (~100 km), and finer scale features (< 1 km). Much about the nature and causes of variability in the climate system was in the process of being sorted out through sustained measurement programs, and emphasis was being placed on establishing connections between the physical variability and other components of the marine environment, e.g., ecosystem ecology and biogeochemical processes associated with carbon and nutrient cycling in the subtropical gyre.

The wind-driven portion of the Sargasso Sea, generally comprising the upper 1000 m and referred to as the main thermocline, arises due to the prevailing atmospheric wind patterns. Easterly Trade Winds in the tropics and the Westerlies at mid-latitudes drive clockwise surface ocean flows that converge toward the gyre centre, with a net downwelling effect within the gyre interior. This creates weak southward Sverdrup transports over the bulk of the gyre, balanced by an intense poleward flowing current along its western edge. Thus, the Sargasso Sea is bounded west and north by the poleward flowing Gulf Stream, with southward recirculation feeding the interior and the westward flowing Antilles Current along its southern boundary (Figure 2.1).

Three long-running time series programs, the Bermuda Atlantic Time-series Study (BATS), Ocean Flux Program (OFP) and Hydrostation 'S', have provided a

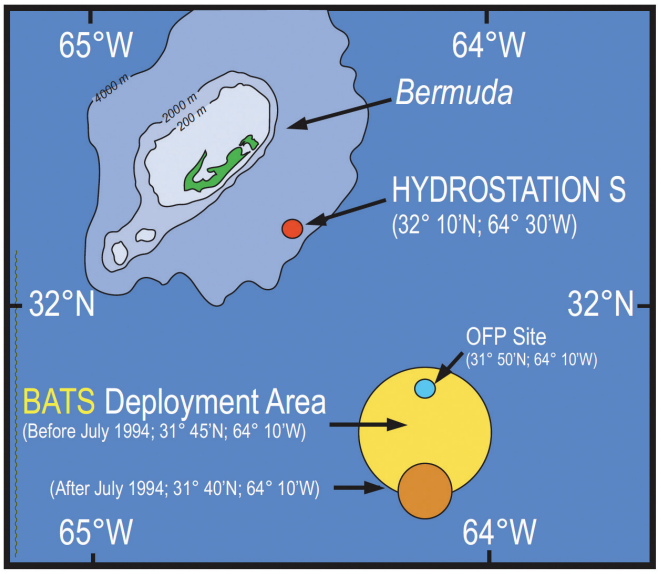

FIGURE 2.1. Location of Bermuda and the reef complex relative to several sustained open–ocean time series, including: Hydrostation S (1954–present); OFP, Ocean Flux Program (1978–present); BATS, Bermuda Atlantic Time-series Study (1988–present). Credit: Bates and Johnson, 2020.

cornerstone reference framework for a broader collection of regional field experiments and modelling studies (Figure 3). Located within 50 miles of the island, the Bermuda time-series sites (BTS) have repeatedly sampled the water column for relatively long periods with monthly sampling at the BATS site since 1987, bi-weekly at Hydrostation 'S' since 1954, and near seasonal sampling at OFP since 1978. The data have been used to identify patterns of variability on timescales of seasons, years, and decades. Moreover, these time series have provided critical data confirming long-term changes in heat and salinity budgets and increasing ocean acidification characterizing the broader subtropical gyre.

The gyre circulation is essentially a cog in a more extensive, inter-hemispheric system, the Atlantic Meridional Overturning Circulation (AMOC), which significantly regulates planetary heat distributions and, thus, Earth's climate. The AMOC consists of two opposing oceanic flows that pass through the Sargasso Sea: the shallower component, or upper limb, has its source in the poleward flowing Gulf Stream and must be balanced by equivalent volumes of equatorward flows in the deeper layers of the gyre beneath the main thermocline. The difference in temperature between the upper and lower limbs determines the amount of heat transported from the tropics toward the pole, which affects, among other things, the buildup or decline of Arctic Ocean sea ice and the Greenland Ice Sheet.

In 2004, two international field collaborations were initiated to monitor the strength of the AMOC in the subtropical North Atlantic. The RAPID Climate Change Program deployed an extensive basin-wide array of moorings across 26°N, supplemented by annual hydrographic measurements. Line W measured flows at the northern gyre boundary in the deep western boundary current (DWBC), Gulf Stream, and Sargasso Sea with 6 moorings installed along a line from the continental slope near 40°N, 70°W to Bermuda. These programs delivered baseline measurements of the strength and variability of the full AMOC and its deep limb, respectively, with analyses from both programs revealing far greater variability than expected (e.g., McCarthy *et al.*, 2012; Toole *et al.*, 2011). An initial decline in the AMOC strength was diagnosed from the RAPID observations over the years 2004 to 2014 (e.g., Smeed *et al.*, 2014; Smeed *et al.*, 2018) but countered by a possible recovery in subsequent years 2014 to 2018 (Moat *et al.*, 2020). Ultimately, it was determined that the 15-year span of the record was insufficient to quantify a significant trend; however, establishing a baseline was extremely important for future assessments of AMOC transports.

Another time series program, the Oleander Project, uses a "Ship of Opportunity" to monitor ocean properties. Since 1992, the commercial container vessel *CMV Oleander*, which transports goods between New Jersey and Bermuda every week, has routinely measured upper ocean currents using an acoustic Doppler current profiler (ADCP) installed in its hull and acquired temperature profiles down to the base of the main thermocline along its route once each month. The overarching objective of this effort has been to monitor transports of mass and heat in the Gulf Stream and surrounding waters. Its 25 years of observations have identified significant warming in the Sargasso Sea, the Gulf Stream and the U.S. shelf region, and year-to-year variations in the Gulf Stream transport, but no long-term trend in the current strength (Rossby *et al.*, 2019).

In light of our planet's growing energy imbalance, there is now more than ever an urgency to understand the patterns and drivers of ocean variability, and a diverse network of instruments, platforms and sampling strategies is essential to achieving this objective. Developing newer, compact sensors that can be deployed on autonomous vehicles, such as floats and gliders, for missions lasting months or years is revolutionizing our ability to measure the global ocean environment with higher resolution measurements at significantly reduced costs compared to ship-based observations. Here, we highlight some research developments and key findings for the Sargasso Sea that have occurred since the publication of the previous report.

2.2 Meteorology and air-sea interaction of the Sargasso Sea

R. Curry and R.J. Johnson

From late fall to early spring, the northern Sargasso Sea is progressively conditioned by the passage of low-pressure systems rolling off the coast of North America. Air masses associated with these storms are typically cold and dry, which, combined with high wind speeds, results in episodes of rapid heat loss from the upper ocean, primarily through latent heat fluxes. In contrast, the Bermuda-Azores high-pressure cell dominates the summer months, associated with relatively stable weather conditions, light winds and high humidity. Tropical cyclones can abruptly alter these conditions and, in tandem, upper ocean heat, salinity and inorganic carbon content (Bates

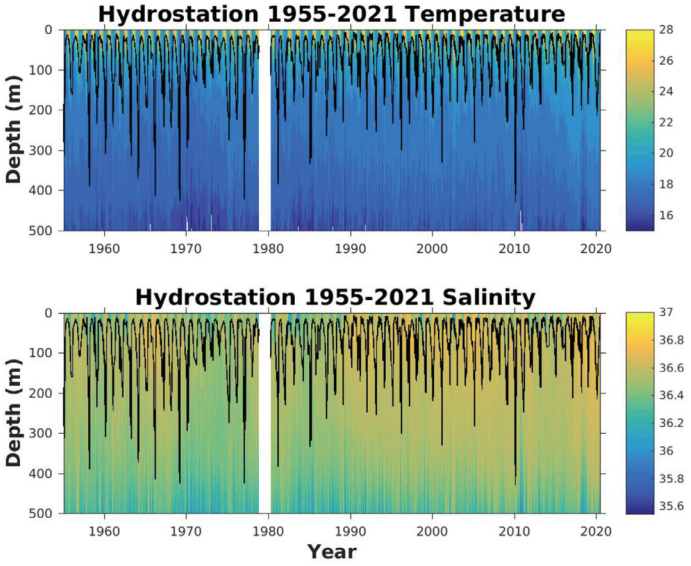

FIGURE 2.2. **Contour plots of temperature and salinity for the upper 500m at Hydrostation 'S' for years 1955 to 2021. Mixed layer depth is overlaid as a solid black line. A gap in the observations occurred in the 1979-1980 period due to a temporary lack of funding. Credit: R.J. Johnson, ASU-BIOS.**

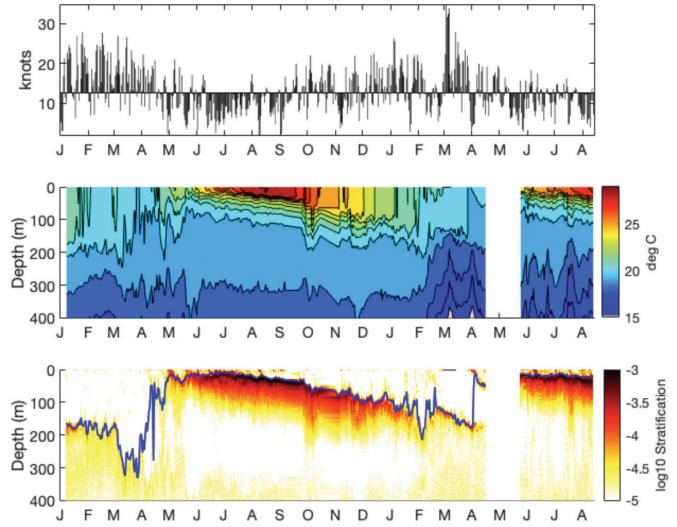

FIGURE 2.3. **The seasonal cycle of winds, temperature, mixing and stratification in the central Sargasso Sea from January 2017 to August 2018. A. wind speed (bars are plotted relative to a baseline of 12 kts, B. temperature and C. vertical stratification with mixed layer depth (blue contour). Wind data are daily averaged values from ERA5; temperature and stratification were measured by autonomous underwater gliders near the BATS site. A gap in observations occurred in spring 2018. Credit: R. Curry, ASU-BIOS.**

et al., 1998; Nelson, 1998). Individual storms, for example, have been observed to reduce SST by ~2.5°C (Dickey *et al.*, 1998).

The upper ocean's response to local atmospheric forcing is manifested as a pronounced seasonal cycle in its physical properties e.g., temperature, density, and vertical stratification. This is a consequence of air-sea heat, freshwater and momentum exchanges. Winter storms create conditions that cool and densify the surface waters, which drives convective mixing in the upper layers. The intensity of mixing and the depth to which it cools and homogenizes the upper ocean varies considerably from year to year. Recorded by the BTS observational records, winter mixed layer depths typically extend from 150 to 400 m with surface temperatures ranging from ~18 to 30°C (Figure 2.2).

The cooling peaks sometime in February/March, after which increasing solar radiance and reduced winds cause surface temperatures to rise to their maximum of ~30°C in late August to early September. The surface warming diffuses heat downward, building strong vertical gradients of temperature (thermocline) and density (pycnocline) throughout the summer months, progressively increasing stratification in the upper 100 m. These gradients impose a barrier to vertical mixing, generally confined to the upper 10-30 m in summer. A transition from net warming to net cooling in September/October re-initiates convective mixing, progressively deepening the mixed layer and entraining the underlying waters, thus eroding the seasonal thermocline in the fall and winter months to begin the annual cycle anew. To illustrate these connections, Figure 2.3 shows a time series of wind, temperature and stratification measured in the central

Sargasso Sea by underwater autonomous gliders from January 2017 to August 2018.

Gyre regions to the north of Bermuda generally experience more intense winter conditions, and thus, gradients of heat loss and mixed layer depth seasonally increase northwards toward the Gulf Stream. By contrast, in the southern portion of the Sargasso Sea, and mainly south of the subtropical convergence zone at 28°N, mixing is relatively weak and leads to reduced seasonality and a permanently stratified water column. Located between these extremes, BTS observations reflect and record interannual variations in the atmospheric forcing of the gyre and have provided an invaluable resource for documenting and investigating variability on interannual, decadal, and anthropogenic timescales (e.g., Dickson *et al.*, 1996; Levitus *et al.*, 1996; Joyce *et al.*, 2000; Bates 2001; Curry and McCartney, 2001; Goodkin, 2008).

2.3 Seasonality of the upper ocean in the Sargasso Sea

R.J. Johnson, R. Curry and N.R. Bates

The seasonality of the Sargasso Sea and the North Atlantic Ocean oligotrophic gyre has been well documented since the early 1960s when Menzel and Ryther (1960) first reported the annual cycle of temperature, salinity, mixed layer depth and ecosystem indicators (e.g., rates of primary production). Sustained ocean observations at the BATS (since 1988) and Hydrostation S (since 1954) sites have revealed complex linkages and interactions between regional and local scale physics e.g., eddies, (McGillicuddy *et al.*, 1999) and convective mixing, (Stevens *et al.*, 2022) and the biology and biogeochemistry, of the Sargasso Sea (e.g., Lomas *et al.*, 2013; Bates and Johnson, 2020; Lomas *et al.*, 2023). The Sargasso Sea is part of the broader North Atlantic Ocean-Arctic Ocean system (Correll *et al.*, 2023). The surface and mixed layer of the Sargasso Sea shows a typical seasonality of temperature with a range of ~9-11°C and with summertime highs of ~28 to 30°C and wintertime lows of ~18 to 20°C (Figure 2.4). The mixed layer depth varies from shallow during summertime (~20-30 m deep) to 150 m to 300 m deep in the wintertime (Lomas *et al.*, 2013), and the euphotic zone is about 100 m deep (Lomas *et al.*, 2013). Surface salinities are higher in wintertime (~36.67) and fresher in summer (~36.45), with a seasonal range of ~0.2 to ~0.3 (Figure 2.4). The freshening during summer is generally associated with precipitation that is distributed across a shallower mixed layer (~10-15 m), while precipitation in the wintertime is distributed through a much deeper mixed layer (~100-300 m; Michaels and Knap, 1996, Lomas *et al.*, 2013). Low salinity events are occasionally apparent (Bates and Johnson, 2020, 2023; Figure 2.4).

Over the past 70 years, an upper-ocean (~0-450 m) warming trend first recognized in the 1970s has strengthened in recent decades (about 1.2° C since the 1970s; an increase in the upper ocean heat content of ~1.2 W m^{-2}). A contemporaneous increase in salinity of ~0.2 was observed over this period (Bates and Johnson, 2020, 2022, 2023). The warming and salinification over the last decade have been ~0.8°C and 0.1, respectively, with rapid changes in the previous five years (Figure 2.4).

2.3.1 *Changes in the seasonality of the Sargasso Sea.*

In the last couple of decades, it has become evident that the seasonality observed at Hydrostation S and the Sargasso Sea near Bermuda has changed (Figure 2.5). The summer surface temperatures have increased at a higher rate than winter (i.e., 0.26 ± 0.01 °C $year^{-1}$ compared to 0.10 ±0.01 °C $year^{-1}$). As an example of these changes, it is notable that the winter ocean season (with waters being cooler than 22°C) is shorter by almost a month in the 2010s compared to the 1980s. In contrast, the summer period (with waters warmer than 25°C) has lengthened by nearly a month (Bates and Johnson, 2020). The profound implication of this finding is that the biology and marine ecosystem have also changed in concert with these physical changes.

2.3.2 *Surface warming trends of the North Atlantic subtropical gyre.*

Hydrostation S observations have proved an invaluable resource for deciphering the complexities of long–term oceanic cycles and decadal to centennial climate variability, and linkages to climate change in the North Atlantic Ocean (e.g., Pocklington, 1972; Frankingoul, 1981; Dickson *et al.* 1996; Houghton, 1996; Joyce and Robbins, 1996; Joyce and Talley, 1996; Levitus *et al.* 1996; Molinari *et al.* 1997; Hazeleger and Drifjhout, 1998; Joyce *et al.*, 2000; Bates, 2001; Curry and McCartney, 2001; Johnson 2003; Goodkin *et al.* 2008, 2015; Molinari 2011; Rhein *et al.*, 2013).

Over the past 40 years (1983–2023), ses surface temperatures have increased by 0.85 ± 0.12°C (Bates and Johnson, 2020), with an increase of 1.2°C ± 0.12°C from the early 1970s to 2022 at Hydrostation S (Figure 2.6). This constitutes the most extended set of sustained data in the global open-ocean that illustrates long-term warming

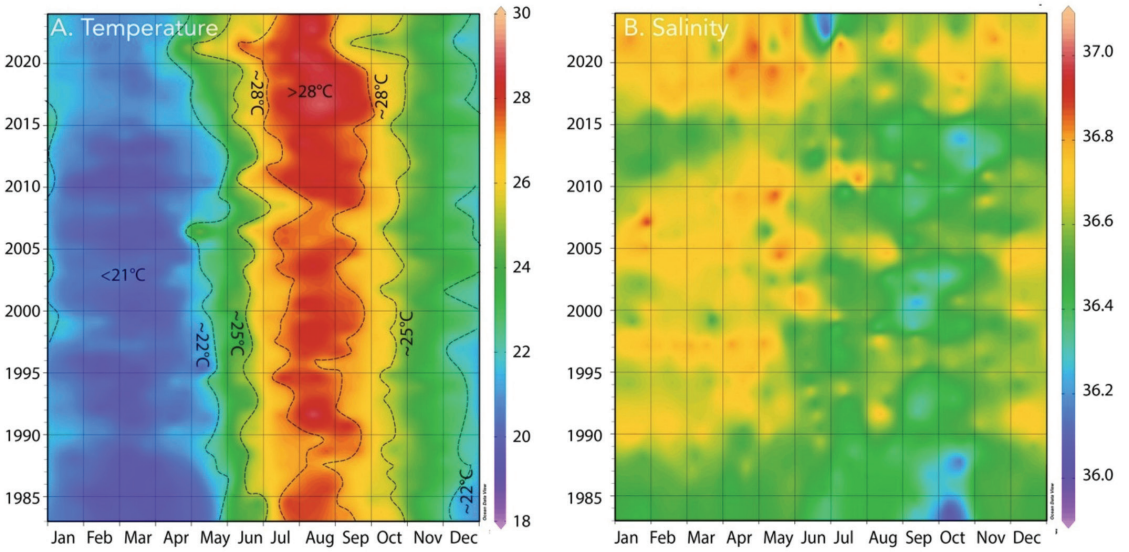

FIGURE 2.4. **The seasonal cycle and inter annual variability of surface (mixed layer) temperature and salinity at BATS (1988–2023) with earlier data (1983-1988) from Hydrostation S. These hovmuller plots show data from January to December on the x-axis and year data from 1983 to 2022 (bottom to top). A. Temperature (°C); B. salinity; Credit: Bates, N.R., and R.J. Johnson, 2023.**

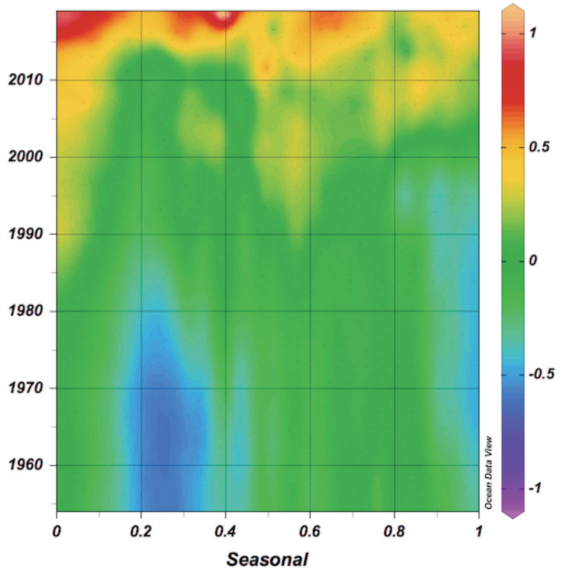

FIGURE 2.5. **Surface temperature anomalies for Hydrostation 'S' from January 1955 through December 2020. In this and following figures, all physical and biogeochemical data was seasonally detrended following methods given elsewhere (Bates and Johnson, 2020). Almost identical temperature changes are shown at the BATS site from 1983 to end of 2020. A data gap from January 1979 through April 1980 represents the period where the hydrowire with all Nansen bottles and reversing thermometers were lost at sea and resources were not available for immediate replacement. Credit: Bates, N.R., and R.J. Johnson, 2023.**

and decadal variation. The warming trend was not steady: the 1980s exhibited a slight warming (+0.26°C) that was followed by slight cooling in the 1990s and 2000s. The most substantial warming in the upper ocean (0-500m), however, has occurred since 2010 with depth integrated mean temperatures increasing by +1.18°C (Bates and Johnson, 2020) compared to an increase of +1.4°C from the early 1970s to the present. This climate relevant metric (integrated temperatures from 0 to 500m) reflects the ocean's uptake and storage of excess heat energy and since 1983, the increase has been equivalent to ~+0.24°C ±0.04°C per decade or +0.97 ±0.15°C from 1983 to 2022 (Figure 2.6).

Long-term trends represent the best data and metrics to quantify climate and ocean changes (Cheng *et al.* (2023). The gradual rise in ocean temperatures is an inevitable outcome of Earth's energy balance, with a faster rate of warming since the 1990s (Cheng *et al.*, 2022a,b). The warming and increasing stratification of the upper ocean in the Sargasso Sea have been reported with earlier datasets (Bates and Johnson, 2020; Lomas *et al.*, 2022), but here, the warming reported is of sufficient

length of time to be statistically significant. Bates and Johnson (2020) documented a ~0.21°C per decade warming (1983 to 2019 data) but this rate of warming has since increased to +0.24°C per decade with the addition of four years of recent data. In the last decade, integrated mean temperatures have rapidly increased by +0.7°C with a substantial increase in upper ocean heat content (Johnson and Bates, 2022).

Warming and increasing heat content of the upper ocean is also observed in the eastern subtropical gyre (e.g., Villarino *et al.*, 2020; Siemer *et al.*, 2021) and subpolar gyre of the North Atlantic Ocean (e.g., Desbruyères *et al.*, 2021; Josey *et al.*, 2022; Rousseau *et al.*, 2023) and this provides a broader regional context. Additionally, annual BATS validation transect cruises from 35°N to 19°N along 66°W reveal upper ocean warming trends consistent with those observed at the BTS highlighting the widespread change throughout the interior of the Sargasso Sea (Johnson et al., 2020). It should also be noted that the formation rates of subtropical mode water formation south of the Gulf Stream have decreased in the last decade (Stevens *et al.*, 2020). The ~+1°C warming of the North Atlantic subtropical gyre observed at the BATS site over the past forty years is thus another indicator of the physical and circulation changes underway in the North Atlantic Ocean that have global implications through changes in overturning circulation (e.g., Lenton *et al.*, 2019; Jackson *et al.*, 2022). It should also be noted that the acceleration of ocean temperatures in the North Atlantic subtropical gyre, particularly in the last decade, is contemporaneous with faster rates of global ocean warming (Cheng *et al.*, 2023).

2.3.3 *Salinification of the North Atlantic subtropical gyre.*

Over the past forty years, surface salinity increased by ~+0.034±0.005 per decade and by +0.136±0.020 from 1983 to 2023 (Bates and Johnson, 2023; Figure 2.6). As with the rate of change of temperature at BATS, salinification has also increased at a faster pace recently when comparing rates of +0.029 (Bates and Johnson; 1983-2019) to the rate (+0.034) computed from this extended dataset (i.e., Bates and Johnson, 2023, 1983-2023; Figure 2.7). Recently, Cheng *et al.*, 2020 proposed the Salinity-Contrast (SC) index as a valuable way to show the reorganization and amplification of the global hydrological cycle. The SC index is a manifestation of the "salty gets saltier and fresh gets fresher" ocean changes as evidenced by long-term regional and hemispheric

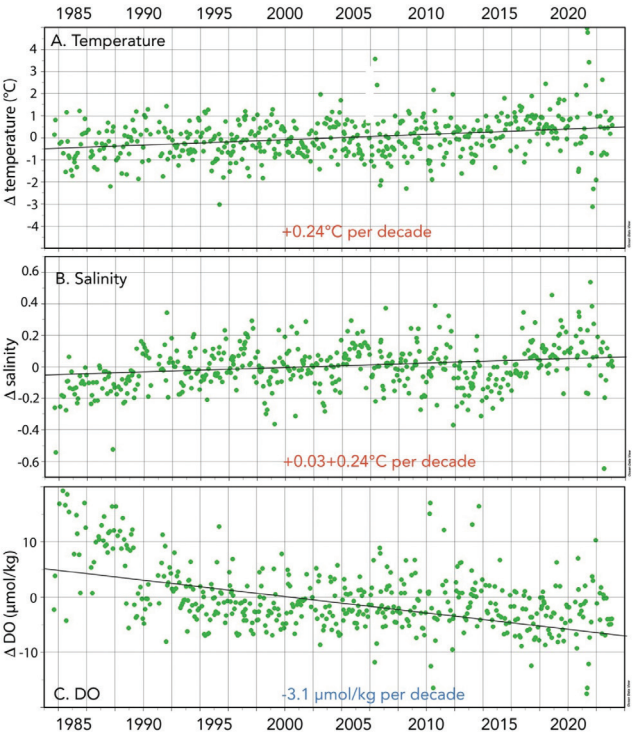

FIGURE 2.6. **Seasonally detrended seawater properties collected at the BATS site (1988–2023) and combined with earlier data from Hydrostation S (1983-1988). A. Surface temperature anomalies (Δtemperature; °C) over time; B. Surface salinity anomalies over time (Δsalinity; C. Surface dissolved oxygen DO anomalies (ΔDO; µmoles kg^{-1}) over time. Credit: Bates, N.R., and R.J. Johnson, 2023.**

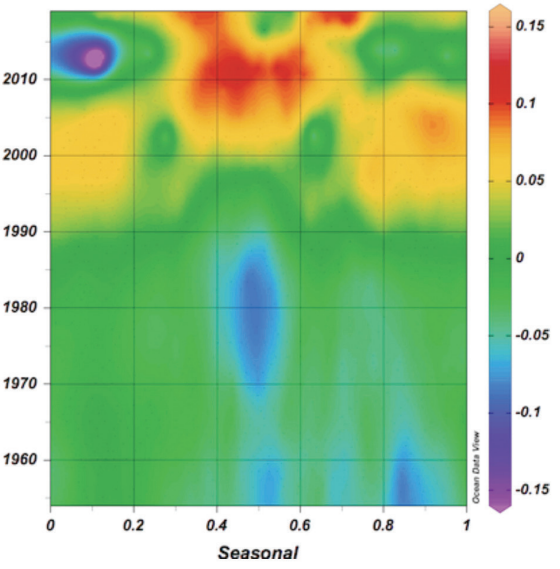

FIGURE 2.7. **Contour plots of surface salinity anomalies for Hydrostation 'S' from January 1955 through December 2020. Almost identical temperature changes are shown at the BATS to 2020. Credit: R.J. Johnson, ASU-BIOS.**

differences in the ocean. It is based on the difference in monthly averaged salinity between high-latitude and low-latitude regions. Cheng *et al*. (2023) report that the SC index has continued to increase, and compared to a 1981-2010 baseline, the North Atlantic has got saltier. This long-term change in the global hydrological cycle has been observed at BATS, and the "saltiness" of the subtropical gyre continues to increase.

Similar to the changes in the physical climate relevant metrics upper ocean biogeochemical parameters have also seen significant change. Over the past thirty years at the BATS site, primary production rates have doubled, chlorophyll biomass has increased by 22% per decade), low nitrate values in the mixed layer have doubled (i.e., an increase of ~0.25 µmoles kg^{-1}), suspended particulate organic matter and dissolved organic carbon have increased by ~30% and 2% per decade, respectively, while organic matter export increased 30% in the Sargasso Sea (Bates, 2017).

2.4 Mesoscale and submesoscale influences on Sargasso Sea variability

R.J. Johnson and R. Curry

For much of the interior of the Sargasso Sea well away from the boundary currents the long-term upper ocean flows are characterized by low (<5cm s^{-1}) westerly to south westerly geostrophic currents (Worthington, 1979) with net Ekman downwelling rates of ~4 cm day^{-1} (McClain and Firestone, 1993). However, in sharp contrast to this long-term canonical flow scheme much of the interior of the Sargasso Sea is continually subjected to the inherent presence of mesoscale eddies resulting in complex rotational flows with typical instantaneous speeds ranging between 10 to 50 cms^{-1} (Figure 2.8; Siegel and Deuser, 1997). Mesoscale eddy phenomena in the Sargasso Sea include cold core rings (Richardson, 1978) and mid-ocean mesoscale eddies (McGillicuddy and Robinson, 1997). The core of these two types of eddies are quite different in that the 'cold-core' contains water from north of the Gulf Stream and thus transport foreign waters to the

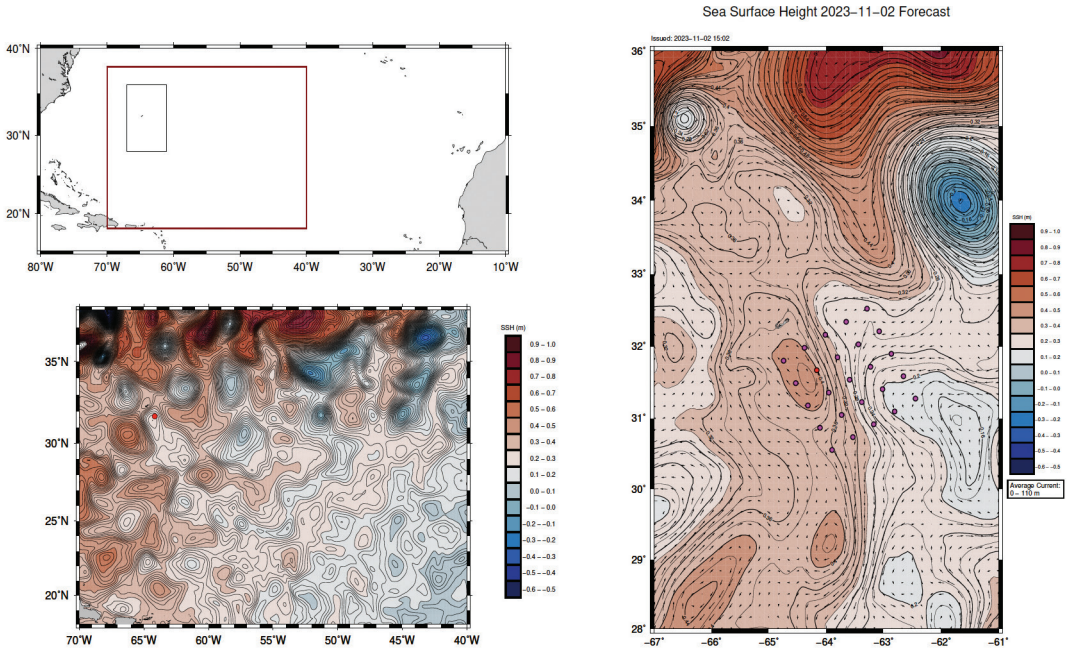

FIGURE 2.8. **Mesoscale eddies in the Sargasso Sea as viewed from satellite altimeter derived Sea Surface Height (SSH). Upper left panel show geographic locations of the far-field (larger red box) and the mid field domain smaller box). Lower left panel is a single typical representative snapshot of the Sargasso Sea SSH showing the rich complex field of interacting cyclones (low SSH- blue) and anticyclones (high SSH red). The right panel shows the mid-field domain SSH used for assessing eddy influence in the region of the BTS programs. Depth averaged (0-110m) geostrophic flows associated with the eddy systems are shown as current vectors (black arrows). BATS site is shown as red dot and other stations are the BATS spatial stations (spacing of 40km). Credit: P.L. Lethaby, ASU-BIOS.**

northern Sargasso Sea. Due to the closed recirculation flow in this region these cold core eddies tend to remain in the northwest sector of the gyre (Cornillion *et al.*, 1986) although have been infrequently observed near the BTS (Siegel *et al.* 1999).

In contrast, mid-ocean eddies are presumed to originate mostly within the eastern Sargasso Sea in response to baroclinic instability driven by the differential poleward heat flux from the tropics such that the temperature-salinity profile through the permanent thermocline of these eddies is mostly consistent with Sargasso Sea gyre water types. Though, it is also cognizant to note that intensive surveys of these features (EDDIES project and on-going work through the BATS program) have identified anomalous water masses at the core of some of these systems and thus mid-ocean eddies permit pathways for foreign waters into the Sargasso Sea (Li *et al.*, 2008).

Advancements in satellite altimetry in the early 90's helped reveal the extent and ubiquitous nature of mid-ocean mesoscale eddies in the Sargasso Sea (Figure 2.8) which was first hypothesized in the MODE and POLYMODE programs. Beyond the seasonal cycle, these mesoscale eddies are the dominant source of variability in the upper ocean through the permanent thermocline (0-1000m) and potentially hinder our ability to assess impacts of atmospheric forcing in the observational datasets over seasonal and shorter time scales e.g., McGillicuddy *et al.*, 1998, 1999, 2007; McGillicuddy, 2016). Viewed from satellite altimetry data, eddies can be recognized by changes in sea level height while using oceanographic observations the strength and eddy type can be determined by displacements of the density surfaces in the upper ocean. They are broadly categorized into three types: (i) cyclonic- density surfaces elevated resulting in anomalously cold water and a depressed sea level at its center (ii) anticyclonic density surfaces depressed resulting in anomalously warm water and an elevated sea level at its center and (iii) mode water or lens eddy. These are formed when a lens of near uniform water resides between two density surfaces causing density surfaces to be elevated and depressed for depths above and below the lens, respectively. In the case of the lens eddy, the density surface perturbation tends to be greater in the deeper layers and thus in terms of sea level height resembles a weak anticyclone (McGillicuddy and Robinson, 1997; McGillicuddy *et al.*, 1999).

Mid ocean eddies have diameters of O (100 km), lifetimes of months to years with central propagation speeds of 3 to 5 km day^{-1}, predominately track on a westerly to north westerly course and their signal is apparent through the base of the permanent thermocline (~1000 m) (McGillicuddy *et al.*, 1999). Mesoscale eddies represent a primary mode of transport for physical and chemical properties in the upper ocean of the Sargasso Sea. However, understanding their full impact through a specific region is difficult since their passage alters upper ocean inventories through both horizontal and vertical mechanisms (Woods, 1988). Further, it has been well documented that mesoscale eddies are typically self-contained rotating bodies of water with unique physical and biogeochemical properties (Benitez-Nelson *et al.*, 2008; McGillicuddy *et al.*, 2008) implying that quantification of the regional eddy flux is imperative for understanding the time varying components of the local system.

In addition to modulating upper ocean physics, mesoscale eddies also impact biogeochemical processes in the upper ocean by lifting or depressing the nutricline into the euphotic zone and subsequently enhancing or reducing primary production. Assessment of this process is important for understanding the role of eddies in the oceanic biological pump (Volk and Hoffert, 1985) and field campaigns in the Sargasso Sea (e.g., EDDIES) have been instrumental for investigating dynamics relating to the eddy processes capable of delivering new nutrients to the euphotic zone (McGillicuddy, 2008). However, quantifying these processes in ocean gyres such as the Sargasso Sea is difficult since mesoscale eddies drive significant spatial variability in the physics and biology over a wide range of length scales (10's to 100's km). Following the insight gained from the eddy process cruises (EDDIES), the BATS program established a spatial component based on fixed spatial stations (nominal 40km station spacing) around the BATS site to help assess the eddy flux through the local region (see Figure 10 right panel). Such spatial information provides valuable upstream conditions for time series analyses and at times, reveal significant heterogeneity, whereby the variability of the upper ocean observed on a single cruise (length scale of ~120 km) is similar to the variability recorded over multiple decades for the same month at the nominal BATS location. This spatial heterogeneity can be particularly pronounced during the deep convective winter mixing periods. For example, in March 2011 profiles from BATS and several spatial stations revealed a mixed layer depth range of 80 to 400 m, with respective mixed layer temperatures of 22.4°C and 18.3°C, which was due the presence of a warm anticyclone to the southwest of BATS and a cold cyclone to the northeast of BATS (length scale ~100 km,

Johnson *et al.*, 2012). Such variability complicates our ability to balance the implied physical budgets and given that this event in 2011 was prior to the spring bloom, highlights potential difficulties in understanding regional vertical convective nutrient supply and subsequent carbon export.

Interior eddy mixing and subsequent nutrient supply to the euphotic zone (and new production potential) differs for each eddy type and complicated by eddy/wind interactions (McGillicuddy *et al.* 2007). Observations from the EDDIES project reveal wind interactions with mode water eddies can amplify the eddy induced upwelling resulting in significantly large biological blooms (single episodic events equivalent to 1–3 times annual new production for the region) whereas for cyclones the eddy/wind interaction reduces the upwelling signal (McGillicuddy *et al.* 2007). Further, assessing the impact of mesoscale eddies is potentially more exacerbated given recent modelling studies revealing complex mechanisms in eddy genesis, whereby wind-eddy interactions can transform eddy types, in particular, anti-cyclones change to a mode water eddy (McGillicuddy, 2015). Additionally, there has been substantial progress in assessing the role of sub-mesoscale processes (0.01 to 10 km length scale) in driving upper ocean mixing and driving instabilities in mesoscale eddies (Brannigan *et al.*, 2017; *personal communication*, Ruth Curry ASU-BIOS MAGIC program) highlighting another important scale of variability for understanding upper ocean mixing and transport in the Sargasso Sea.

The spatial and temporal evidence from the BTS and other regional programs strongly imply that the upper ocean in this region is intimately modulated by mesoscale eddies which in turn has consequences for understanding upper ocean system processes. This is an issue when trying to understand monthly variability at the BATS site as evidenced in upper ocean inventories of heat and salinity, whereby a local 1-dimensional balance on consideration of air-sea fluxes can be achieved over multi-year time scales yet over shorter monthly intervals significant imbalances (from a 1-dimensional solution) of order of the seasonal amplitude exist (Doney, 1999; Johnson *et al.*, 2008). These imbalances are the direct consequence of the passage of mesoscale eddies and implies the need for advection to balance the system (Glover, 2002). To help assess regional eddy influence efforts are underway to develop a robust consensus of eddies using global hindcast eddy resolving models (provided by the Copernicus Marine Environment Monitoring Service, CMEMS) to establish origin, age, and dominant physical and biogeochemical characteristics as they transit through the interior of the Sargasso Sea. Initial results of these eddy tracking analyses are encouraging and further document the rich eddy environment of the BTS region determining that for years 1993-2021, a total of 1268 significant eddies (694 anticyclones, 574 cyclones) passed through the local area with a long-term monthly average of 8 features in the local region (Figure 2.9). Additionally, several modelling strategies are being developed to best integrate observations and provide a realistic 3D framework for

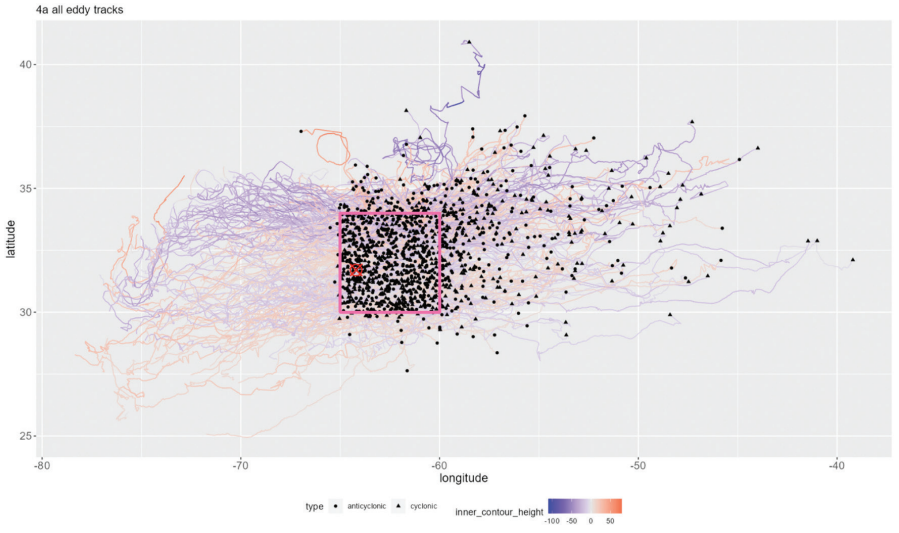

FIGURE 2.9. Trajectories of mesoscale eddies in the Sargasso Sea for 1993-2021 derived from model output and eddy tracking software developed by CMEMS. The red box (30-34°N and 60-65 °W or ~450 km x 450 km) is considered the local eddy region capable of influencing the BTS and for the time period of analyses a total of 694 anticyclones and 574 cyclones transited through the local region. Symbols indicate the location when first detected with a black circle depicting anticyclones and black triangle for cyclones. Relative strength of the eddy is shown using the SSH colourbar (blue and red for strong cyclones and anticyclones respectively). BATS site is shown as a red circle with a red cross. Credit: R. Bakker, ASU-BIOS.

quantifying eddy transport of physical and biogeochemical parameters through the Sargasso Sea.

2.5 Physical characteristics and changes in the deep water of the Sargasso Sea

R. Curry, R.J. Johnson and N.R. Bates

2.5.1 *Subtropical mode water (STMW) variability.*

Considerable attention has been given to the Subtropical Mode Water (STMW), readily identifiable by its temperature, density, and potential vorticity characteristics. It is formed by wintertime convective mixing in the northern Sargasso Sea and is subsequently subducted beneath the sea surface and advected laterally into the gyre interior. Its importance derives from several attributes: (1) its notably large volume and homogeneous characteristics, for which it was named Eighteen Degree Water (EDW) by Worthington (1959); (2) because its potential vorticity characteristics strongly influence the mean circulation in the Sargasso Sea (Schmitz, 1996; Forget *et al.*, 2011; Maze and Marshall, 2011); (3) because its properties are set by large-scale air-sea exchanges that both reflect and govern Atlantic climate variability (Joyce et al., 2000; Olsina *et al.*, 2013); and 4) because the STMW serves as a repository of heat, carbon and oxygen that circulates around the gyre (Bates *et al.*, 2002).

The CLIVAR Mode water Dynamic Experiment (CLIMODE) field campaign (Marshall *et al.*, 2009), a synergistic deployment of moorings, profiling floats, surface drifters and ship-based observations, made significant strides toward resolving STMW formation and dispersal dynamics questions. In 2006-2007, the project obtained direct observations of the coevolution of the atmospheric and oceanic boundary layers undergoing vigorous convection and placed that evolution in the context of the larger-scale gyre circulation (for overview see Marshall *et al.*, 2009). New perspectives on STMW formation sites, magnitudes of air-sea fluxes, production rates, and dynamical causes of property variability emerged (Joyce *et al.*, 2009; Maze and Marshall, 2011; Joyce *et al.*, 2013; Olsina *et al.*, 2013). In contrast to the prevailing views of STMW formation as a 1-dimensional cooling-driven convection process, a substantial portion of new STMW was observed to form in a separate region within the Gulf Stream between 67°W and 52°. There, cross-frontal fluxes of salinity were required to account for the regional salinity budget, while the heat balance in its production was determined to be primarily a product of both lateral advection by the Gulf Stream and air-sea fluxes. Thus, STMW formation within a given winter can have at least two sets of dominant physics and distinct locations.

The above findings may have wider-reaching implications. In a recent study, Berglund *et al.* (2022) suggested that the gyre exerts a more significant impact on the AMOC than previously envisioned through extensive recirculation pathways. This paradigm, described as the "downward spiralling nature" of the gyre, results in cooling and densification as water parcels complete repeated circuits within the subtropical gyre before passing into the subpolar gyre. Hence, the formation of STMW and the spiral dynamics may be connected, and changes in the former could potentially lead to changes in the AMOC's future pathways and strength.

Hydrostation S observations have enabled investigators to track the distinctive physical properties and variability of the STMW over seven decades. As discussed above this water mass typically sits directly between the locally convected upper ocean layer and the permanent thermocline which for Hydrostation S is at depths ranging from 250 to 400m (e.g., Schroeder *et al.*, 1959; Talley and Raymer, 1982). STMW serves as a reservoir for upper ocean inorganic nutrient inventories since seasonal convective winter mixing extends into this layer and entrains new nutrient into the euphotic zone and thus STMW plays an essential role in sustaining phytoplankton photosynthesis and growth rates. Early studies estimated that ~5-15 Sv (1 Sv = 10^6 m^3 s^{-1}) of STMW was annually formed and transported through the North-Atlantic mid– latitudes (e.g., Marsh and New, 1996; Marshall *et al.*, 2009), with interannual differences strongly influenced by climate variability such as the North Atlantic Oscillation (e.g., Talley and Raymer, 1982; Hurrell, 1995; Marsh and New, 1996; Talley, 1996; Hazeleger and Drifjhout, 1998; Joyce *et al.*, 2000). In the past decade, however, STMW formation rates have essentially been halved from ~11 Svy (1 Svy = 3.15 x 10^{13} m^3 volume per year) to less than 5 Svy (Stevens *et al.*, 2020) with as yet uncertain physical and biogeochemical impacts on the Sargasso Sea

2.5.2 *Oxygen minimum zone changes.*

The oxygen minimum zone (OMZ, a water mass where dissolved oxygen (DO) levels fall to <180 µmoles kg^{-1}) occupies deeper Atlantic Central waters found at depths between 600 - 900 m at Hydrostation S. While the temperature and salinity properties of this water mass have not significantly changed since 1970, DO concentrations have decreased at a rate of -2.5 µmoles kg^{-1} $decade^{-1}$ (p-value <0.01), representing a loss of ~7% in the past

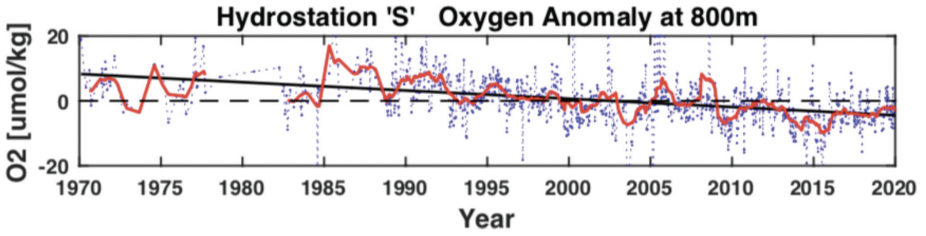

FIGURE 2.10. **Time-series of the oxygen minimum zone (OMZ) dissolved oxygen anomalies for Hydrostation 'S' from 1970 to present. The blue dots are observed data, and the red line represents a 12- month running mean. The anomalies represent the time-series data minus the overall mean. Credit: R.J. Johnson, ASU-BIOS.**

fifty years (Figure 2.10). The OMZ has also expanded volumetrically with its upper horizon lifting from ~600 m to ~500 m, particularly in the last decade. This may reflect changes in source water physical conditions, ventilation time and/or increased remineralization (Parsons, Johnson and Bates, *in preparation*), but these potential causes remain to be solved.

2.5.3 *Ventilation and deeper water flow within the subtropical gyre.*

Whereas the water masses comprising the main thermocline of the Sargasso Sea are predominantly ventilated within the subtropical gyre, the waters circulating through its deeper levels are formed remotely at higher latitudes, e.g., in the northern subpolar gyre, the Nordic Seas and in the seas around Antarctica. As they transit through the Sargasso Sea, the deep waters are characterized by temperatures colder than 6°C with salinities in the range of 34.8–35.2. Their physical properties are initially set by air-sea interactions (wind and buoyancy forcing) at their winter ventilation locations. However, these are subsequently modified by mixing and stirring along their flow paths.

Cold, dense waters from the northern source regions enter the subtropical gyre via the deep western boundary current (DWBC). This relatively narrow system flows around the Grand Banks of Newfoundland and hugs the continental shelf en route to the equator, where it crosses into the southern hemisphere. Near Cape Hatteras, the DWBC encounters the poleward-flowing Gulf Stream, and significant amounts of cold, dense water become entrained into a deep expression of that eastward-flowing current while the remainder continues southward. Interactions with topography (e.g., the New England Seamounts, Bermuda Rise and the Mid Atlantic Ridge) shape the interior trajectories such that the net flows through the deep Sargasso Sea are westward and rejoin the DWBC south of 30°N.

The coldest, densest waters in the Sargasso Sea flow northward across the equator from the South Atlantic through gaps in the seafloor topography. The temperature of this water mass, the Antarctic Bottom Water (AABW), is in the range of 1.5°-1.8°C. As it flows through the deepest basins, it progressively warms and mixes with ambient waters. Through a series of recirculation cells, the AABW ultimately upwells into the overlying layers, collectively referred to as North Atlantic Deep Water (NADW) and characterized by temperatures of 1.8° to 5°°C.

The net volume of NADW flowing equatorward through the Sargasso Sea and the lower limb of the AMOC is ~18 Sv. This however reflects extremely strong and highly variable flows in the DWBC that are balanced by a network of circulations, generally more diffuse, through the interior of the basin (Bower *et al.*, 2009; Bower *et al.*, 2019; Lozier *et al.*, 2013; Frajka-Williams *et al.* 2019). An array of moorings installed along the southeast flank of Bermuda Rise as part of the DynAMITE program from 2010-2012 (Figure 2.11) measured an average of 10 Sv of westward flow below 3000 meters (Curry, unpublished manuscript). The bulk of this flow was mainly concentrated inshore of the 4500m isobath. Chemical tracer measurements indicated these waters were tagged with northern source characteristics (elevated CFCs and O_2, low nutrient concentrations) that contrasted sharply to water masses and much weaker flows found farther down the Bermuda Rise slope. This implies separate source regions for the upslope and downslope waters: the former supplied by water masses recirculating from the DWBC and Gulf Stream to the north, the latter emanating from the basin interior to the east and/or south.

The NADW is routinely measured at the BATS in the depth range of 1,300 to 4,000m with AABW found at deeper levels. The deep ocean ultimately offers a broader (temporal and spatial) perspective for detecting long–term change. Analyses of Hydrostation S records have revealed significant thermohaline changes in the

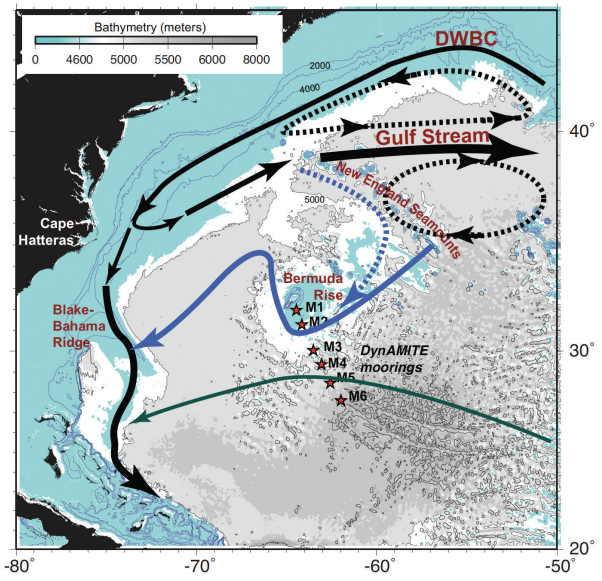

FIGURE 2.11. Deep circulation pathways of NADW in the Sargasso Sea with the location of moorings for the DYNAMITE program. Credit: R. Curry, ASU-BIOS.

deep ocean (Joyce and Talley, 1996; Joyce and Robbins, 1996; Levitus *et al.*, 1996; Talley, 1996; Curry *et al.*, 1998; Whitefield *et al.*, 2008). Hydrostation S observations have also offered insight into the variability of deeper water masses in the North Atlantic mid–latitudes (e.g., Aucan and Llovel, 2013; section 2.3.2) and climate/deep water formation. Early studies of Labrador Sea water, transiting through the Sargasso Sea and sampled at Hydrostation S, revealed an approximate six–year transit from the site of formation in the Labrador Sea to Bermuda (Curry *et al.*, 1998). The utility of Hydrostation S observations for determining Labrador Sea water formation dynamics and transport has continued with subsequent studies (e.g., Dickson *et al.*, 1996; Curry and McCartney, 2001; Rossby *et al.*, 2005).

Deep ocean trends continue to emerge in response to changing atmospheric forcings in the formation sites. For example, recent analyses on deep–water (e.g., Labrador Sea Water, LSW at 2,000m depth) changes over the past three decades suggest a significant long-term decline in both temperature (~0.08°C decade^{-1}) and salinity (~0.02 decade^{-1}) in stark contrast to upper ocean trends. While these trends are shown since the 1950s, slight warming and salinification is evident since 2000 (Figure 2.12) presumably reflecting changes in the Arctic Ocean (freshening in the Arctic and Labrador Sea).

2.6 Modelling and autonomous technologies

R. Curry, R.J. Johnson and N.R. Bates.

As highlighted above, the Sargasso Sea and in particular the immediate region off Bermuda, supports an invaluable framework of sustained and integrated field research programs which have resulted in new insight, paradigm adaptions, and documented significant climate relevant emerging trends (e.g., Bates and Johnson, 2020; Bates and Johnson, 2023). These programs span many decades with varying parameters, and although integrated at some complementary level they lack primary hydrodynamic data and are mostly insufficiently sampled in time and space to allow for 'connectivity' at a direct process level of understanding. Hence, although trends can be qualitatively linked to large scale climate type processes, it remains problematic to assign quantitative metrics to direct forcing mechanisms which is fundamental for predicative capability especially with changing environmental conditions. New ocean modelling approaches and the progressive development of autonomous technologies (e.g., gliders, profiling floats) offer synergistic solutions to help constrain the relevant physics and advance the synthesis of ocean processes through data fusion of observations and modelling, across physical scales and biogeochemical disciplines.

The time series programs have been the cornerstone and impetus for numerous modelling studies in the Sargasso Sea over the past few decades (e.g., Fasham, 1990; Sarmiento *et al.*, 1993; Doney, 1996; Spitz *et al.*, 2001; Anderson *et al.*, 2003; Johnson, 2008; Vallino *et al.*, 2008; Letscher *et al.*, 2016; LeGland *et al.*, 2020) with the most prominent growth period in the late 90's as part of the US JGOFS (Joint Global Ocean Flux Study) Synthesis and Modelling Project (SMP). Much of the SMP efforts were in response to the collective success of the JGOFS process cruises, JGOFS Atlantic time-series sites (BATS and North Atlantic Bloom Experiment sites) and new output from primitive global numerical biogeochemical models. The overarching focus of the SMP was processes that control carbon partitioning within oceanic reservoirs, with five specific objectives all of which remain at the forefront of current research questions (Doney et al., 2002).

The SMP program ranged from development phase and basic 1-D physical models (e.g., bulk mixed layer models) and simple biogeochemical models (e.g., Phytoplankton-Zooplankton Nutrient-Detritus, PZND), to establish more robust 3D global solutions with more

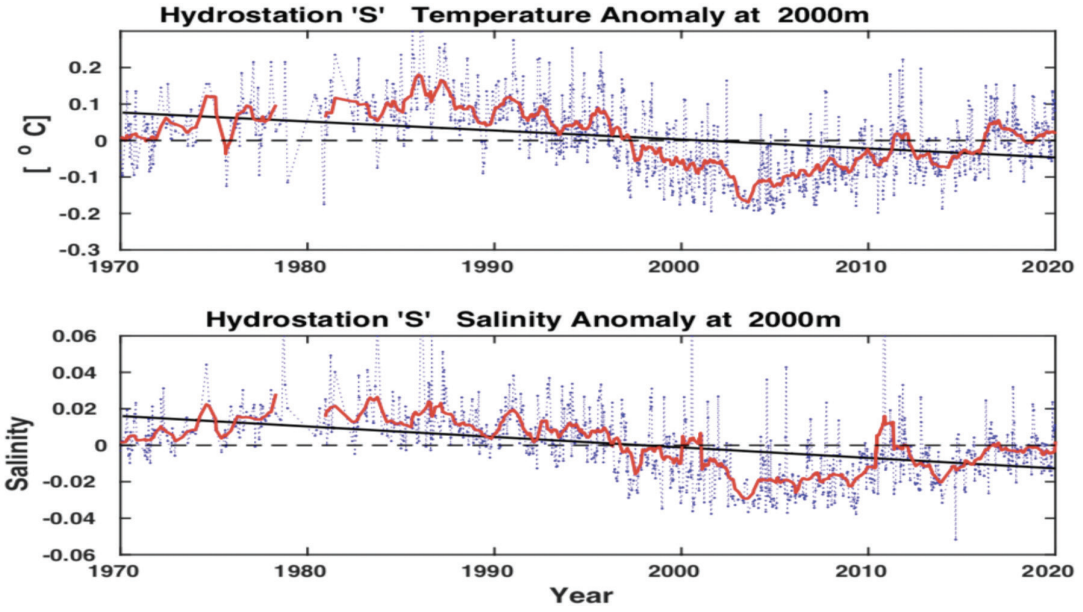

FIGURE 2.12. Time-series of temperature and salinity anomalies at 2,000 m at Hydrostation 'S' from 1970 to present. The blue dots are observed data, and the red line represents a 12-month running mean. The anomalies represent the time-series data minus the overall mean. The regressions are statistically significant (p-values <0.01) with cooling and freshening of -0.13°C and -0.033 over the past 50 years (caveat is the multidecadal oscillation of cooling/warming and salinification/freshening superimposed on the overall fifty-year trend. Credit: R.J. Johnson, ASU-BIOS.

realistic treatment of ecosystem process (e.g., Aumont *et al.*, 2001, though the emergence of model complexity revealed substantial deficiencies in observational parameter constraints (Ward et al., 2013). Tasked with understanding impacts of anthropogenic forcing on the functioning of North Atlantic ecosystems through an integrative modelling package, EURO-BASIN (European Basin scale Analysis and Synthesis, a joint EU/North American program initiated in 2013) provided a key foundation for sustained ocean model development for regional and global purposes (Holt *et al.*, 2014). Based on NEMO (Nucleus for European Modelling of the Ocean), EURO-BASIN helped create a legacy of state-of-the-art physical and biogeochemical models (benefited from incremental developments, advances in parameterisation, testing and validation) which continue to evolve and serve the ocean community through NEMO and CMEMS (Copernicus Marine Environmental Monitoring System, operated by Mercator Ocean International) with global ocean modelling products at high resolution.

CMEMS model output which include both forecast and reanalysis products are derived from an eddy resolving model with a resolution of 1/12° (~ 9 km) with daily output of physical variables (T, S, *U*, *V*) for full ocean depth. Validation of the CMEMS physical data has been performed at the BATS site (Figure 2.13; Johnson *et al.*, 2014; Hiron *et al.*, 2016) verifying excellent model skill demonstrating its appropriate application for Sargasso Sea studies. Additionally, output from the CMEMS global biogeochemical hindcast model based on the EURO-BASIN evolved lower trophic PISCES (Pelagic Interactions Scheme for Carbon and Ecosystem Studies) model with a grid resolution of 1/4° (~27 km) provides users with daily output of ecosystem parameters (nutrients, chlorophyll, pCO_2, and primary productivity) which has also proven valuable for Sargasso Sea studies. For example, a recent time series program off Bermuda (Bermuda Atlantic Iron Time-series project (BAIT; Sedwick *et al.*, 2022) focused on iron modelling at BATS using global NEMO PISCES solutions. A key aspect of the BAIT work is the two-year time series which measured all forms of iron species to allow refinement of the model parametrizations. Initial PISCES model runs using conventional parameterization schemes significantly over predicted the seasonal accumulation of dissolved iron in the upper ocean. Through the modelling and observational fusion efforts, a new process namely the 'colloidal shunt' was established and when implemented in algorithms, model output aligns

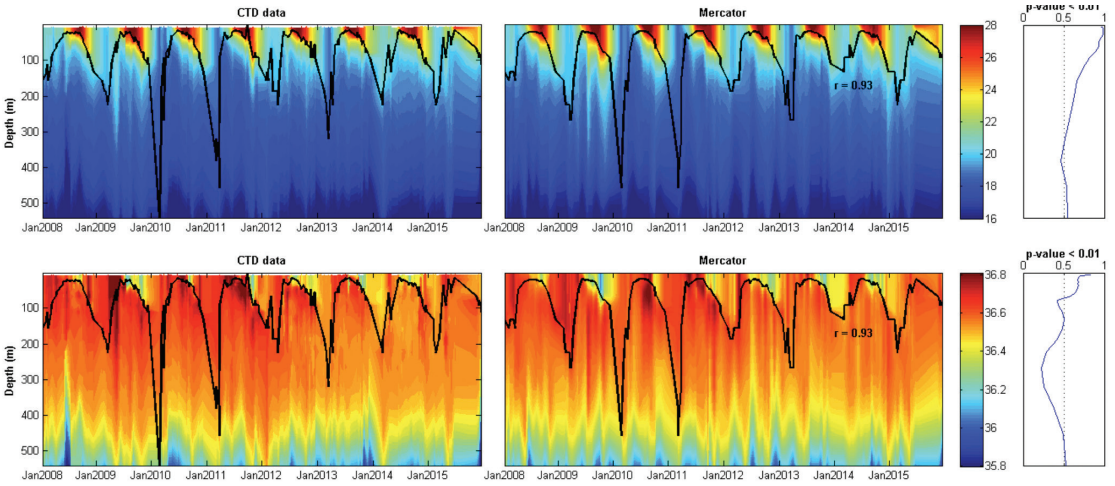

FIGURE 2.13. Comparison of Mercator (CMEMS) model output with observed CTD profiles of temperature (upper) and salinity (lower) at the BATS site for years 2008 through 2015. Plots to the right of the contours show the correlation coefficient between model and observed data with significant correlations for upper 500m. Mixed layer depth is overlaid as sold black line (r=0.93). (Hiron *et al.*, 2015)

with the seasonal observations (Tagliabue *et al.*, 2023). Subsequently, these model algorithms developed at the BATS site were used for PISCES global model runs and hence solutions established at BATS through intensive field campaigns provide new insight globally. Potentially, the global model solutions could also highlight local measurement deficiencies, though it is fundamentally this progressive and perpetual feedback from observations to model, and local to global scale, that empowers modelling to quantify system processes fit for prediction purposes. The wealth of observational data and history of modelling in the Sargasso Sea provides this region with valuable opportunities to advance our understanding of relevant physical and biogeochemical processes and should be considered as a modelling testbed region.

All BATS related cruises since 2015 use CMEMS forecast data for cruise planning purposes, and to determine spatial variability. Real time data collected during the cruises are used to validate the model forecast data and typically the model skill is appropriate though at times depends on the recent availability of satellite altimetry data (used as an input to the modelling). For synthesis efforts the CMEMS reanalysis products are used which agree very well with the observed physical parameters temperature and salinity (Figure 2.13) and velocity fields (Figure 2.14). Validation efforts with CMEMS data are in progress with a 28-year statistical assessment with Hydrostation S and BATS data, and a consensus of mesoscale eddies through the local region which will detail the subsequent model-observation research path. As such efforts are in

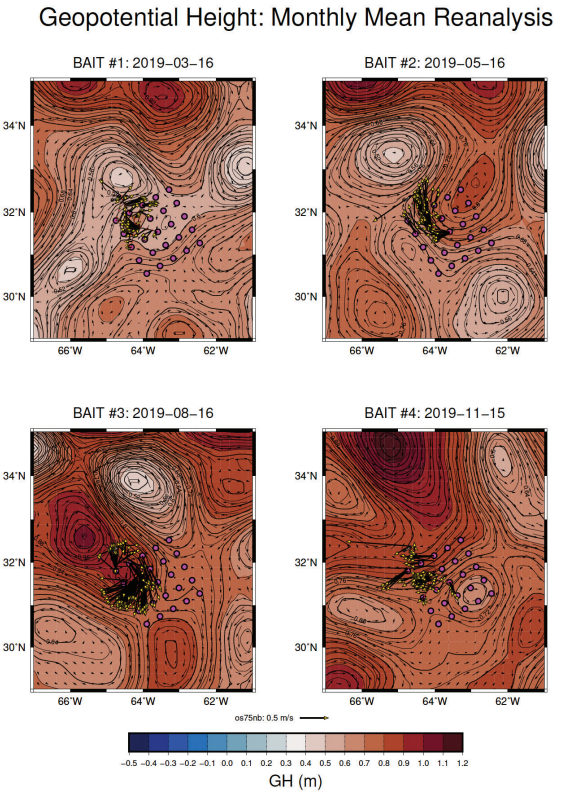

FIGURE 2.14. Comparison of Mercator (CMEMS) reanalysis model velocity fields with observed ADCP data (black arrows with yellow head) overlaid on geopotential height. Observed data from the R/V Atlantic Explorer for all four BAIT cruises in the Sargasso Sea during 2019. Scaling arrow is shown above the colorbar and pink filled circles and the BATS spatial stations. Credit: P. Lethaby, ASU-BIOS.

progress to establish a formal modelling framework for the Sargasso Sea in the region of the BTS. Operationally the modelling framework will comprise of pelagic and coastal modelling domains with the latter being coupled to the offshore system through boundary conditions. Additionally, one dimensional modelling approaches are being developed with recent analyses highlighting the important role of advection in balancing the upper ocean heat budget at BATS (Jones and Johnson, 2023) and the PISCES modelling working group have endorsed efforts to establish BATS as a global testbed for 1D model development for the NEMO-PISCES program.

Modelling offers an attractive tool for enhancing system understanding however robust observations in space, time and parameter space, are vital for model initialization, boundary conditions and verification. Advancements in ocean instrumentation (e.g., nutrient sensors, turbulence probes) and autonomous platforms (e.g., gliders, ARGO floats) have accelerated in recent years such that these technologies can provide new insight on oceanographic processes not possible with conventional measurement protocols. For example, gliders can be used as virtual moorings for long time periods providing high resolution profile data over diel to seasonal time scales. Such high resolution data can better quantify changes in upper ocean inventories and capture physical and biological events at important sub-mesoscale length scales. Additionally, gliders can be equipped with a range of instrumentation such as turbulence probes that determine dissipation rates and vertical diffusion, which are vital for understanding ocean mixing and typically not well parametrized in models. The Mid-Atlantic Glider Initiative and Collaboration (MAGIC) project at BIOS launched at BIOS in 2014 has successfully delivered numerous glider missions shedding new insight on ocean variability and mixing in the Sargasso Sea.

2.7 References

Aucan, J., and Llovel, W., 2013. Deep water trends and variability at the BATS site in the subtropical North Atlantic and consequences on local sea level budget. *Deep Sea Research, II*, January 2013, doi:10.1016/j.dsr2.2013.01.003.

Balmaseda, M. A., Smith, G.C., Haines, K., Anderson, D., Palmer, T.N., and Vidard A., 2007. Historical reconstruction of the Atlantic Meridional Overturning circulation from the ECMWF operational ocean reanalysis, *Geophys. Res. Lett.*, **34**, doi:10.1029/2007GL031645.

Bates, N.R., Knap, A.H. and Michaels, A.F., 1998. The effect of hurricanes on the local to global air-sea exchange of CO_2. *Nature*, **395**, 58–61.

Bates, N.R., 2001. Interannual variability of oceanic CO_2 and biogeochemical properties in the Western North Atlantic subtropical gyre. *Deep–Sea Research II*, **48** (8–9), 1507–1528, doi:10.1016/S0967–0645(00)00151–X.

Bates, N.R., and Johnson, R.J., 2020. Acceleration of ocean warming, salinification, deoxygenation, and acidification in the surface subtropical North Atlantic Ocean. *Nature Communications in Earth and Environment*, **1**, 1–12.

Bates, N.R., and Johnson, R.J., 2022. Ocean observing in the North Atlantic subtropical gyre. *Oceanography*, 34(4), 32–33.

Bates, N.R., Michaels, A.F., and Knap, A.H., 1996. Seasonal and interannual variability of oceanic carbon dioxide species at the US JGOFS Bermuda Atlantic Time-series Study (BATS) site. *Deep Sea Research Part II,* 43, 347–383.

Bates, N.R., Michaels, A.F., and Knap, A.H., 1996. Alkalinity changes in the Sargasso Sea: geochemical evidence of calcification? *Marine Chemistry*, **51**, 347–358.

Bates, N.R., Pequignet, A.C., Johnson, R.J., and Gruber, N. 2002. A short–term sink for atmospheric CO_2 in subtropical mode water of the North Atlantic Ocean. *Nature*, **420** (6915), 489–493, doi:10.1038/nature01253, Dec. 5, 2002.

Benitez-Nelson, C.R. and McGillicuddy, D.J., 2008. Mesoscale physical-biological biogeochemical linkages in the open ocean: An introduction to the results of the E-Flux and EDDIES programs - Preface. *Deep Sea Res., Part II*, **55**, 1133–1138.

Berglund, D., Groeskamp, S., and McDougall, T., 2022. The downward spiralling nature of the North Atlantic Subtropical Gyre. *Nature Communications*.

Bower, A., Lozier, S.M., Gary, S.F. and Böning, C.W., 2009. Interior pathways of the North Atlantic Meridional Overturning Circulation. *Nature*, **459** (7244), 243–247. https://doi.org/10.1038/nature07979.

Bower, A., Lozier, S., Biastoch, A., Drouin, K., Foukal, N., Furey, H., et al., 2019. Lagrangian views of the pathways of the Atlantic Meridional Overturning Circulation. *Journal of Geophysical Research: Oceans*, 124, 5313–5335. https://doi.org/10.1029/2019JC015014.

Brannigan, L., Marshall, D.P., Naveira Garabato, A.C., George Nurser, A.J., and Kaiser, J., 2017. Submesoscale instabilities in mesoscale eddies. J. Physical Oceanography, **47**, 12, 3061–3085. https://doi.org/10.1175/JPO-D-16-0178.1

Cheng, L., K. E. Trenberth, N. Gruber, J. P. Abraham,J. T. Fasullo, G. Li, M. E. Mann, X. Zhao, and J. Zhu, 2020. Improved estimates of changes in upper ocean salinity and the hydrological cycle. J. Climate, **33**, 10357–10381, https:// doi.org/10.1175/JCLI-D-20-0366.1.

Cheng, L., von Schuckmann, K., Abraham, J.P., Trenberth, K.E., Mann, M.E., Zanna, L., England, M.H., Zika, J.D., Fasullo, J.T., Yu, Y., Pan, Y., Zhu, J., Newsom, E.R., Bronselaar, B., and Lin, X., 2022a. Past and future ocean warming. *Nature Reviews Earth and Environment*, **3**, 776–794, https:// doi.org/10.1038/s43017-022-00345-1.

Cheng, L. J., Foster, G., Hausfather, Z., Trenberth, K.E., and Abraham, J., 2022b. Improved quantification of the rate of ocean warming. J. *Climate*, **35**, 4827–4840, https://doi.org/10. 1175/JCLI-D-21-0895.1.

Cheng, L., Abraham, J., Trenberth, E.E., Fasullo, J., Boyer, T., Mann, M.E., Zhu, J., Wang, F., Locarnini, R., Li, Y., Zhang, B., Yu, F., Wan, L., Chen, X., Feng, L., Song, X., Liu, Y., Reseghetti, F., Simoncelli, S., Gouretski, V., Chen, G., Mishonov, A., Reagan, J., and Li, G., 2023. Another year of record heat for the ocean. *Advances in Atmospheric Sciences*, 40, 963–974.

Cornillion, P.D., Evans, D. and Large, W., 1986. Warm outbreaks of the Gulf Stream into the Sargasso Sea. *Journal of Geophysical Research*, **91**, 6853–6596.

Curry, R. G. and McCartney M.S., 2001. Ocean Gyre Circulation Changes Associated with the North Atlantic Oscillation, *J. Phys. Oceanogr.*, **31**, 3374–3400.

Curry, R.G., McCartney, M.S. and Joyce, T.M., 1998. Ocean transport of subpolar climate signals to mid-depth subtropical waters. *Nature*, 391 (5), 575–577.

Danabasoglu, G. and McWilliams, J.C., 2000. An upper-ocean model for short-term climate variability. *Journal of Climate*, **13**, 3380–3411.

Desbruyères, D., Chafik, L., and Maze, G., 2021. A shift in the ocean circulation has warmed the subpolar North Atlantic Ocean since 2016. *Nature Communications Earth and Environment*, **2**, 48.

Dickey, T.D., Frye, D., Jannasch, H., Boyle, E.A., Manov, D., Sigurdson, D., McNeil, J., Stramska, M., Michaels, A.F., Nelson, N.B., Siegel, D.A., Chung, G., Wu, J. and Knap, A.H., 1998. Initial results from the Bermuda Testbed Mooring Program. *Deep-Sea Res.*, **45**, 771–794.

Dickson, R., Lazier, J., Meincke, J., Rhines, P., and Swift, J., 1996. Long-Term Coordinated Changes in the Convective Activity of the North Atlantic. *Progress in Oceanography* 38, 241–295.

Doney, S.C., 1996. A synoptic atmospheric surface forcing data set and physical upper ocean model for the U.S. JGOFS Bermuda Atlantic Timeseries Site. *J. Geophys. Res.*, 101, 25,615–26,634.

Forget, G., Maze, G., Buckley, M., and Marshall, J. 2011. Estimated Seasonal Cycle of North Atlantic Eighteen Degree Water, J. Phys. Ocean., 41, 269–286, doi:10.101175/2010JPO4257.1

Frajka-Williams, E., Ansorge, I.J., Baehr. J., Bryden, H.L., Chidichimo, M.P., Cunningham, S.A., Danabasoglu, G., Dong, S, Donohue, K.A., Elipot, S., Heimbach, P., Holliday, N.P., Hummels, R., Jackson, LC, Karstensen. J, Lankhorst M., Le Bras. I.A., Lozier, M.S., McDonagh, E.L., Meinen, CS, Mercier, H, Moat. BI, Perez, RC, Piecuch, CG, Rhein, M, Srokosz, MA, Trenberth, K.E., Bacon, S., Forget, G., Goni, G., Kieke, D, Koelling, J, Lamont, T, McCarth.y G.D., Merten,s C., Send, U, Smeed, DA, Speich, S, van den Berg, M, Volkov, D. and Wilson, C. 2019. Atlantic Meridional Overturning Circulation: Observed Transport and Variability. *Front. Mar. Sci.*, **6**, 260, doi: 10.3389/fmars.2019.00260.

Frankignoul, C., 1981. Low-frequency temperature fluctuations off Bermuda. *J.Geophys. Res.*, **86**, 6522-6528.

Glover, D.M., Doney, S.C., Mariano, A.J., Evans, R.H., and McCue, S.J., 2002. Mesoscale variability in time series data: Satellite based estimates for the U.S. JGOFS Bermuda Atlantic Time-series study (BATS) site. *Journal of Geophysical Research*, **107**, C8, 3092, doi:10.1029/2000JC000589.

Gonçalves, A., Johnson, R.J., and Bates, N.R., 2016. Understanding the steric height long term variability at the Bermuda Atlantic Time-Series Study (BATS) site with a neutral density approach. Ocean Sciences Meeting, New Orleans, 2016.

Goodkin, N.F., Hughen, K.A., Cohen, A.L. and Smith, S.R., 2005. Record of little ice age sea surface temperatures at Bermuda using a growth-dependent calibration of coral Sr/Ca. *Paleoceanography*, **20**, PA4016.

Goodkin, N.F., Hughen, K.A., Curry, W.B., Doney, S.C. and Ostermann, D.R., 2008. Sea surface temperature and salinity variability at Bermuda during the end of the Little Ice Age. *Paleoceanography*, **23**, PA3203.

Goodkin, N.F., Wang, B.-S., You, C.-F., Hughen, K.A., Grumet-Prouty, N., Bates, N.R., and Doney, S.C., 2015. Ocean circulation and biogeochemistry moderate interannual and decadal surface water pH changes in the Sargasso Sea. *Geophysical Research Letters*, **42**(12), 4931–4939.

Hazeleger, W. and Drijfhout, S.S., 1998. Mode water variability in a model of the subtropical gyre: response to anomalous forcing. *J. Phys. Oceanogr.*, 28, 266-288.

Henson, S.A., 2014. Slow science: the value of long ocean biogeochemistry records. *Philosophical Transactions of the Royal Society of London A: Mathematical, Physical and Engineering Sciences*, **372** (2025), 20130334.

Hiron, L., Gonçalves, A., Bates, N.R., and Johnson, R., 2016. Evaluation of an eddy resolving global model at the Bermuda Atlantic Time-series Study site. *Ocean Sciences Meeting*, New Orleans, 2016.

Houghton, R.W., 1996. Subsurface quasi-decadal fluctuations in the North Atlantic. *Journal of Climate*, **9**, 1363–1373.

Hurrell, J.W., 1995. Decadal trends in the North Atlantic Oscillation regional temperature and precipitation, *Science*, **269**, 676–679.

Jackson, L.C., Biastoch, A., Buckley, M.C., Desbruyères, D., Frajka-Williams, E., Moat, B., and Robson, J., 2022. The evolution of the North Atlantic Meridional Overturning Circulation since 1980. *Nature Reviews Earth and Environment*, **3**, 241–254.

Jenkins, W.R., 1982. On the climate of a subtropical ocean gyre: decade timescale variations in water mass renewal in the Sargasso Sea. *Journal Marine of Research Supplement*, 40: 265–290.

Jenkins, W.R. and Goldman, J.C., 1985. Seasonal oxygen cycling and primary production in the Sargasso Sea. *Journal of Marine Research*, **43**, 465–491.

Johnson, R.J., 2003. Climatic and mesoscale modulation of the upper ocean at the Bermuda time-series sites. Ph.D thesis, University of Southampton, U.K.

Johnson, R.J., Knap, A.H., Bates, N.R., Whitefield, J.D, Kadko, D. and Lomas, M.L. 2008. Coordinated change in the heat, salinity and CO_2 Budgets of the mesopelagic zone at the Bermuda time-series sites. Paper presented at the Ocean Sciences meeting, *Am. Soc. of Limnol. and Oceanogr.*, Orlando, Fla., 2–7 March

Johnson, R.J., Evans, D.G., McGillicuddy, D., Bates, N.R., Lomas, M.W. and Knap. A.H., 2012. Observations of mesoscale eddies near the Bermuda Atlantic Time-series study site and implications for the local hydrography and nutrient budgets. *ASLO 2012 Ocean Sciences meeting, February 19–24, Salt Lake City.*

Johnson, R.J., Hyder, P., Evans, D.G., Koffi, U., and Bates, N.R., 2014. Assessment of reanalysis and operational numerical models in the Sargasso Sea to help quantify advection at the Bermuda Atlantic Time-series Site. *(Abstract ID: 13513), ASLO Ocean Sciences Meeting, February 2014.*

Johnson, R.J., Bates, N.R., Lomas, M.W., Stevens, S., Lethaby, P., Anderson, A., Pacheco, F., and Knap, A.H., 2020. Meridional heat and salinity budgets of the Sargasso Sea inferred from two decades of ocean time-series and transect observations. *Ocean Sciences Meeting, San Diego, February 2020.*

Johnson, R.J., Bates, N.R., Hiron, L., Gonçalves, A., and Knap, A.H., 2023a. Surface ocean warming and steric height changes in the Sargasso Sea at Hydrostation S, 1954 to present. *Geophysical Research Letters* (in preparation).

Johnson, R.J., Bates, N.R., Hiron, L., and Knap, A.H., 20213b. Deep water cooling in the Sargasso Sea at Hydrostation S, 1954 to present. *Geophysical Research Letters* (in preparation).

Josey, S.A., and Sinha, B., 2022. Subpolar Atlantic Ocean mixed layer heat content variability driven by an active ocean. *Nature Communications Earth and Environment*, **3**, 111. Joyce, T.M. and Robbins, P., 1996. The Long-Term Hydrographic Record at Bermuda. *Journal of Climate*, **9**, 3121–3131.

Joyce, T.M. and Talley, L., 1996. The Bermuda Hydrostation 'S' – A long-running oceanographic show. *Oceanus*, **39** (2), 14–15.

Joyce, T.M., Deser, C., and Spall, M.A., 2000. The relation between decadal variability of subtropical mode water and the North Atlantic Oscillation. *Journal of Climate*, **13** (14), 2550–2569.

Joyce, T.M., Thomas, L.N., and Bahr, F., 2009. Wintertime observations of subtropical mode water formation within the Gulf Stream. *Geophysical Research Letters*, **36**, 2. https://doi.org/10.1029/2008GL035918

Joyce, T.L. Thomas, N., Dewar, W.K., and Girton J.B., 2013. Eighteen Degree Water formation within the Gulf Stream during CLIMODE. *Deep Sea Research Part II: Topical Studies in Oceanography*, **91**, 1–10.

Klein, P. and Coste, B., 1984. Effects of wind-stress variability on nutrient transport into the mixed layer. *Deep Sea Research*, **31**, 21–37.

Latif, M., Collins M., Pohlmann, H., and Keenlyside, N., 2006. A review of predictability studies of the Atlantic sector climate on decadal time scales, *Journal of Climate*, **19**, 5971-5987. Lenton, T.M., Rockström, J., Gaffney, O., Rahmsdorf, S., Richardson, K., Steffen, W., and Schellnhuber, H.J., 2019. Climate tipping points-too risky to bet against. *Nature*, **575**, 592–595.

Leonelli, F.E., Bellicicco, M., Organelli, E., Buongiorno Nardelli, B., de Toma, V., Cammarota, C., Marullo, S., and Santoleri, R., 2021. Ultra-oligotrophic expansion in the North Atlantic subtropical gyre relvealed by 21 years of satellite observations. *Geophysical Research Letters*, 49, 21, e2021GL096965.

Levin, L.A., and Le Bris, N., 2015. The deep ocean under climate change. *Science*, 350, 766–768 Levitus, S., Antonov, J., Zhou, X., Dooley, H., Selemenov, K. and Tereschenkov, V., 1996. Decadal-Scale Variability of the North Atlantic Ocean. Eds. D.G. Martinson, K. Bryan, M. Ghil, M.M. Hall, T.M. Karl, E.S. Sarachik, S. Sorooshian, and L.D. Talley. Natural Climate Variability on decade-to-century time scales. National Academy of Sciences Press, 318-324. Li, Q.P., McGillicuddy, D.J., Hansell, D.A., Bates, N.R., and Johnson, R.J., 2008. Uncertainty in the biogeochemical impact of a cyclonic eddy in the Sargasso Sea. *Journal of Geophysical Research*, **113**, C10006, doi:10.1029/2008JC004840.

Lima, I. D. and Doney, S.C, 2004. A three-dimensional, multinutrient and size-structured ecosystem model for the North Atlantic. *Global Biogeochemical Cycles* **18**.

Lomas, M.W., Bates, N.R., Buck, K.R., and Knap, A.H., 2011. Oceanography of the Sargasso Sea Overview of Scientific Studies. Sargasso Sea Commission, 94 pp.

Lomas, M.W., Bates, N.R., Johnson, R.J., Knap, A.H, Steinberg, D.K., Carlson, C.A., 2013. Two decades and counting: 23–years of sustained open ocean biogeochemical measurements in the Sargasso Sea. *Deep–Sea Research II*, **93**, 16–32, doi: 10.1016/j.dsr2.2013.01.008.

Lomas, M.W., Bates, N.R., Johnson, R.J., Steinberg, D.K., and Tanioka, T., 2022. Adaptive carbon response to warming in the Sargasso Sea. *Nature Communications*, **13** (1), 1211.

Losa, S.N., Kivman, G.A. and Ryabchenko, V.A. 2004. Weak constraint parameter estimation for a simple ocean ecosystem model: what can we learn about the model and data? *Journal of Marine Systems*, **45**, 1–20.

Lozier, M.S., Roussenov, V., Reed M.S.C, and Williams R.G., 2010. Opposing decadal changes for the North Atlantic meridional overturning Circulation, *Nature Geoscience*, **3**, 728-734.

Lozier, M.S., Dave, A.C., Palter J.B., Gerber, L.M. and Barber, R.T., 2011. On the relationship between stratification and primary productivity in the North Atlantic. *Geophysical Research Letters*, **38**, LI8609, doi:10.1029/2011GL049414.

Lozier, M.S., Gary, S.F., and Bower, A.S., 2013. Simulated pathways of the overflow waters in the North Atlantic: Subpolar to subtropical export. *Deep Sea Research Part II: Topical Studies in Oceanography*, **85**, 147–153. https://doi.org/10.1016/j.dsr2.2012.07.037.

Marsh, R., and New, A.L., 1996. Modeling 18 Degree Water Variability. *Journal of Physical Oceanography*, **26**, 1059–180.

Marshall, J., Andersson, A., Bates, N.R., Dewar, W., Doney, S., Edson, J., Ferrari, R., Fratantoni, D., Gregg, M., Joyce, T., Kelly, K., Lozier, S., Lumpkin, R., Samuelson, R., Skyllingstad, E., Straneo, F., Talley, L., Toole, J., and Weller, R., 2009. Observing the cycle of convection and restratification over the Gulf Stream system and the subtropical gyre of the North Atlantic Ocean: preliminary results from the CLIMODE field campaign. *Bulletin of the American Meteorological Society*, **90**, 1337–1350, doi:10.1175/2009BAMS2706.1, Sep. 2009.

Maze, G., and Marshall, J., 2011. Diagnosing the observed seasonal cycle of Atlantic subtropical mode water using potential vorticity and its attendant theorems. *Journal of Physical Oceanography*, **41**, 1986-1999.

McCarthy, G., Frajka-Williams, E., Johns, W. E., Baringer, M. O., Meinen, C. S., Bryden, H. L., Rayner, D., Duchez, A., Roberts, C. D., and Cunningham, S. A.: Observed Interannual Variability of the Atlantic Meridional Overturning Circulation at 26.5° N. *Geophysical Research Letters*, **39**, L19609, 2012.

McClain, C.R., and Firestone, J.,1993. An investigation of Ekman upwelling in the North Atlantic. *Journal of Geophysical Research*, **98**, 12237–12339.

McGillicuddy, D.J., and Robinson, A.R., 1997. Eddy induced nutrient supply and new production in the Sargasso Sea. *Deep Sea Research*, **44**, 1427–1450.

McGillicuddy, D.J., Robinson, A.R., Siegel, D.A., Jannasch, H.W., Johnson, R.J., Dickey, T.D., McNeil, J., Michaels, A.F., and Knap, A.H., 1998. Influence of mesoscale eddies on new production in the Sargasso Sea. *Nature*, **394**, 263–266.

McGillicuddy, D.J., Johnson, R., Siegel, D.A., Michaels, A.F., Bates, N.R., Knap, A.H., and Michaels, A.F., 1999. Mesoscale variations of biogeochemical properties in the Sargasso Sea. *Journal of Geophysical Research*, **104** (C6), 13,381–13,394, doi: 10.1029/1999JC900021, Jun. 15, 1999.

McGillicuddy, D.J., Anderson, L.A., Bates, N.R., Bibby, T., Buesseler, K.O., Carlson, C.A., Davis, C.S., Ewart, C., Falkowski, P.G., Goldthwait, S.A., Hansell, D.A., Jenkins, W.J., Johnson, R., Kosnyrev, V.K., Ledwell, J.R., Li, Q.P., Siegel, D.A., and Steinberg, D.K., 2007. Eddy/wind interactions stimulate extraordinary mid-ocean plankton blooms. *Science*, 316 (5827), 1016-1021, doi:10.1126/science.1136256.

McGillicuddy DJ Jr. 2016. Mechanisms of Physical-Biological-Biogeochemical Interaction at the Oceanic Mesoscale. Ann Rev Mar Sci. 2016;8:125-59. doi: 10.1146/annurev-marine 010814-015606. Epub 2015 Sep 10. PMID: 26359818.

Menzel, D.W., and Ryther, J.H., 1960. The annual cycle of primary production in the Sargasso Sea off Bermuda. *Deep Sea Research*, **6**, 351–367.

Menzel, D.W., and Ryther, J.H., 1961. Annual variation in primary production of the Sargasso Sea off Bermuda. *Deep Sea Research*, **7**, 282–288.

Michaels, A.F., and Knap, A.H., 1996. Overview of the U.S. JGOFS Bermuda Atlantic Time series Study and the Hydrostation S program. *Deep-Sea Research II*, 43, 2–3, 157–198. Moat, B. I., Smeed, D. A., Frajka-Williams, E., Desbruyères, D. G., Beaulieu, C., Johns, W. E., Rayner, D., Sanchez-Franks, A., Baringer, M. O., Volkov, D., Jackson, L. C., and Bryden, H. L.: Pending recovery in the strength of the meridional overturning circulation at 26° N. *Ocean Sci.*, **16**, 863–874, https://doi.org/10.5194/os-16-863-2020, 2020.

Molinari, R.L., Mayer, D., Festa, J. and Bezdek, H., 1997. Multi-year variability in the near surface temperature structure of the midlatitude western North Atlantic Ocean. *Journal of Geophysical Research*, **102**, 3267–3278.

Nelson, N.B., 1998. Spatial and temporal extent of sea surface temperature modifications by hurricanes in the Sargasso Sea during the 1995 season. *Monthly Weather Rev.*, 126, 1364–1368.

Olsina, O., Wienders, N. Dewar, W.K., 2013. The climatology and variability of Eighteen Degree Water potential vorticity forcing. *Deep-Sea Research. II*, **91**, 84–95. Phillips, H.E. and Joyce T.M., 2007. Bermuda's tale of two time series: Hydrostation 'S' and BATS. *Journal of Physical Oceanography*, **37**, 554–571

Pocklington, R. 1972. Secular changes in ocean off Bermuda. *Journal of Geophysical Research*, **77**, 6604–6637.

Powell, T.M., and Steele, J.H., 2012. *Ecological time series*. Springer Science and Business Media.

Reid, P.C., Fischer, A., Lewis-Brown, E., Meredith, M., Sparrow, M., Andersson, A.J., Antia, A., Bates, N.R., Bathmann, U., Beaugrand, G., Brix, H., Dye, S., Edwards, M., Furevik, T., Gangstø, R., Hátún, H., Hopcroft, R.R., Kendall, M., Kasten, S., Keeling, R., Corinne Le Quéré, C., Mackenzie, F.T., Malin, G., Mauritzen, C., Ólafsson, J., Paull, C., Rignot, E., Shimada, K., Vogt, M., Wallace, C., Wang, Z., and Washington R., 2009. Impacts of the oceans on climate change. **Advances In Marine Biology**, **56**, 1–150, doi: 10.1016/S0065- 2881(09)56001-4.

Rhein, M., Rintoul, S.R., Aoki, S., Campos, E., Chambers, D., Feely, R.A., Gulev, S., Johnson, G.C., Josey, S.R., Kostianoy, A., Mauritzen, C., Roemmich, D., Talley, L.D., and Wang, F., 2013. Observations: Ocean. In: Climate Change 2013: The Physical Science Basis. Contribution of Working Group I to the Fifth Assessment Report of the Intergovernmental Panel on Climate Change [Stocker, T.F., D. Qin, G.-K. Plattner, M. Tignor, S.K. Allen, J. Boschung, A. Nauels, Y. Xia, V. Bex and P.M. Midgley (eds.)]. Cambridge University Press, Cambridge, United Kingdom and New York, NY, USA (N.R. Bates was one of 61 contributing authors).

Richardson, P.L., Cheney, R.E. and Worthington, L.V., 1978. A census of Gulf Stream rings, spring 1975. **Journal of Geophysical Research**, **83**, 6136–6144.

Robbins, P.E., Price, J.F., Owens, W.B., and Jenkins, W.J., 2000. The importance of lateral diffusion for the ventilation of the lower thermocline in the subtropical North Atlantic. *Journal of Physical Oceanography*, **30**, 67–89.

Rossby, T., Flagg, C.N., and Donohue, K., 2005. Interannual variations in upper-ocean transport by the Gulf Stream and adjacent waters between New Jersey and Bermuda. *Journal of Marine Research*, **63**, 203–226.

Rossby, T., Flagg, C.N., Donohue, K., Fontana, S., Curry, R., Andres, M., and Forsyth, J., 2019. *Oleander* is more than a flower: Twenty-five years of oceanography aboard a merchant vessel. *Oceanography*, **32** (3), 126–137.

Rousseau, V., Fraudeau, R., Hammond, M., Houndegnonto, O. J., Ablain, M., Blazquez, A., Calafat, F. M., Desbruyères, D., Foti, G., Llovel, W., Marti, F., Meyssignac, B., Restano, M., and Benveniste, J., 2023. Monitoring the regional Ocean Heat Content change over the Atlantic Ocean with the space geodetic approach, Earth Syst. Sci. Data Discuss. [preprint], https://doi.org/10.5194/essd-2023-236, in review.

Sarmiento, J.L., Slater, R.D., Fasham, M.J.R., Ducklow, H.W., Toggweiler, J.R. and Evans, G.T., 1993. A seasonal 3-dimensional ecosystem model of nitrogen cycling in the North Atlantic euphotic zone. *Global Biogeochemical Cycles*, **7**(2), 417–450.

Schmitz, W.J., 1996. On the World Ocean Circulation: Volume 1 Some Global Features/North Atlantic Circulation. WHOI Technical Report, WHOI-96-03, 141p.

Schroeder, E. and Stommel, H., 1969. How representative is the series of Panulirus stations of monthly mean conditions off Bermuda? *Progress in Oceanography*, **5**, 31–40. Schroeder, E., Stommel, H., Menzel, D.W. and Sutcliffe, W.Jr., 1959. Climatic stability of the eighteen degree water at Bermuda. *Journal of Geophysical Research*, **64** (3):363–366. Shaw, E. and Donn, T., 1964. Sea level variation at Iceland and Bermuda. *Journal of Marine Research*, 22(2), 111–122.

Siegel, D.A., and Deuser, W.G., 1997. Trajectories of sinking particles in the Sargasso Sea: Modelling of "statistical funnels" above deep ocean sediment traps. *Deep Sea Research, I*, **44**, 1519–1541.

Siegel, D.A., McGillicuddy, D.J. and Fields, E.A., 1999. Mesoscale eddies, satellite altimetry and new production in the Sargasso Sea. *Journal of Geophysical Research*, **104**, 13,359–13,379.

Siemer, J.P., Machín, F., González-Vega, A., Arrieta, J.J., Gutiérrez-Guerra, M.A., Pérez Hernández, M.D., Vélez-Belchí, P., Hernández-Guerra, A., and Fraile-Nuez, E., 2021. Recent trends in SST, Chl-*a*, productivity and wind stress in upwelling and open ocean areas in the upper eastern North Atlantic subtropical gyre. *Journal of Geophysical Research Oceans*, **126**, 8, e2021JC017268.

Smeed, D. A., McCarthy, G. D., Cunningham, S. A., Frajka-Williams, E., Rayner, D., Johns, W. E., Meinen, C. S., Baringer, M. O., Moat, B. I., Duchez, A., and Bryden, H. L.: Observed decline of the Atlantic meridional overturning circulation 2004–2012, *Ocean Sci.*, **10**, 29–38.

Smeed, D. A., Josey, S., Johns, W., Moat, B., Frajka-Williams, E., Rayner, D., Meinen, C., Baringer, M., Bryden, H., and McCarthy, G.: The North Atlantic Ocean is in a state of reduced overturning. *Geophysical Research Letters*, **45**, 1527–1533, 2018.

Sprintall, J., and Tomczak, M., 1992. Evidence of the barrier layer in the surface layer of the tropics. *Journal of Geophysical Research*, **97**, 7305–7316.

Stevens, S.W., Johnson, R.J., Maze, G., and Bates, N.R. 2020. A recent decline in North Atlantic subtropical mode water formation. *Nature Climate Change*, **10** (4), 335–341.

Stramska, M., 2010. The diffusive component of particulate organic carbon export in the North Atlantic estimated from SeaWiFS ocean color. *Deep-Sea Res., I*, 57, 284–296.

Talley, L.D., 1996. North Atlantic Circulation and Variability, Reviewed for the CNLS conference *Physica D.*, **98**, 625–646.

Talley, L.D. and Raymer, M.E., 1982. Eighteen Degree Water Variability. *Journal of Marine Research*, **40**, 757–775.

Toole, J., Curry, R., Joyce, T., McCartney, M., and Peña-Molino, B., 2011. Transport of the North Atlantic Deep Western Boundary Current about 39°N, 70°W: 2004–2008, Deep Sea Research Part II, 58, 1768–1780.

Villarino, E., Irigoien, X., Villate, F., Iriate, A., Uriate, I., Zervoudaki, S., Carstensen, J., O'Brien, T., and Chust, G., (2020). Response of copepod communities to ocean warming in three time-series across the North Atlantic and Mediterranean Sea. *Marine Ecology Progress Series*, 636, 47–61.

Volk, T. and Hoffert, M.I., 1985. Ocean carbon pumps: analysis of relative strengths and efficiencies in ocean-driven atmospheric CO_2 changes. In *The Carbon Cycle and Atmosphere CO_2: Natural variations Archeaan to Present* (Sundquist, E.T. and Broecker, W.S., Eds.) American Geophysical Union, *Geophysical Monograph* 32, Washington D.C., 99–110.

Whitefield, J.D., Johnson, R.J. and Knap A.H., 2008. Deep water variability at the Bermuda Timeseries Sites. *Ocean Sciences meeting, Orlando 2008* (poster presentation). Worthington, L.V., 1976. On the North Atlantic circulation. *The John Hopkins Oceanography Studies*, **6**, 1–110.

Wunsch, C., 1972a. The spectrum from two years to two minutes of temperature fluctuations in the main thermocline at Bermuda. *Deep Sea Research*, **19**, 577–593.

Wunsch, C. 1972b. Bermuda sea level in relation to tides, weather and baroclinic fluctuations. *Rev. Geophysical Space Physics*, **10** (1), 1–49.

Wunsch, C., 1981. Low frequency variability of the sea. Chapter 11. *In*: Evolution of Physical Oceanography, B. Warren and C. Wunsch. ed. MIT Press. Cambridge.

Wunsch, C., and Heimbach, P., 2006. Estimated Decadal Changes in the North Atlantic meridional overturning circulation and heat flux 1993–2004. *Journal of Physical Oceanography*, **36**, 2012–2024.

CHAPTER 3

Chemical oceanography of the Sargasso Sea

D.S. Grundle, N.R. Bates, S. Murdock and R.J. Johnson

3.1 Nutrients in the Sargasso Sea

D.S. Grundle and N.R. Bates

The basic hydrographic properties of seawater, temperature and salinity control the density of seawater and, ultimately, vertical exchange processes in the global ocean. This control of vertical exchange has essential implications for the Sargasso Sea, as deeper ocean waters contain the nutrients required to support the surface sunlit ocean ecosystem.

3.1.1 *Nutrient cycling in the Sargasso Sea.*

The global ocean nutrient cycles supporting the marine food web also appear to be impacted by human activities, climate-related physical processes, and a dynamic marine nitrogen and phosphorus cycle. For example, the inputs of anthropogenic nutrients to the coastal ocean (e.g., Galloway *et al.*, 2008) and fixed nitrogen to the open ocean (via atmospheric deposition) are expected to increase (e.g., Duce *et al.*, 2008; Seitzinger *et al.*, 2010). Ocean warming appears to be increasing the stratification of the surface ocean, potentially reducing nutrient supply and the rates of phytoplankton primary production globally (Boyce *et al.*, 2010). However, there are complex and counteracting processes that control the physical supply of nutrients to the surface ocean, thereby influencing the global ocean nutrient cycles (e.g., Williams *et al.*, 2006; Cianca *et al.*, 2007; Wong *et al.*, 2007; Di Lorenzo *et al.*, 2009; Steinhoff *et al.*, 2010; Canfield et al., 2010). The marine nitrogen cycle is very dynamic, with, for example, complex linkages between eutrophication, nutrients and carbon (e.g., Chen and Borges, 2009; Borges and Gypens, 2010). Recent studies in the Sargasso Sea indicate that the potential rate of nitrification (i.e., the biological oxidation of ammonia to nitrate) is declining with ocean acidification (Beman *et al.*, 2011), while the significance of oceanic nitrogen fixation, especially in the Sargasso Sea, is highly debated (e.g., Michaels *et al.*, 1996; Gruber and Sarmiento, 1997; Hansell *et al.*, 2004; Bates and Hansell 2004; Hansell *et al.*, 2008; Gruber, 2008; Singh *et al.*, 2013).

Many of these atmospheric processes impact one nutrient biogeochemical cycle, nitrogen or phosphorus, more than the other, resulting in potentially large deviations from the canonical Redfield Ratio, which defines not only the relative concentrations of inorganic nitrate and phosphate in the deep ocean but also which nutrient limits primary production. The Sargasso Sea is already characterized by a ratio of inorganic nitrate and phosphate much higher than the canonical Redfield Ratio (Singh *et al.*, 2013). However, the response of phytoplankton and their control over this ratio of available nutrients is currently being challenged (e.g., Mills and Arrigo, 2010). Anthropogenic modifications of the global biogeochemical cycles of nitrogen and sulphur have led to acidic deposition from the atmosphere, which has affected sensitive terrestrial and ocean ecosystems (e.g., Farrell, 1995; Rodhe *et al.*, 2002; Bouwman *et al.*, 2003; Holland *et al.*, 2005; Lamarque *et al.*, 2005; Dentener *et al.*, 2006; Doney *et al.*, 2007). In those regions with acid deposition, industrial emissions of sulfur and nitrogen compounds (e.g., North America, Europe and East Asia) or intensive agricultural practices contribute to the acidity of rainwater with pH typically ranging from about 4 to 6 (e.g., Rodhe *et al.*, 2002).

If nitrogen is the primary limiting nutrient for primary production in the Sargasso Sea, 'new nitrogen' availability from upwelled nitrate or nitrogen fixation should regulate export production, the principal route for marine carbon export via the biological pump (Stanley *et al.*, 2015). Nitrate is considered to be the predominant form of new nitrogen in the ocean, owing to the assumption that nitrification only occurs in the aphotic regions of the water column (Horrigan *et al.*, 1981; Peng *et al.*, 2018; Schön and Engel 1962; Shiozaki *et al.*, 2019). In more recent years, however, nitrification has been shown to occur in the euphotic zone of several coastal and oceanic regions (e.g., Dore and Karl, 1996; Grundle and Juniper, 2011; Grundle *et al.*, 2013; Wankel et al., 2007, Ward 1987), including the Sargasso Sea (Grundle unpublished). This suggests that not all nitrate in the euphotic zone should be considered as supporting export production and that measures of new production arising from nitrate

uptake by phytoplankton have likely been overestimated. However, this overestimate depends on the importance of euphotic zone nitrification in a given location.

Time-series measurements in the Sargasso Sea, starting with Hydrostation S (1954) and later with the Bermuda Atlantic Time-series Station (BATS; 1988), have played a critical role in our understanding of new production in the subtropical ocean regions (Lipschultz et al. 2002). Indeed, Hydrostation S served as one of the sampling stations for the first measurements of ^{15}N NO_3^- uptake rates (Dugdale and Georing 1967). This led Lipschultz *et al.* (2002) to describe the concept of new production as being "intimately tied" to the Sargasso Sea. Natural variations in the nitrogen and oxygen isotopes of nitrate indicate that nitrification is not an essential process in the euphotic zone of the Sargasso Sea and, therefore, nitrate assimilation rates remain a valuable approximation of organic carbon export in this location (Fawcett *et al.*, 2015). Nitrogen-fixing organisms, which convert atmospheric N_2 to bioavailable ammonium, have also been identified as potentially significant and underestimated contributors to global carbon export (Bonnet *et al*., 2023). This may be crucial in nitrogen-limited regions like the Sargasso Sea. Estimates of nitrogen fixation in the Sargasso Sea range from 44 to 95 mmol N m^{-2} $year^{-1}$ (Bates and Hansell, 2004; Singh *et al.*, 2013).

3.1.2 *Atmospheric deposition of nitrogen.*

The Sargasso Sea is downwind of pollution sources from the North American continent and consequently experiences acid deposition with rainfall pH levels typically ranging from about 4.4 to 5.6 (Jickells *et al.*, 1982; Bates and Peters, 2007). Early studies of atmospheric deposition of nitrogen or sulphur were focused on the contributions from H_2SO_4, HNO_3, $CaCO_3$, organic acids, soil dust and reduced and oxidized sulfur and nitrogen compounds to the acidity of wet deposition (e.g., Keene and Galloway, 1988; Whelpdale *et al.*, 1996). The pH and chemical composition of rainwater have been monitored on the island of Bermuda since the early 1980s (Jickells *et al.*, 1982; Galloway *et al.*, 1993; Chen and Siefert, 2004), initially as part of the Western Atlantic-Ocean Experiment (WATOX; Galloway *et al.*, 1987 and Atmosphere-Ocean Chemistry Experiments (AEROCE; Huang *et al.*, 1996) projects. AEROCE was a multi disciplinary collaborative program focused on the North Atlantic Ocean region's linked atmospheric and marine chemical processes. Under this initiative, several atmospheric research towers were constructed at critical sites in the North Atlantic Ocean region, including a 23 m tower completed in 1988 at Tudor Hill, Bermuda. This facility was used for daily sampling of gases, aerosol and precipitation for over a decade and continues to be maintained and used as a research facility.

The results of the AEROCE program were summarized by Prospero (2001). Some of the key findings relevant to the Sargasso Sea include: (1) seasonal cycles in aerosol pollutants in Bermuda are determined more by the speed and duration of atmospheric transport than by strength of source emissions (e.g., Moody *et al.*, 1995; Huang *et al.*, 1999; Nevison *et al.*, 2003, 2013; Dadashazar *et al.*, 2021; Menzel-Barraqueta, 2019; Xiu *et al.*, 2021); (2) anthropogenic sources contribute a significant amount to the atmospheric loadings of sulphur and nitrogen species (e.g., Savoie *et al.*, 1992); (3) sea-salt aerosol is a significant reaction medium and sink for sulphur and nitrogen species over the North Atlantic Ocean (e.g., Keene *et al.*, 1998, 2014); (4) records of deposition of African dust to the Sargasso Sea were consistent with loadings of atmospheric dust observed at Bermuda, and annual variations in sediment trap fluxes were linked to changes in atmospheric transport rather than source strength (Jickells *et al.*, 1998); and; (5) mineral dust is the dominant light scattering aerosol over a large part of the tropical and subtropical North Atlantic Ocean (e.g., Maring *et al.*, 2000).

Atmospheric deposition of nitrogen species also can support ocean primary production, although it varies widely by ocean region (e.g., Jickells *et al.*, 1989; Paerl, 1997; de Leeuw *et al.*, 2003; Hastings *et al.*, 2003; Spokes and Jickells, 2005; Boulart *et al.*, 2006; Jickells, 2006). Annual rates of primary production at BATS are typically ~150 g C m^{-2} $year^{-1}$ (Steinberg *et al.*, 2001; Lomas *et al.*, 2013), and the amount supported by atmospheric nitrogen deposition is typically insignificant (0.2–0.5%) except potentially for rare high rainfall events (e.g., Knap *et al.*, 1986; Fanning, 1989; Owens *et al.*, 1992; Michaels *et al.*, 1993; Altieri *et al.*, 2014, 2016). However, future changes in atmospheric nitrogen deposition (e.g., Duce *et al.* 2008), coupled with the long-term reductions in nutrient supply from below and changes in nitrogen fixation (Sarmiento and Gruber, 1997), might enhance this mechanism supporting oceanic primary production. In terms of supporting primary production, atmospheric iron inputs are perhaps more critical than atmospheric nitrogen deposition, which keeps the Sargasso Sea replete with a biologically important trace metal (Sedwick *et al.*, 2007).

3.2 Dissolved oxygen in the Sargasso Sea

N.R. Bates and R.J. Johnson

Since the late 1980s, waters in this subtropical region of the North Atlantic Ocean have lost oxygen at a rate of ~2% per decade (~8% over the past 40 years; Bates and Johnson, 2020). The trends of declining DO at Hydrostation S over the past 60 years, and especially over the past 30 years, are slightly lower than the range of global ocean deoxygenation of ~0.3 to ~0.7 µmoles kg^{1} year^{-1} in the thermocline (e.g., Keeling *et al.* 2010; Helm *et al.*, 2011; Stendardo and Gruber, 2012). While ocean warming has likely contributed to overall deoxygenation by decreasing oxygen solubility, in the North Atlantic subtropical gyre, contemporaneous increases in biological productivity have partially offset these DO losses.

Physico-chemical changes over the past forty years in the Sargasso Sea have also resulted in the loss of dissolved oxygen (i.e., ocean deoxygenation), higher than other areas in the globalocean (Bates and Johnson, 2020). The upper-ocean record of DO shows an overall decline of ~17.8 ± 2.4 µmoles kg^{-1} (-0.37 µmoles kg^{-1} yr^{-1}) over the past 40 years (Bates and Johnson), with short-term year-to-year variability (Figure 3.1). The longer-term

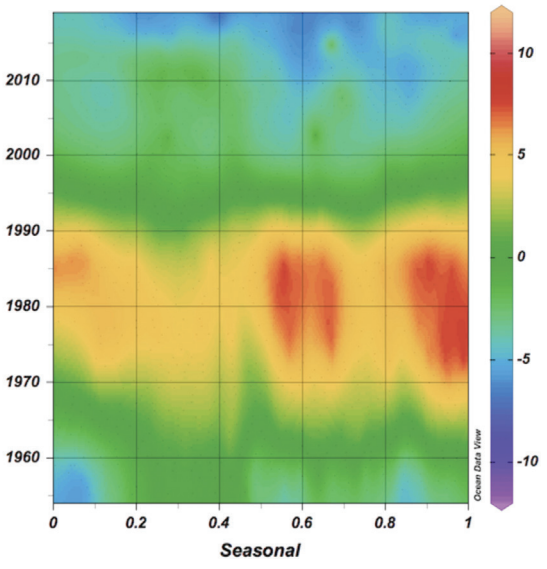

FIGURE 3.1. Contour plots of surface dissolved oxygen anomalies for Hydrostation 'S' from 1955 through December 2020. Almost identical dissolved oxygen changes are shown at the BATS site from 1983 to end of 2020. DO data prior to 1958 is not included due to changes in DO methods after the International Geophysical Year (IGY). Credit: R.J. Johnson, ASU-BIOS.

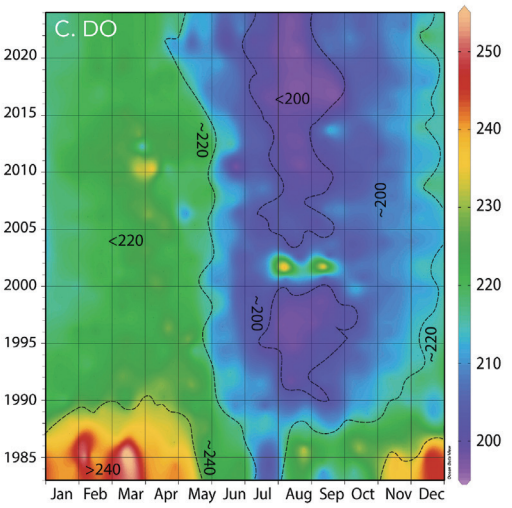

FIGURE 3.2. Hovmuller contour plot of surface dissolved oxygen anomalies for the BATS site from 1983 to 2023. Credit: Bates and Johnson, 2023.

data represents a loss of DO of ~8.1% or ~2% per decade. The trend of DO decline in the Sargasso Sea since the 1980s is in the range shown for global ocean deoxygenation (ODO) rates of ~0.3 to ~0.7 µmoles kg^{-1}year^{-1} (~3– 7 µmoles kg^{-1} decade^{-1}) in the thermocline (Stendardo *et al.*, 2012; Cianca *et al.*, 2013; Stendardo *et al.*, 2015, 2016; Montes *et al.*, 2016). Apparent oxygen utilisation (AOU), as a calculated parameter (Garcia and Gordon, 1992), offers a few clues as it reflects changes in oxygen due to the combined effect of biological processes such as primary production and respiration but also diffusion, circulation, and ventilation (Stramma and Schmidtko, 2019). The trend in AOU in the upper 500 m is about -0.54 µmoles kg^{-1} year^{-1}, slightly higher than the contemporaneous decrease in DO. As with temperature and salinity changes, several decades were notable with significant loss of oxygen (-30.2 and -17.6 µmoles kg^{-1} decade^{-1}) accompanying "*warming*" decades. The 1990s and 2000s had only slight changes in surface oxygen (Bates and Johnson, 2020) associated with "*cooling*" decades.

The cause for deoxygenation of the Sargasso Sea over the past 40 years appears only partly due to solubility changes associated with warming (Bates and Johnson, 2020; the contribution of nitrification and denitrification to AOU is considered minor in surface waters). Given the ocean warming observed in the Sargasso Sea, the warming impact on DO solubility would likely have contributed to about 13% of the total decline of DO over the past nearly 40 years (Figure 3.2). The remaining deoxygenation (~87%) must result from the combined effect of

ocean biology and physics changes. Recent warming in the 2010s of +1.18°C contributed about 18% of the concurrent decline in DO in that decade.

Although the Sargasso Sea is characteristically well-oxygenated, a persistent zone of decreased oxygen (approximately 14-28% lower than mixed layer oxygen values and 31-42% lower than oxygen values below 1500 m) exists between 500-1000 m depth at the BATS site. It is expanding in vertical extent (Figure 3.2).

3.3 Nitrous oxide in the Sargasso Sea

D.S. Grundle and S.A. Murdock

Dissolved oxygen (DO) concentrations play a crucial role in determining the favorability of microbial nitrogen cycling processes (Berman-Frank *et al.*, 2008), including those that produce nitrous oxide (N_2O), a potent greenhouse and ozone-destroying gas. Atmospheric levels of nitrous oxide have steadily increased in recent decades (Prinn *et al.*, 2018; Ravishankara *et al.*, 2009), and current estimates are that one-quarter to one-third of naturally produced N_2O flux to the atmosphere comes from open ocean regions (Tian *et al.*, 2020). Nitrogen cycling processes that generate N_2O primarily occur under low DO, while those that consume N_2O occur under anoxic conditions, making understanding the effects of increasing ocean deoxygenation on N_2O production a growing area of research. Most marine N_2O is produced within stable oxygen deficient zones (ODZ) in, for example, highly productive eastern boundary upwelling regions in the Pacific, Atlantic, and Arabian Sea (e.g., Ji *et al.*, 2019; Wright *et al.*, 2012) and low oxygen mesoscale eddies (Grundle *et al.*, 2011). Conditions in the cores of ODZs where minimal amounts of oxygen remain present (~5-10 µmol O_2 L^{-1}; Grundle *et al.*, 2017) are ideal for N_2O production via anaerobic processes like denitrification. At the same time, oxic and hypoxic boundaries favour N_2O formation as a byproduct of nitrification, with nitrification derived N_2O increasing substantially below ~20 µmol O_2 L^{-1}. Although the Sargasso Sea is characteristically well-oxygenated (>180 µM O_2), a band of decreased DO between 500-1000 meters depth has increased potential to promote N_2O-producing processes as ocean deoxygenation intensifies.

To provide baseline data on N_2O in the Sargasso Sea, Meyer *et al.* (2022) reported BATS station N_2O distributions and yields from the oxic process of nitrification, from the surface down to 4500 m depth and estimated air-sea fluxes. The highest reported N_2O concentrations coincided with the zone of lowest oxygen (~ 150 µmol L^{-1}) during the September to November 2018 and June 2019 cruises. Concentrations were in the same order as those measured elsewhere in the North Atlantic (10-20 nmol L^{-1}; Ji and Ward 2017; Nevison *et al.* 2003) but generally lower than those measured in the tropical Atlantic and Pacific (25-200 nmol L^{-1}; Babbin *et al.* 2015; Frame *et al.* 2014; Grundle *et al.* 2017; Ji *et al.* 2019; Kelly *et al.* 2021; Nevison *et al.* 2003). N_2O in the mixed layer (upper 35-70 m for the four months sampled) ranged from being mostly undersaturated, a net sink for atmospheric N_2O, to slightly supersaturated, a weak source of N_2O to the atmosphere. N_2O in deeper waters, below the peak in the low oxygen zone, remained relatively stable at 10-12 nmol L^{-1}. Besides flux to the atmosphere, microbial reduction to N_2 is the only known mechanism for removing marine N_2O. Because this microbial process is oxygen sensitive, the oxic-deep Sargasso Sea retains N_2O. However, this deep N_2O may become available for atmospheric flux during eddy-induced upwelling. While N_2O data from the BATS station is not amenable to making gyre-wide conclusions, this long-standing time-series location does offer an opportunity to track changes in N_2O concentrations and fluxes with the steady decline in oxygen (see section 3.2) and vertical expansion of the oxygen minimum zone (see section 3.2).

3.4 Rare earth elements in the Sargasso Sea

D.S. Grundle and S.A. Murdock

Methane, another potent greenhouse gas, supports a marine microbial community of methanotrophic organisms that play a vital role in the global carbon cycle (Khmelenina *et al.*, 2018). Low levels of methane in the Sargasso Sea (1-3 nmol L^{-1}) (Jones 1991) indicate the need for novel techniques to study microbial methane cycling in this region. Meyer et al. (2021) capitalize on the requirement for rare earth elements (REE) by some aerobic bacterial methanotrophs (Keltjens *et al.*, 2014; Pol *et al.*, 2014) to investigate REE molar ratios as possible biosignatures of methane oxidation. In a commonly expressed form of methanol dehydrogenase, an enzyme used in the bacterial methane oxidation pathway, a REE acts as a cofactor on the enzyme's active site (Picone and Op den Camp, 2019). The REE cofactors observed are lanthanides with an atomic mass <147, called light REEs (LREE). Thus, in the first full-depth profile (24 depths, surface to 5 m above the seafloor) of REE concentrations at the BATS site, Meyer *et al.* (2021) measured light and

heavy (HREE; lanthanides with atomic mass ≥ 147) REEs, under the assumption that depletion of LREE relative to HREE could act as an indicator of methanotrophic activity.

Ocean REE concentrations exhibited three different profile types: 1) HREEs varied little with depth, except for a minimum roughly coinciding with the deep chlorophyll maximum, likely indicative of scavenging onto particles. 2) Surface LREE concentrations were high relative to HREEs, with a minimum value between 200-500 m depth and a slow increase to maximum levels in the deep. 3) The LREE cerium expressed a unique depth profile, with the highest values at the surface, a minimum near the top of the OMZ, and a slight increase with depth below. The depleted LREE: HREE ratio between 200-500 m also coincided with successful culturing on growth media with single-carbon compounds as the sole carbon source, indicating an active community of methane-oxidizing microbes at these depths. Meyer *et al.* (2021) recommend additional measurements across regions and seasons to build on the success of this first use of REE molar ratios as indicators of methane oxidation.

3.5 References

Altieri, K.E., Hastings, M.G., Peters, A.J., Oleynik, S., and Sigman, D.M., 2014. Isotopic evidence for a marine ammonium source in rainwater at Bermuda. *Global Biogeochemical Cycles*, 28 (10), 1066–1080.

Altieri, K.E., Fawcett, S.E., Peters, A.J., and Hastings, M.G., 2016. Marine biogenic source of atmospheric organic nitrogen in the subtropical North Atlantic. *Earth, Atmosphere, and Planetary Sciences*, 113 (4), 925–930.

Babbin, A.R., Bianchi, D., Jayakumar, A., and Ward, B.B., 2015. Rapid nitrous oxide cycling in the suboxic ocean. *Science* **348**, 1127–1129.

Bates, N.R., and Hansell, D.A., 2004. Temporal variability of excess nitrate in the subtropical mode water of the North Atlantic Ocean. *Marine Chemistry*, 84 (3–4), 225–241, doi:10.1016/j.marchem.2003.08.003, Jan. 2004.

Bates, N.R., and Johnson, R.J. 2020. Acceleration of ocean warming, salinification, deoxygenation and acidification in the surface subtropical North Atlantic Ocean. *Nature Communications in Earth and Environment*, **1**, 33.

Bates, N.R., and Peters, A.J., 2007. The contribution of atmospheric acid deposition to ocean acidification in the subtropical North Atlantic Ocean. *Marine Chemistry*, **107** (4), 547–558, doi:10.1016/j.marchem.2007.08.002.

Beman, J.M., Chow, C.-E., King, A.L., Feng, Y., Fuhrman, J.A., Andersson, A., Bates, N.R., Popp, B.N., and Hutchins, D.A., 2011. Global declines in oceanic nitrification rates as a consequence of ocean acidification. Proceedings of the National Academy of Sciences, 108: 208–213.

Berman-Frank, I., Chen, Y-B., Gao, Y., Fennel, K., Follows, M.J., Milligan, A.J. *et al.*, 2008. Chapter 35. *Feedbacks Between the Nitrogen, Carbon and Oxygen Cycles*. In: Capone D.G., Bronk D.A., Mulholland M.R., and Carpenter E.J. (eds). *Nitrogen in the Marine Environment (Second Edition)*. Academic Press: San Diego. pp 1537–1563.

Bonnet, S., Benavides, M., Le Moigne, F.A.C., Camps, M., Torremocha, A., Grosso O., *et al.* 2023. Diazotrophs are overlooked contributors to carbon and nitrogen export to the deep ocean. *The ISME Journal 17*: 47–58.

Borges, A.V. and Gypens, M., 2010: Carbonate chemistry in the coastal zone responds more strongly to eutrophication than ocean acidification. Limnology Oceanography, 55, 346–353. Boulart, C., Flament, P., Gentilhomme, V., Deboudt, K., Migon, C., Lizon, F., Schapira, M., and Lefebvre, A., 2006. Atmospherically-promoted photosynthetic activity in a well-mixed ecosystem: significance of wet deposition events of nitrogen compounds. *Estuarine, Coastal and Shelf Science*, **69** (3–4), 449–458.

Bouwman, A.F., Van Vuuren, D.P., Derwent, R.G., and Posch, M., 2003. A global analysis of acidification and eutrophication of terrestrial ecosystems. *Water, Air and Soil Pollution*, **141** (1–4), 349–382.

Boyce, D.G., Lewis, M.R., and Worm, B., 2010. Global phytoplankton decline over the past century. *Nature*, **466**, 591–596.

Canfield, D.E., Glazer, A.N., and Falkowski, P.G., 2010. The evolution and future of Earth's nitrogen cycle. *Science*, **330**, 192–196.

Chen, C.T.A., and Borges, A.V., 2009. Reconciling opposing views on carbon cycling in the coastal ocean: continental shelves as sinks and near-shore ecosystems as sources of atmospheric CO_2. *Deep-Sea Research II*, **56**, 578–590.

Chen, L., and Siefert, R. L., 2004. Seasonal and spatial distribution and dry deposition fluxes of atmospheric total and labile iron over the tropical and subtropical North Atlantic Ocean. *Journal of Geophysical Research*, **109**, D09305.

Cianca, A., Helmke, P., Mouriño, B., Rueda, M. J., Llinás, O., and Neuer, S., 2007. Decadal analysis of hydrography and in situ nutrient budgets in the western and eastern North Atlantic subtropical gyre. *Journal of Geophysical Research*, **112**, C07025.

Cianca, A., Santana, R., Hartman, S.E., Martin–Gonzalez, J.M., Gonzalez–Davila, M., Rueda, M.J., Llinas, O., and Neuer, S., 2013. Oxygen dynamics in the North Atlantic subtropical gyre. *Deep Sea Research*, **93**, 135–147.

The CLIMODE Group (Marshall, J., Andersson, A., Bates, N., Dewar, W., Doney, S., Edson, J., Ferrari, R., Fratantoni, D., Gregg, M., Joyce, T., Kelly, K., Lozier, S., Lumpkin, R., Samuelson, R., Skyllingstad, E., Straneo, F., Talley, L., Toole, J., and Weller, R., 2009. Observing the cycle of convection and restratification over the Gulf Stream system and the subtropical gyre of the North Atlantic Ocean: preliminary results from the CLIMODE field campaign. *Bulletin of the American Meteorological Society*, September, 2009, 1337–1350, doi:10.1175/2009BAMS2706.1.

de Leeuw, G., Spokes, L., Jickells, T., Skjoth, C.A., Hertel, O., Vignati, E., Tamm, S., Schulz, M., Sorensen, L.L., Pedersen, B., Klein, L., and Schlunzen, K.H., 2003. Atmospheric nitrogen inputs into the North Sea: effect on productivity. *Continental Shelf Research*, **23** (17–19), 1743–1755.

Dadashazar, H., Painemal, D., Alipanah, M., Brunke, M., Chellappan, S., Corral, A.F., Crosbie, E., Kirschler, S., Liu, H., Moore, R.H., Robinson, C., Scarino, A.J., Shook, M., Sinclair, K., Thornhill, K.L., Voigt, C., Wang, H., Winstead, E., Zeng, X., Ziemba, L., Zuidema, P., and Sorooshian, A., 2021. Cloud drop number concentrations over the western North Atlantic Ocean: seasonal cycle, aerosol interrelationships, and other influential factors. *Atmospheric Chemistry and Physics*, **21** (3), 10499–10526.

Dentener, F., Drevet, J., Lamarque, J.F., Bey, I., Eickhout, B., Fiore, A.M., Hauglustaine, D., Horowitz, L.W., Krol, M., Kulshrestha, U.C., Lawrence, M., Galy-Lacaux, C., Rast, S., Shindell, D., Stevenson, D., Van Noije, T., Atherton, C., Bell, N., Bergman, D., Butler, T., Cofala, J., Collins, B., Doherty, R., Ellingsen, K.K., Galloway, J., Gauss, M., Montanaro, V.,Muller, J.F., Pitari, G., Rodriguez, J., Sanderson, M., Solmon, F., Strahan, S., Schultz, M., Sudo, K., Szopa, S., Wild, O., 2006. Nitrogen and sulfur deposition on regional and global scales: a multimodel evaluation. *Global Biogeochemical Cycles*, **20** (4), GB4003. doi:10.1029/2005GB002672.

Di Lorenzo, E., Cobb, K.M., Furtado, J.C., Schneider, N., Anderson, B.T., Bracco, A., Alexander, M.A., and Vimont, D.J., 2009. Nutrient and salinity decadal variations in the central and eastern North Pacific. *Geophysical Research Letters*, **36**, L14601, doi:10.1029/2009GL038261.

Doney, S.C., Mahowald, N., Lima, I., Feely, R.A., Mackenzie, F.T., Lamarque, J.-F., and Rasch, P.J., 2007. The impact of anthropogenic atmospheric nitrogen and sulfur deposition on ocean acidification and the inorganic carbon system. *Proceedings of the National Academy of Sciences*, **104** (37), 14580–14585.

Dore, J.E., and Karl, D.M., 1996. Nitrification in the euphotic zone as a source for nitrite, nitrate, and nitrous oxide at Station ALOHA. *Limnology and Oceanography* **41**, 1619–1628.

Duce, R.A., LaRoche, J., Altieri, K., Arrigo, K.R., Baker, A.R., Capone, D.G., Cornell, S., Dentener, F., Galloway, J., Ganeshram, R.S., Geider, R.J., Jickells, T., Kuypers, M.M., Langlois, R., Liss, P.S., Liu, S.M., Middelburg, J.J., Moore, C.M., Nickovic, S., oschlies, A., Pedersen, T., Prospero, J., Schlitzer, R., Seitzinger, S., Sorensen L.L., Uematsu, M.,Ulloa, O., Voss, M., Ward, B., and Samora, L., 2008, Impacts of atmospheric anthropogenic nitrogen on the open ocean. *Science*, **320**, 893-897. doi: 10.1126/science.1150369**.**

Fanning, K.A., 1989. Influence of atmospheric pollution on nutrient limitation in the ocean. *Nature*, **339** (6224), 460–463.

Farrell, E.P., 1995. Atmospheric deposition in maritime environments and its impact on terrestrial ecosystems. *Water, Air and Soil Pollution*, **85** (1), 123–130.

Fawcett, S.E., Ward, B.B., Lomas, M.W., and Sigman, D.M., 2015. Vertical decoupling of nitrate assimilation and nitrification in the Sargasso Sea. *Deep Sea Research Part I: Oceanographic Research Papers* **103**, 64–72.

Frame, C.H., Deal, E., Nevison, C.D., and Casciotti, K.L., 2014. N_2O production in the eastern South Atlantic: Analysis of N_2O stable isotopic and concentration data. *Global Biogeochemical Cycles* **28**, 1262–1278.

Galloway, J.N., Church, T.M., Knap, A.H., Whelpdale, D.M., and Miller, J.M., 1987. The Western Atlantic-Ocean Experiment. ACS Symposium Series, **349**, 39–55.

Galloway, J.N., Savoie, D.L., Keene, W.C., and Wilson, P.A., 1993. The temporal and spatial variability of scavenging ratios for NSS sulphate, nitrate, methanesulfonate and sodium in the atmosphere over the North-Atlantic Ocean. *Atmospheric Environment Part A– General Topics*, **27** (2), 235–250.

Galloway, J.N., Townsend, A.R., Erisman, J.W., Bekunda, M., Cai, Z.C., Freney, F.R., Martinelli, L.A., Sietzinger, S.P., and Sutton, M.A., 2008. Transformation of the nitrogen cycle: Recent trends, questions, and potential solutions. *Science*, **320**, 889–892, doi: 10.1126/science.1136674.

Garcia, H.E., and Gordon, L.I., 1992. Oxygen solubility in seawater: Better fitting equations. *Limnology and Oceanography*, **37** (6), 1307–1312.

Gruber, N., 2008. The marine nitrogen cycle: overview and challenges. In *Nitrogen in the Marine Environment*, (Capone, D.G., D.A. Bronk, M.R. Mulholland, E.J. Carpenter, eds.) Academic, Burlington, MA pp. 1–50.

Gruber, N., and Sarmiento, J.L., 1997. Global patterns of marine nitrogen fixation and denitrification. *Global Biogeochemical Cycles*, **11**, 235–266.

Grundle, D.S., and Juniper, S.K., 2011. Nitrification from the lower euphotic zone to the sub oxic waters of a highly productive British Columbia fjord. *Marine Chemistry*, **126**, 173–181.

Grundle, D.S., Juniper, S.K., and Giesbrecht, K.E., 2013. Euphotic zone nitrification in the NE subarctic Pacific: Implications for measurements of new production. *Marine Chemistry*, **155**, 113–123.

Grundle, D.S., Löscher, C., Krahmann, G., Altabet, M.A., Bange, H.W., Karstensen, J., Körtzinger, A., and Fiedler, B., 2017. Low oxygen eddies in the eastern tropical North Atlantic: Implications for N_2O cycling. *Scientific Reports*, **7** (1), 4806.

Hansell, D.A., Bates, N.R., and Olson, D.B., 2004. Excess nitrate and nitrogen fixation in the North Atlantic Ocean. *Marine Chemistry*, **84**, 243–265.

Hansell, D.A., Olson, D.B., Dentener, F., and Zamora, L.M., 2008. Assessment of excess nitrate development in the subtropical North Atlantic. *Marine Chemistry*, **106**, 562–579.

Helm, K.P., Bindoff, N.L., and Church, J.A., 2011. Observed decreases in oxygen content of the global ocean. *Geophysical Research Letters*, https://doi.org/10.1029/2011GL049513.

Hastings, M.G., Sigman, D.M., and Lipschultz, F., 2003. Isotopic evidence for source changes of nitrate in rain at Bermuda. *Journal of Geophysical Research*, **108**, ACH4790.

Holland, E.A., Braswell, B.H., Sulzman, J., and Lamarque, J.F., 2005. Nitrogen deposition onto the United States and Western Europe: synthesis of observations and models. *Ecological Applications*, **15** (1), 38–57.

Horrigan S.G., Carlucci A.F., and Williams, P.M., 1981. Light inhibition of nitrification in sea surface films. *Journal of Marine Research*.

Huang, S.L., Arimoto, R., and Rahn, K.A., 1996. Changes in atmospheric lead and other pollution elements at Bermuda. *Journal of Geophysical Research [Atmospheres]*, **101** (D15), 21033–21040.

Huang, S., Rahn, K.A., Arimoto, R., Graustein, W.C., and Turekian, K.K., 1999. Semiannual cycles of pollution at Bermuda. *Journal of Geophysical Research*, **104**, 30309–30318.

Ji., Q, and Ward, B.B., 2017. Nitrous oxide production in surface waters of the mid-latitude North Atlantic Ocean. *Journal of Geophysical Research: Oceans* **122**, 2612–2621.

Ji, Q., and Grunde, D.S., 2019. An automated, laser-based measurement for nitrous oxide isotope and isotopomer rations at nanomolar levels. *Rapid Communications in Mass Spectrometry*, **33**, 1533–1540.

Jickells, T.D., Knap, A.H., Sherriff-Dow, R. and Galloway, J.N., 1989. No ecosystem shift. *Nature*, **347**, 25–26.

Jickells, T., 2006. The role of air–sea exchange in the marine nitrogen cycle. Biogeosciences 3, 271–280.

Jickells, T., Knap, A., Church, T., Galloway, J., and Miller, J., 1982. Acid- rain on Bermuda. Nature, 297 (5861), 55–57.

Jickells, T.D., Dorling, S., Deuser, W.G., Church, T.M., Arimoto, R. and Prospero, J. 1998. Airborne dust fluxes to a deep water sediment trap in the Sargasso Sea. *Global Biogeochemical Cycles*, 12, 311–320.

Jones, R.D., 1991. Carbon monoxide and methane distribution and consumption in the photic zone of the Sargasso Sea. *Deep Sea Research Part A Oceanographic Research Papers* **38:** 625–635.

Keene, W.C., and Galloway, J.N., 1988. The biogeochemical cycling of formic and acetic acids through the troposphere: An overview of current understanding. *Tellus*, 40B, 322–334.

Keene, W.C., Sander, R., Pszenny, A.A.P., Vogt, R., Crutzen, P.J. and Galloway, J.N., 1998. Aerosol pH in the marine boundary layer: A review and model evaluation. Journal of Aerosol Science, 29, 339–356.

Keene, W.C., Moody, J.L., Galloway, J.N., Prospero, J.M., Cooper, O.R., Eckhardt, S., and Maben, J.R., 2014. Long-term trends in aerosol and precipitation composition over the western North Atlantic Ocean at Bermuda. *Atmospheric Chemistry and Physics*, **14** (15), 8119–8135.

Keeling, R.F., Körtzinger, A., and Gruber, N., 2010. Ocean deoxygenation in a warming world. Annu. Rev. Mar. Sci. 2010, **2**, 199–229

Kelly, C.L., Travis, N.M., Baya, P.A., and Casciotti, K.L., 2021. Quantifying nitrous oxide cycling regimes in the eastern Tropical North Pacific Ocean with isotopomer analysis. *Global Biogeochemical Cycles* **35**, e2020GB006637.

Keltjens, J.T., Pol, A., Reimann, J., and Op den Camp, H.J.M., 2014. PQQ-dependent methanol dehydrogenases: rare-earth elements make a difference. *Applied Microbiol Biotechnology*, **8**, 6163–6183.

Khmelenina, V.N., Murrell, C.J., Smith, T.J., and Trotsenko, Y.A., 2018. Physiology and Biochemistry of the Aerobic Methanotrophs. In: Rojo F (ed). *Aerobic Utilization of Hydrocarbons, Oils and Lipids*. Springer International Publishing, pp 1–25.

Knap, A.H., Jickells, T.D., Pszenny, A. and Galloway, J.N., 1986. The significance of atmospheric derived fixed nitrogen on the productivity of the Sargasso Sea. *Nature*, **320**, 158–160.

Lamarque, J.-F., Kiehl, J.T., Brasseur, G.P., Butler, T., Cameron-Smith, P., Collins, W.D., Collins, W.J., Granier, C., Hauglustaine, D., Hess, P.G., Holland, E.A., Horowitz, L., Lawrence, M.G., McKenna, D., Merilees, P., Prather, M.J., Rasch, P.J., Rotman, D., Shindell, D., Thornton, P., 2005. Assessing future nitrogen deposition and carbon cycle feedback using a multimodel approach: analysis of nitrogen deposition. *Journal of Geophysical Research*, **110**, D19303. doi:10.1029/2005JD005825.

Lipschultz, F., Bates, N.R., Carlson, C. A., and Hansell, D.A., 2002. New production in the Sargasso Sea: History and current status. *Global Biogeochemical Cycles*, **16**, 1001.

Lomas, M.W., Bates, N.R., Johnson, R.J., Knap, A.H, Steinberg, D.K., Carlson, C.A., 2013. Two decades and counting: 23–years of sustained open ocean biogeochemical measurements in the Sargasso Sea. *Deep–Sea Research II*, 93, 16–32, doi: 10.1016/j.dsr2.2013.01.008.

Maben, J.R., Izaguirre, M.A., and Galloway, J.N., 2013. Flow climatology for physicochemical properties of dichotomous aerosol over the western North Atlantic Ocean at Bermuda. *Atmospheric Chemistry and Physics*, **13**, 22383–22444.

Maring H., Savoie, D.L., Izaguirre, M.A., McCormick, C., Arimoto, R., Prospero, J.M. and Pilinis, C., 2000. Aerosol physical and optical properties and their relationship to aerosol composition in the free troposphere at Izaña, Tenerife, Canary Islands during July 1995. *Journal of Geophysical Research*, **105**, 14,677–14,700.

Menzel-Barraqueta, J-L.M., Klar, J.K., Gledhill, M., Schlosser, C., Shelley, R., Planquette, H.F., Wenzel, B., Sarthou, G., and Achterberg, E.P., 2019. Atmospheric deposition fluxes over the Atlantic Ocean: a GEOTRACES case study. *Biogeosciences*, **16** (7), 1525–1546.

Michaels, A.F., Siegel, D.A., Johnson, R.J., Knap, A.H., and Galloway, J.N., 1993. Episodic inputs of atmospheric nitrogen to the Sargasso Sea-contributions to new production and phytoplankton blooms. Global Biogeochemical Cycles, 7(2), 339–351.

Michaels, A.F., and Knap, A.H., 1996. Overview of the US JGOFS Bermuda Atlantic Time series Study and the Hydrostation S program. *Deep-Sea Research Part II-Topical Studies in Oceanography*, **43**, 157–198.

Meyer, A.C.S., Grundle D.S., and Cullen, J.T., 2021. Selective uptake of rare earth elements in marine systems as an indicator of and control on aerobic bacterial methanotrophy. *Earth and Planetary Science Letters* **558**, 116756.

Meyer, A.C.S., Cullen, J.T., and Grundle, D.S., 2022. Nitrous oxide distributions in the oxygenated water column of the Sargasso Sea. *Atmosphere-Ocean*, 1–13.

Mills, M.M., and Arrigo, K.R., 2010. Magnitude of oceanic nitrogen fixation influenced by the nutrient uptake ratio of phytoplankton. *Nature Geoscience*, **3**, 412–416.

Montes, E., Muller-Karger, F.E., Cianca, A., Lomas, M.W., Lorenzoni, L., and Habtes, S., 2016. Decadal variability in the oxygen inventory of North Atlantic subtropical underwater captured by sustained, long-term oceanographic time series observations. *Global Biogeochemical Cycles*, **30** (3), 460–478.

Moody, J.L., Oltsman, S.J., Levy, H., and Merrill, J.T., 1995. Transport climatology of tropospheric ozone: Bermuda, 1988-1991. *Journal of Geophysical Research*, **100**, 7179–7194.

Nevison, C., Butler, J.H., and Elkins, J.W., 2003. Global distribution of N2O and the N_2O AOU yield in the subsurface ocean *Global Biogeochemical Cycles*, **17**, 4.

Owens, N.J.P., Galloway, J.N., and Duce, R.A., 1992. Episodic atmospheric nitrogen deposition to oligotrophic oceans. *Nature*, **357** (6377), 397–399.

Paerl, H.W., 1997. Coastal eutrophication and harmful algal blooms: importance of atmospheric deposition and groundwater as "'new"' nitrogen and other nutrient sources. *Limnology and Oceanography*, **42** (5), 1154–1165.

Peng, X., Fawcett, S.E., Van Oostende, N., Wolf, M.J., Marconi, D., Sigman, D.M. *et al* 2018. Nitrogen uptake and nitrification in the subarctic North Atlantic Ocean. *Limnology and Oceanography* **63**, 1462–1487.

Picone, N, and Op den Camp, H.J.M., 2019. Role of rare earth elements in methanol oxidation. *Current Opinion in Chemical Biology* **49:** 39–44.

Pol, A., Barends, T.R.M., Dietl, A., Khadem, A.F., Eygensteyn, J., Jetten, M.S.M. *et al* (2014). Rare earth metals are essential for methanotrophic life in volcanic mudpots. *Environ Microbiol* **16**, 255–264.

Prinn, R.G., Weiss, R.F., Arduini, J., Arnold, T., DeWitt, H.L., Fraser, P.J. *et al* 2018. History of chemically and radiatively important atmospheric gases from the Advanced Global Atmospheric Gases Experiment (AGAGE). *Earth System Science Data*, **10**, 985–1018.

Prospero, J.M., 2001. The Atmosphere-Ocean Chemistry Experiment (AEROCE): Background and major accomplishments. *IGACctivities Newsletter*, **24**, 3–5.

Rodhe, H., Dentener, F., and Schulz, M., 2002. The global distribution of acidifying wet deposition. *Environmental Science and Technology*, **36**, 4382–4388.

Ravishankara, A.R., Daniel, J.S., and Portmann, R.W., 2009. Nitrous oxide (N_2O): the dominant ozone-depleting substance emitted in the 21st century. *Science* **326**, 123–125.

Sarmiento, J. L., and Gruber, N., 1997. Global patterns of marine nitrogen fixation and denitrification. *Global Biogeochemical Cycles*, **11**, 235–266.

Schön, G.H., and Engel, H., 1962. Der Einfluß des Lichtes auf Nitrosomonas europaea Win. *Archiv für Mikrobiologie* **42**, 415–428.

Sedwick, P.N., Sholkovitz, E.R. and Church, T.M. 2007. Impact of anthropogenic combustion emissions on the fractional solubility of aerosol iron: Evidence from the Sargasso Sea. Geochemistry, Geophysics, Geosystems 8: 10.1029/2007GC001586.

Seitzinger, S.P., Mayorga, E., Bouwman, A.F., Kroeze, C., Beusen, A.H.W., Billen, G., Van Drecht, G., Dumont, E., Fekete, B.M., Garnier, J., and Harrison, J.A., 2010: Global river nutrient export: A scenario analysis of past and future trends. *Global Biogeochemical Cycles*, **24**, GB0A08 doi:10.1029/2009GB003587.

Shiozaki, T., Ijichi, M., Fujiwara, A., Makabe, A., Nishino, S,. and Yoshikawa, C., *et al.* 2019. Factors regulating nitrification in the Arctic Ocean: potential impact of sea ice reduction and ocean acidification. *Global Biogeochemical Cycles* **33**: 1085–1099.

Singh, A., Lomas, M.W., and Bates, N.R., 2013. Revisiting N_2 fixation in the North Atlantic Ocean: Significance of Redfield ratio and climate variability. *Deep-Sea Research II*, **93**, 148–158, doi: 10.1016/j.dsr2.2013.04.008.

Spokes, L.J., and Jickells, T.D., 2005. Is the atmosphere really an important source of reactive nitrogen to coastal waters? *Continental Shelf Research*, **25** (16), 2022–2035.

Stanley, R.H.R., Jenkins, W.J., Doney, S.C., and Lott, D.E., 2015. The ^{3}He flux gauge in the Sargasso Sea: a determination of physical nutrient fluxes to the euphotic zone at the Bermuda Atlantic Time-series site. *Biogeosciences*, **12** (17), 5199–5210.

Steinhoff, T, Friedrich, T., Hartman, S.E., Oschlies, A., Wallace, D.W.R., and Kortzinger, A., 2010: Estimating mixed layer nitrate in the North Atlantic Ocean. *Biogeosciences*, **7**, 795–807 doi:10.5194/bg-7-795-2010.

Steinberg, D.K, Carlson, C.A., Bates, N.R., Johnson, R.J., Michaels, A.F., and Knap, A.H., 2001. Overview of the US JGOFS Bermuda Atlantic Time–series Study (BATS): a decade–scale look at ocean biology and biogeochemistry. *Deep–Sea Research II*, 48 (8–9), 1405–1447, doi:10.1016/S0967–0645(00)00148–X.

Stendardo, I., and Gruber, N., 2012. Oxygen trends over five decades in the North Atlantic. Journal of Geophysical Research, **117**, C111.

Stendardo, I., Rhein, M., and Hollman, R., 2016. A high resolution time-series 1993–2012 in the North Atlantic from Argo and altimeter data. *Journal of Geophysical Research*, **121** (4), 2523–2551.

Stendardo, I., Kieke, D., Rhein, M., Gruber, N., and Steinfeldt, R., 2015. Interannual to decadal oxygen variability in the mid-depth water masses of the eastern North Atlantic. *Deep Sea Research I*, **95**, 85–98.

Stramma, L., and Schmidtko, S., 2019. Global evidence of deoxygenation. in *Ocean Deoxygenation: Everyone's Problem*. (editors Laffoley, D., and Baxter, J. M.) 25–36, (IUCN).

Tian, H., Xu, R., Canadell, J.G., Thompson, R.L., Winiwarter, W., Suntharalingam, P., *et al.* 2020. A comprehensive quantification of global nitrous oxide sources and sinks. *Nature*, **586**, 248–256.

Wankel, S.D., Kendall, C., Pennington, J.T., Chavez, F.P., and Paytan, A., 2007. Nitrification in the euphotic zone as evidenced by nitrate dual isotopic composition: Observations from Monterey Bay, California. *Global Biogeochemical Cycles* **21**.

Ward, B.B., 1987. Nitrogen transformations in the Southern California Bight. *Deep Sea Research Part A Oceanographic Research Papers* **34**, 785–805.

Whelpdale, D.M., Summers, P.W., Sanhueza, E., Artz, R.A., Ayers, G., Delmas, R.J., Dovland, H., Galloway, J.N., Gillett, R., Hara, H., Lacaux, J.-P., Luke, W., Pedersen, U., Ryaboshapko, A., 1996. A global overview of acid deposition. In: Whelpdale, D.W., Kaiser, D.M. (Eds.), World Meteorological Organization/Global Atmospheric Watch Report, 106. WMO/GAW Report 106.

Williams, R. G., Roussenov, V., and Follows, M. J., 2006: Nutrient streams and their induction into the mixed layer. GlobalBiogeochemical Cycles, 20, GB1016, doi:10.1029/2005GB002586.

Wong, C.S., Xie, L., and Hsieh, W.W., 2007. Variations in nutrients, carbon and and other hydrographic parameters related to the 1976/77 and 1988/89 regime shifts in the sub-arctic Northeast Pacific. *Progress in Oceanography*, **75**, 326–342.

Wright, J.J., Konwar, K.M., and Hallam S.J., 2012. Microbial ecology of expanding oxygen minimum zones. *Nature Reviews Microbiology* **10**: 381–394.

Xiu, P., and Chai, F., 2021. Impact of atmospheric deposition on carbon export to the deep ocean in the subtropical Northwest Pacific. *Geophysical Research Letters*, **48** (6), e2020GL089640.

CHAPTER 4

Biological oceanography of the Sargasso Sea

D.S. Grundle, N.R. Bates, S. Murdock and R.J. Johnson

4.1 Food web overview, ocean optics and remote sensing

The use of satellite and other remote sensing systems has advanced the field of oceanography in the last decades, allowing for fast and global studies impossible to attain by other means. In the Sargasso Sea, the presence of the continuous measurements provided by the many time series, both oceanic and atmospheric, allows to ground truth those remote sensing readings with *in situ*, actual measurements of the object of study (e.g., temperature, oceanic chlorophyll, aerosols, etc.). The monthly observations of optical and biogeochemical properties of the Bermuda Bio Optics Project (BBOP) at the Bermuda Atlantic Time-series Study (BATS) site, carried out from 1995 until the mid-2010s, showed an increase of the diffuse attenuation in the upper photic layer (Allen *et al.*, 2017). The results suggest long-term ongoing changes in the phytoplankton community, and they agree with measured changes in the phytoplankton at BATS (Lomas *et al.*, 2022), discussed in a later section. These direct comparisons also improved the models calculating primary production from satellite measurements (Kovač *et al.*, 2018). Similar validation approaches were included in global models for dissolved organic matter cycling (Swan *et al.*, 2012; Swan *et al.*, 2013). The data from the Sargasso Sea have been vital to understand the limits of models and disentangle the interaction between the spatial and temporal resolution of the proposed models.

To date, most of the oceanic remote sensing approaches focused on passive sensors, such as those measuring organic matter and phytoplankton. In recent years, there has been an increase in the use of satellite-mounted light-detection-and-ranging (lidar) instruments. This system detects the distribution of animals both during the day and at night, allowing for a global study of the zooplankton's diel vertical migration (DVM) at a worldwide scale (Behrenfeld *et al.*, 2019). Using remote sensing to measure DMV at the spatial and temporal resolution that satellite could provide would significantly improve our calculations of the biogeochemical impact of the zooplankton. The inclusion of the BATS data in the Sargasso Sea allowed, again, a better understanding of the spatial *versus* seasonal variability. It also proved the agreement between the satellite readings and the known seasonality in the total biomass of the zooplankton (Behrenfeld *et al.*, 2019).

4.2 Microbial Ecology, Genomics and eDNA

Far away from fading or slowing down, the impulse given in the previous decades by molecular techniques to research the smaller components of the plankton (viruses and prokaryotes) has continued to deliver a vast amount of new knowledge. The combination of the historical framework provided by the long-term study sites (BATS, Hydrostation, OFP, OMO) and the development of new techniques and instruments in the field made the Sargasso Sea the perfect open ocean laboratory.

Using the molecular metabarcoding techniques developed in the early 2000s (Sogin *et al.* 2006), the composition of whole communities can be characterized by amplifying specific fragments of conserved regions of the genome, sequencing in parallel millions of those fragments. This method opened the door to understanding the community dynamics of those groups for which optical methods could not be applied to the species level, such as the prokaryotes (Bacteria and Archaea). These studies showed very strong seasonal dynamics in the Sargasso Sea, as well as the role of depth conditioning the prokaryotic community in the water column (Vergin *et al.*, 2013b). These dynamics were linked to changes to the yearly cycles of stratification and mixing events (Vergin *et al.*, 2013b), mesoscale events such as eddies (Nelson *et al.*, 2014) or, in a few cases, to other non-cyclical events or disturbances of unknown origin at the time. Within the Sargasso Sea discovered SAR11 clade, there were single lineages linked to specific depths or environmental conditions (ecotypes), indicating the presence of continuous evolutionary processes in the ocean even at fine spatial scales. These ecotypes could finely tune to their ecological niche and often occupy adjacent niches if competing with

other groups (Vergin *et al.*, 2013a). Widespread in the global ocean, temperature and nutrient concentration are accurate predictors for which ecotype might be dominant at any time in any location (Bolaños *et al.*, 2022). Together, data suggested that community assembly, succession and evolution did not follow a neutral pattern but were controlled by niche-dependent, deterministic processes (Vergin *et al.*, 2017). These studies, in which the whole community was characterized, were the basis for processes-oriented studies, in which the observed transitions were studied in depth, with the aid of other methods and experiments, to understand the underlying mechanisms and their consequences in the biogeochemical cycles.

Having characterized the community composition and dynamics paved the way to advance our knowledge in the metabolic pathways of the prokaryote community, both considering a few lineages or even considering the whole community. Many focused on the interaction between bacteria and dissolved organic matter (DOM) and carbon (DOM), such as the role of bacteria in the production of the climatically–active trace gas dimethylsulfide (DMS) in the upper ocean (Vila-Costa *et al.*, 2014). Although the results were not conclusive, they suggested that the metabolic pathway responsible for the production of DMS depends on the metabolic demand of sulfur by the prokaryotic community and the availability of labile carbon and energy (Parsons *et al.*, 2012; Vila-Costa *et al.*, 2014).

Another research focus continued focusing on the SAR lineages, especially in SAR11. The primary questions related to the role of SAR11 in the multiple paths of degradation of organic matter: which pathways, when, and how much of those different components of DOM were passing through SAR11. One of the critical components of the DOM in the oceans is vitamins, which are rare but essential for essential metabolic pathways. SAR11 could synthesize vitamin B1, one of the key coenzymes for all living organisms, from a precursor and could not use exogenous B1 (Carini *et al.*, 2014). The precursor is actually a typical exudate in marine cyanobacteria, phytoplankton and bacteria but remains almost undetectable in most of the water column, suggesting that SAR11 efficiently processes the precursor, funnelling this organic compound into its metabolic pathway (Carini *et al.*, 2014). Another SAR lineage of interest is SAR202 since its high densities and the evolutionary placement suggested from its discovery a potential role in the metabolic degradation of recalcitrant (that is, resistant to microbial degradation) organic matter. Genome analyses, including samples from the Sargasso Sea, have shown that they have the metabolic machinery (or, at least, the genes) for oxidizing a fair number of relatively recalcitrant compounds (Landry *et al.*, . 2017). Similar to SAR11, ocean depth studies of the abundance and distribution of these genomes in the water column also depicts the presence of different evolutionary lineages, each with a different metabolic specialization (Saw *et al.*, 2020).

Multidisciplinary efforts in the Sargasso Sea allow the link between different facets of biological oceanography. Combining zooplankton incubations, bacterial remineralization experiments and dissolved targeted metabolites via quantitative mass spectrometry, the first steps towards a mechanistic understanding between zooplankton behaviour and organic matter production, and bacterial growth and organic matter consumption have been characterized. Copiotrophic bacteria, able to rapidly utilize the large number of labile carbon molecules produced for growth, actively respond to the zooplankton byproducts (Maas *et al.*, 2020). Further studies should investigate the fate of the less labile molecules of the zooplankton-originated DOM and the effect on the prokaryotic community. On a similar approach, but using only field data, the injection of surface DOM into the deep ocean that happens in the Sargasso at the end of the summer (Carlson *et al.*, 1994) produced a growth of specific bacterial lineages (such as the aforementioned SAR11 and SAR202). Different bacterial lineages and ecotypes peaked at other times after the injection, which is linked to the changes in the DOM total amount and composition over time, suggesting a tight link between DOM variability and prokaryotic community abundance and composition (Liu *et al.*, 2022).

During the last decade, there has been a growing interest in the viral component of the plankton, the virioplankton. In the Sargasso Sea, these fraction seems to be dominated in the epipelagic by virus lineages with affinity for the cyanobacteria *Prochlorococcus* (Parsons *et al.*, 2012). The community, however, follows a seasonal cycle controlled by hydrography (Goldsmith *et al.*, 2015). Interestingly, the viral abundance did not correlate with the most abundant bacteria, SAR11. Ongoing studies analyzing the phylogenetic composition of the viral community and their taxonomic affinity should shed light on the dynamics of virioplankton in the oligotrophic gyre of the Sargasso Sea.

4.3 Phytoplankton, protist diversity and productivity

L. Blanco-Bercial

4.3.1 *Introduction*

The phytoplankton community in the Sargasso Sea is dominated by the picophytoplankton (~0.7 – 2 µm). This group alone represents ~50% to 85% of the community chlorophyll-*a* biomass, and they include cyanobacteria (*Prochlorococcus* and *Synechococcus*) and a very diverse community of microscopic eukaryotes (Blanco-Bercial *et al.*, 2022; Cotti-Rausch *et al.*, 2020). This group is also responsible for most of the primary production and photosynthetic carbon fixation, representing almost 100% of it in the deeper layers. The larger size fractions, the nanophytoplankton (2 – 20 µm) and the microphytoplankton (> 20 µm), find their peak in biomass at the 80–100 m depth range, although their maximum contribution to the total primary production happens however in the upper 50 m (Cotti-Rausch *et al.*, 2020). These findings agree with the assumption that picophytoplankton is the main driver of primary production in the oligotrophic areas. This community shows a large variation on a seasonal basis instead of a steady community throughout the year.

The long-term trends of the phytoplankton community show a further increase in the picophytoplankton community over the last decades (Lomas *et al.*, 2022), especially favouring the cyanobacteria. After some initial data indicating a long-term increase in phytoplankton biomass (Wallhead *et al.*, 2014), this trend decayed over the last years of the 2010s decade, when the eukaryote biomass declined to the baseline of the previous decades. The prokaryotic picophytoplankton did not decrease, which resulted in an apparent reorganization of the community. One of the consequences of this reorganization is that phytoplankton-mediated carbon export was maintained thanks to the different nutrient stoichiometry of both groups, favouring cyanobacteria in the present conditions of lower nutrient availability in the epipelagic (Lomas *et al.*, 2022). Despite this apparent long-term stability of the community, there are noticeable shifts in biomass and community composition linked to regional oscillations, such as the NAO (Casey *et al.*, 2013; Lomas *et al.*, 2013). Maintaining a time series that extends beyond the natural duration of such cycles is thus essential to characterize the real long-term trend in the phytoplankton community in the Sargasso Sea. Finally, although the results summarised above represent a general picture and trend of the Sargasso Sea, and more specifically of the BATS time series, mesoscale structures such as eddies could significantly influence the phytoplankton community, driving it away from the pattern mentioned above (Cotti-Rausch *et al.*, 2016). Depending on the season and nature of the eddy (cyclonic or anticyclonic), the community shifted more towards cyanobacteria (when oligotrophy was promoted) or towards eukaryotes (when it resulted in nutrient supply). Those changes affected the carbon export, with lower values associated with the *Prochlorococcus-dominated*, anticyclonic structures (Cotti-Rausch *et al.*, 2016).

As indicated above, the community is dominated by the smaller size fractions (< 20 µm), which, combined with the high diversity typical from oligotrophic areas, makes very difficult and time-consuming any research involving approaches combining quantification and identification at the individual level. Microscopy-based approaches are highly time-consuming and require broad taxonomic expertise; they provide a quantitative measurement that other methods currently lack. One of the few microscopy studies indicated a dinoflagellate-dominated community in the epipelagic (Wolverton, 2016), although mixotrophic ciliates could, under some circumstances, represent a larger biomass than any other group. The limited dataset of this work (the summers and winters from two years) did not allow for validating some of the existing hypotheses about the relevance of mixotrophy (Mitra *et al.*, 2014) in the trophic web and biological pump at BATS. It offered some hints of the possible prey preferences by nano flagellates, dinoflagellates and ciliates, most of which can feed on the cyanobacteria that dominate the phytoplankton biomass at BATS (Wolverton, 2016). The balance between prey availability, nutrient budgets and depth of the photosynthetically active radiation would then condition which taxa groups can overcompete the others. The ability of mixotrophs to combine nutrient acquisition from predation with carbon fixation through photosynthesis should give them an advantage during stratification periods; meanwhile, the deep mixing in spring would favour those lineages with more efficient photosynthetic systems.

In the last decade, our knowledge of the ocean's unicellular eukaryote components has increased with molecular applications such as metabarcoding or metagenomics. Together with more established methods, they have improved our understanding of the community and processes involving the unicellular components. The research carried out in the Sargasso Sea was not

an exception to this rule, and several publications have seen the light using these tools alone or combined with other methods. Based on these approaches, it has been characterized that mixotrophic lineages, especially dinoflagellates, dominate throughout the whole year in the epipelagic. However, autotroph prasinophytes bloom during the rapid transition between the winter mixing and the stratified summer; meanwhile, heterotrophs have their peak at the end of summer, when the base of the thermocline reaches its deeper depth, and nutrients are more scarce in the epipelagic (Blanco-Bercial *et al.*, 2022; Choi *et al.*, 2020; Treusch *et al.*, 2012). Below the photic zone, the community is dominated by Rhizaria, where different lineages are organized in a depth-stratified fashion, relatively constant throughout the year, and mirror local hydrographic and biological features such as the oxygen minimum zone. The results suggest a dynamic partitioning of the water column, where the niche vertical position for each community changes throughout the year, likely depending on light, nutrient availability, mixed layer depth, and other hydrographic features. Finally, the protist community closely followed mesoscale events (eddies), with the communities mirroring the hydrographic uplift, raising the deeper communities for hundreds of meters, and compressing the communities above (Blanco-Bercial *et al.*, 2022).

4.3.2 *Marine fungi.*

In the last decade, there has been a growing interest in marine fungi, initially due to their role in the natural cycle of organic compounds. Fungi can degrade recalcitrant organic matter, which might be the missing link in how organic matter, especially those complex organic molecules, is used by the planktonic community. Furthermore, fungi are known to produce secondary metabolites with potential use in industry, making this group a focus for applied-oriented research, including drug discovery, cosmetics, or bioreactors. In the Sargasso Sea, a preliminary study has been carried out, exploring the vertical distribution in the epipelagic and upper mesopelagic of planktonic fungi by molecular methods. This first data indicated an increase of filamentous fungi (compared to unicellular, yeast-like ones) with depth, as well as an increase of parasitic forms in the chlorophyll maximum and the upper mesopelagic, compared to the surface (Godfrey *et al.*, 2022). Moreover, Ascomycota dominated the community. There was a shift in the composition within Basidiomycota, with different Classes dominating at each depth. Finally, this study also highlighted that most of the community belonged to lineages without references in the existing databases. The role in the community and biogeochemical cycles, and the applied potential for these lineages, is then unknown, opening the door for future studies focusing on this community to understand their ecology, their role in the biogeochemical cycles, and their potential use in industry.

4.4 Zooplankton in the Sargasso Sea

L. Blanco-Bercial

The zooplankton, small animals that live drifting in the water column, are a vital component of the ocean ecosystem. They are the essential link between primary producers and the upper trophic levels, channelling 15 to > 50% of ocean production toward upper trophic levels (Steinberg and Landry, 2017). In the last decade, our acquired knowledge of the zooplankton community in the Sargasso Sea (composition, seasonality, biogeochemical roles, long-term trends, etc.) has enriched our understanding of local and global processes (Ivory *et al.*, 2019; Steinberg and Lomas, 2012; Stone and Steinberg, 2016). Recent studies include biomass-derived to high-throughput (molecular and images) datasets and observational-based to experimental studies that build up over the previous research and on the shoulders of the plethora of data accumulated by the BATS program.

Long-term trends in zooplankton biomass indicated a nearly 70% increase from 1994 to 2011 (Lomas *et al.*, 2013; Steinberg *et al.*, 2012), especially around the spring bloom. This increase in biomass was flagged as one of the plausible reasons for the detected increase of POC flux in the winter-spring at BATS (Lomas *et al.*, 2010). This trend did not seem homogeneous across all size fractions and suggested that only a fraction of the community responded to the increase in temperatures (Steinberg *et al.*, 2012). Later studies, however, indicate that this increase did not continue in the next decade when it was registered an actual decrease of a similar magnitude (Lomas *et al.* 2022). Data would then suggest a long-term steady state in the biomass of the zooplankton community, with oscillations related to long-term, cyclical forcings.

Recent microscopy work in zooplankton community composition agreed with the historical data from previous decades; copepods were the dominant group, with a high taxonomic diversity across all groups and depths (Stefanoudis *et al.* 2019). In the southern Sargasso Sea, a highly diverse group of copepods were also the dominant group, with biomass peaks associated with

frontal structures (Andersen *et al.*, 2011). At BATS, recent image-analyses-based technology using a zooscan (Gorsky *et al.*, 2010) has advanced our understanding of the zooplankton community beyond biomass measurements. Image data also detected an increase in biomass and was able to associate the increase in the specific groups with the increase of temperatures in the 2002-2010 period (Ivory *et al.*, 2019); future research should address the group-specific response to the decay in general biomass during the last decade. More extended studies have reflected some cycles in specific groups of taxa with possible impact on biogeochemical cycles (Stone and Steinberg, 2014, 2016). Using images also allows for calculating total biomass and derived physiological calculations with applications for biogeochemical cycle models, especially after developing a local, taxonomically specific, size-image-biomass calibration set for this region (Maas *et al.*, 2021). In recent years, but already far away from the foundational (Venter *et al.*, 2004), molecular techniques to describe planktonic communities have significantly increased compared to those using morphology. In the Sargasso Sea, this technique has allowed the description of separate communities that form a seasonal succession related to the hydrographic changes and identify such communities' main components and indicators (Blanco-Bercial, 2020). These successional changes were also associated with the measured carbon and nitrogen export, indicating a measurable link between the seasonality in community composition and its impact on biogeochemical cycles. Future work, merging both sources of high-throughput data (imaging and molecular), should improve our understanding of the zooplankton community at BATS.

Experimental work on the zooplankton in the Sargasso Sea has continued, focusing primarily on the copepod *Pleuromamma xiphias*. Studies have focused on its circadian cycle and its potential impact on biogeochemical cycling (Maas *et al.*, 2018; Tarrant *et al.*, 2021), as well as the interaction between the diel vertical migration pattern of this species, their production of exudates and the response of the microbial community to these dissolved organic compounds in depth (Maas *et al.*, 2020). These studies have shown variability in the diel physiological rhythm depending on the season and the environmental conditions, with implications in the larger scale role of the zooplankton as a critical player in the vertical transport of carbon to sequestration depths. They have also shown the relevance of active flux (the amount of carbon, nitrogen, and other organic compounds that are released directly at depth) driven by the zooplankton, in contrast with the passive flux of surface-originated particles that passively sink in the water column to deeper layers. Accurate quantification of this path and the role of the resident community are two of the following questions that should be addressed in the future to understand the contribution of the zooplankton to the generation, modification and attenuation of sinking particles in the ocean.

Although not a focus of this report, there have been several new studies on the biology and function of eels in the Sargasso Sea (e.g., Righton *et al.*, 2016; Hanel *et al.*, 2014; Rypina *et al.*, 2014) and cephalopods (Lischka *et al.*, 2017).

4.5 Decadal changes in the Sargasso Sea

L. Blanco-Bercial

All the knowledge accumulated not only in the last decade but from the foundation of the time series makes the Sargasso Sea, in general, and BATS, in particular, one of the locations of choice when testing global models of biogeochemical cycles or when testing new approaches that would improve our measurements, about the zooplankton community (e.g., Archibald *et al.*, 2019; Doherty *et al.* 2021). Richardson *et al.* (2017) have recently studied the effects of warming on zooplankton in the Sargasso Sea using observational data and models.

4.6 Modelling approaches

L. Blanco-Bercial

All the knowledge accumulated not only in the last decade but from the foundation of the time series makes the Sargasso Sea in general, and BATS in particular, one of the locations of choice when testing global models of biogeochemical cycles, or when testing new approaches and equipment that would improve our measurements. Studies include, for example, the contribution of zooplankton to global biogeochemical cycles, combining in situ measurements and satellite estimates (Archibald *et al.*, 2019), the calibration of compound-specific isotope analysis of amino acids (Doherty *et al.*, 2021), developing a machine-learning model to relate hydrography and primary productivity in the ocean (D'Alelio *et al.*, 2020), or modelling the controls on carbon export in the ocean (Yumruktepe *et al.*, 2020), to name a few. The continuous use of data originating in the Sargasso Sea highlights the relevance of this location for the scientific community.

4.7 References

Allen, J.G., Nelson, N.B., and Siegel, D.A., 2017. Seasonal to multi-decadal trends in apparent optical properties in the Sargasso Sea. *Deep-Sea Research I*, **119**, 58–67.

Andersen, N.G., Nielsen, T.G., Jakobsen, H.H., Munk P., and Riemann, L., 2011. Distribution and production of plankton communities in the subtropical convergence zone of the Sargasso Sea. II. Protozooplankton and copepods. *Marine Ecology Progress Series*, **426**, 71–86.

Archibald, K.M., Siegel, D.A., and Doney, S.C., 2019. Modeling the impact of zooplankton diel vertical migration on the carbon export flux of the biological pump. *Global Biogeochemical Cycles*, **33**, 181–199.

Behrenfield, M.J., Moore, R.H., Hostetler, C.A., Graff, J., Gaube, P., Russell, L.M., *et al.*, 2019. The North Atlantic aerosol and marine ecosystem study (NAAMES): Science motive and overview. *Frontiers in Marine Science*, **6**, https://doi.org/10.3389/fmars.2019.00122.

Blanco-Bercial, L., 2020. Metabarcoding analyses and seasonality of the Zooplankton community at BATS. *Frontiers in Marine Science*, **7**.

Blanco-Bercial, L., Parsons, R., Bolaños, L., Johnson, R., Giovannoni, S.J., and Curry, R., 2022. The protist community mirrors seasonality and mesoscale hydrographic features in the oligotrophic Sargasso Sea. *Authorea Preprints*.

Bolaños, L.M., Tait, K., Somerfield, P.J., Parsons, R., Giovannoni, S.J., Smyth, T., and Temperton, B., 2022. Influence of short and long term processes on SAR11 communities in open ocean and coastal systems. *bioRxiv*, 2022.2006.2017.496560.

Carini, P., Campbell, E.O., Morré, J., Sañudo-Wilhelmy, S.A., Thrash, J.C., Bennett, S.E., Temperton, B., Begley, T., and Giovannoni, S.J., 2014. Discovery of a SAR11 growth requirement for thiamin's pyrimidine precursor and its distribution in the Sargasso Sea. *The ISME Journal*, **8**, 1727–1738.

Carlson C.A., Ducklow H.W., and Michaels A.F., 1994. Annual flux of dissolved organic carbon from the euphotic zone in the northwestern Sargasso Sea. *Nature*, **371**, 405–408.
Casey, J.R., Aucan, J.P., Goldberg, S.R., and Lomas M.W., 2013. Changes in partitioning of carbon amongst photosynthetic pico- and nano-plankton groups in the Sargasso Sea in response to changes in the North Atlantic Oscillation. *Deep Sea Research Part II: Topical Studies in Oceanography*, **93**, 58–70.

Choi, C.J., Jimenez, V., Needham, D.M., Poirier, C., Bachy, C., Alexander, H., Wilken, S., Chavez, F.P., Sudek, S., Giovannoni, S.J., and Worden, A.Z., 2020. Seasonal and geographical transitions in eukaryotic phytoplankton community structure in the Atlantic and Pacific Oceans. *Frontiers in Microbiology*, **11**.

Cotti-Rausch, B.E., Lomas, M.W., Lachenmyer, E.M., Baumann, E.G., and Richardson, T.L., 2020. Size-fractionated biomass and primary productivity of Sargasso Sea phytoplankton. *Deep Sea Research Part I: Oceanographic Research Papers*, **156**, 103141.

Cotti-Rausch, B.E., Lomas, M.W., Lachenmyer, E.M., Goldman, E.A., Bell, D.W., Goldberg, S.R., and Richardson, T.L., 2016. Mesoscale and sub-mesoscale variability in phytoplankton community composition in the Sargasso Sea. *Deep Sea Research Part I: Oceanographic Research Papers*, **110**, 106–122.

D'Alelio, D., Rampone, S., Cusano, L.M., Russo, L., Sanseverino, N., Cloern, J.E., and Lomas, M.W., 2020. Machine learning identifies a strong association between warming and reduced primary productivity in an oligotrophic ocean gyre. *Scientific reports*, **10**, 3287.

Doherty, S.C., Maas, A.E., Steinberg, D.K., Popp, B.N., and Close, H.G., 2021. Distinguishing zooplankton fecal pellets as a component of the biological pump using compound-specific isotope analysis of amino acids. *Limnology and Oceanography*, **66**, 2827–2841.

Godfrey, R.C., Jones, H.E., Green, N.J., and Lawrence, A.L., 2022. Unified total synthesis of the brevianamide alkaloids enabled by chemical investigations into their biosynthesis. *Chemical Science*, **13**, 1313–1322.

Goldsmith, D.B., Brum, J.R., Hopkins, M., Carlson, C.A., and Breitbart, M., 2015. Water column stratification structures viral community composition in the Sargasso Sea. *Aquatic Microbial Ecology*, **76**, 85–94.

Gorsky, G., Ohman, M.D., Picheral, M., Gasparini, S., Stemman, L., Romagnan, J.-B., Cawood, A., Pesant, S., García, C., and Prejger, F., 2010. Digital zooplankton image analysis using the ZooScan integrated system. *Journal of Plankton Research*, **32**, 285–303.

Hanel, R., Stepputtis, D., Bonhommeau, S., Castonguay, M., Schaber, M., Wysujack, K., Vobach, M., and Miller, M.J., 2014. *Naturewissenschaften*, **101**, 1041–1054.

Ivory, J.A., Steinberg, D.K., and Latour, R.J., 2019. Diel, seasonal, and interannual patterns in mesozooplankton abundance in the Sargasso Sea. *ICES Journal of Marine Science*, **76**, 217–231.

Kovač, Z., Platt, T., Ninčević-Gladen, Z., Morović, M., Sathyendranath, S., Raitsos, D.E., Grbec, B., Matić, F., and Veža, J., 2018. A 55-year time-series station for primary production in the Adriatic Sea: Data correction, extraction of photosynthesis parameters and regime shifts. *Remote Sensing*, **10** (9), 1460.

Landry, Z., Swan, B.K., Herndl, G.J., Stepanauskas, R., and Giovannoni, S.J., 2017. SAR202 genomes from the dark ocean predict pathways for the oxidation of recalcitrant dissolved organic matter. *mBio*, **8**, e00413–00417.

Lischka, A., Piatkowski, U., and Hanel, R., 2017. Cephalopods of the Sargasso Sea: distribution patterns in relation to oceanography. *Marine Biodiversity*, **47**, 685–697.

Liu, S., Longnecker, K., Kujawinski, E.B., Vergin, K., Bolaños, L.M., Giovannoni, S.J., Parsons, R., Opalk, K., Halewood, E., Hansell, D.A., Johnson, R., Curry, R., and Carlson, C.A., 2022. Linkages among dissolved organic matter export, dissolved metabolites, and associated microbial community structure response in the northwestern Sargasso Sea on a seasonal scale. *Frontiers in Microbiology*, **13**.

Lomas, M.W., Steinberg, D.K., Dickey, T.D., Carlson, C.A., Nelson, N.B., Condon, R.H., and Bates, N.R., 2010. Increased ocean carbon export in the Sargasso Sea is countered by its enhanced mesopelagic attenuation. *Biogeosciences*, **7** (1), 57–70.

Lomas, M.W., Bates, N.R., Johnson, R.J., Knap, A.H, Steinberg, D.K., Carlson, C.A., 2013. Two decades and counting: 23–years of sustained open ocean biogeochemical measurements in the Sargasso Sea. *Deep–Sea Research II*, **93**, 16–32, doi: 10.1016/j.dsr2.2013.01.008.

Lomas, M.W., Bates, N.R., Johnson, R.J., Steinberg, D.K., and Tanioka, T., 2022. Adaptive carbon export response to warming in the Sargasso Sea. *Nature Communications*, **13**, 1211. Maas, A.E., Blanco-Bercial, L., Lo, A., Tarrant, A.M., and Timmins-Schiffman, E., 2018. Variations in copepod proteome and pespiration rate in association with diel vertical migration and circadian cycle. *The Biological Bulletin*, **235**, 30–42.

Maas, A.E., Gossner, H., Smith, M.J., Blanco-Bercial, L., 2021. Use of optical imaging datasets to assess biogeochemical contributions of the mesozooplankton. *Journal of Plankton Research*, **43**, 475–491.

Maas, A.E., Liu, S., Bolaños, L.M., Widner, B., Parsons, R., Kujawinski, E.B., Blanco-Bercial, L., and Carlson, C.A., 2020. Migratory zooplankton excreta and its influence on prokaryotic communities. *Frontiers in Marine Science*, **7**.

Mitra, A., Flynn, K.J., Burkholder, J.M., Berge, T., Calbet, A., Raven, J.A., Granéli, E., Glibert, P.M., Hansen, P.J., Stoecker, D.K., Thingstad, F., Tillmann, U., Våge, S., Wilken, S., and Zubkov, M.V., 2014. The role of mixotrophic protists in the biological carbon pump. *Biogeosciences*, **11**, 995–1005.

Nelson, C.E., Carlson, C.A., Ewart, C.S., and Halewood E.R., 2014. Community differentiation and population enrichment of Sargasso Sea bacterioplankton in the euphotic zone of a mesoscale mode-water eddy. *Environmental Microbiology*, **16**, 871–887.

Parsons, R.J., Breitbart, M., Lomas, M.W., and Carlson, C.A., 2012. Ocean time-series reveals recurring seasonal patterns of virioplankton dynamics in the northwestern Sargasso Sea. *ISME J*, **6**, 273–284.

Richardson, K., and Bendtsen, J., 2017. Photosynthetic oxygen production in a warmer ocean: the Sargasso Sea as a case study. *Philosophical Transaction of the Royal Society, A*, 07 August 2017, https://doi.org/10.1098/rsta.2016.0329.

Righton, D., Westerberg, H., Feunteun, E., Økland, F., Gargan, P., Amilhat, E., Metcalfe, J., Lobon-Cervia, J., Sjöberg, N., Simon, J., Acou, A., Vedor, M., Walker, A., Trancart, T., Brämcart, U., and Aarestrup, K., 2016. Empirical observations of the spawning migration of European eels: The long and dangerous road to the Sargasso Sea. *Science Advances*, **2** (10), doi.10.1126/sciadv.1501694.

Rypina, I.I., Llopiz, J.K., Pratt, L.J., and Lozier, M.S., 2014. Dispersal pathways of American eel larvae from the Sargasso Sea. *Limnology and Oceanography*, **59** (5), 1704–1714.

Saw, J.H.W., Nunoura, T., Hirai, M., Takaki, Y., Parsons, R., Michelsen, M., Longnecker, K., Kujawinski, E.B., Stepanauskas, R., Landry, Z., Carlson, C.A., and Giovannoni, S.J., 2020. Pangenomics analysis reveals diversification of enzyme families and niche specialization in globally abundant SAR202 bacteria. *mBio*, **11**, e02975–02919.

Sogin, M.L., Morrison, H.G., Huber, J.A., and Herndl, G.J., 2006. Microbial diversity in the deep sea and the under-explored rare biosphere. *Proceedings of the National Academy of Sciences*, **103**, 12115–12120.

Stefanoudis, P.V., Rivers, M., Ford, H., Yashayaev, I.M., Rogers, A.D., and Woodalll, L.C., 2019. Changes in zooplankton communities from epipelagic to lower mesopelagic waters. *Marine Environmental Research*, **146**, 1–11.

Steinberg, D.K., and Lomas, M.W., 2012. Long-term increase in mesozooplankton biomass in the Sargasso Sea: Linkage to climate and implications for food web dynamics and biogeochemical cycling. *Global Biogeochemical Cycles*, **26** (1).

Steinberg, D.K., and Landry, M.R., 2017. Zooplankton and the ocean carbon cycle. *Annual Review of Marine Science*, **9**, 413–444.

Steinberg D.K., Lomas M.W., and Cope J.S., 2012. Long-term increase in mesozooplankton biomass in the Sargasso Sea: Linkage to climate and implications for food web dynamics and biogeochemical cycling. *Global Biogeochemical Cycles*, **26**, GB1004.

Stone, J.P., and Steinberg, D.K., 2014. Long-term time-series study of salp population dynamics in the Sargasso Sea. *Marine Ecology Progress Series*, **510**, 111–127.

Stone, J.P., and Steinberg, D.K., 2016. Salp contributions to vertical carbon flux in the Sargasso Sea. *Deep Sea Research Part I: Oceanographic Research Papers*, **113**, 90–100.

Swan, C.M., Nelson, N.B., Siegel, D.A., and Kostadinov, T.S., 2012. The effect of surface irradiance on the absorption spectrum of chromophoric dissolved organic matter in the global ocean. *Deep Sea Research, I*, **63**, 52–64.

Swan, C.M., Nelson, N.B., Siegel, D.A., and Fields, E.K., 2013. A model for remote estimation of ultraviolet absorption by chromophoric dissolved organic matter based on the global distribution of the spectral slope. *Remote Sensing of the Environment*, **136**, 277–285.

Tarrant, A.M., McNamara-Bordewick, N., Blanco-Bercial, L., Miccoli, A., and Maas A.E., 2021. Diel metabolic patterns in a migratory oceanic copepod. *Journal of Experimental Marine Biology and Ecology*, **545**, 151643.

Treusch, A.H., Demir-Hilton, E., Vergin, K.L., Worden, A.Z., Carlson, C.A., Donatz, M.G., Burton, R.M., and Giovannoni, S.J., 2012. Phytoplankton distribution patterns in the northwestern Sargasso Sea revealed by small subunit rRNA genes from plastids. *The ISME Journal*, **6**, 481–492.

Venter, J.C., Remington, K, Heidelberg, J.F, A.L.Halpern, Rusch, D., Eisen, J.A., Wu, D., Paulsen, I., Nelson, K., Nelson, W., Fouts, D.E., Levy, S., Knap, A.H., Lomas, M.W., Nealson, K., White, O., Peterson, J., Hoffman, J., Parsons,

R., Baden-Tillson, H., Pfannkock, C., Rogers, Y. and Smith, H.O., 2004. Environmental genome shotgun sequencing of the Sargasso Sea. *Science*, **304**, 5667, 66–74.

Vergin, K.L., Beszteri, B., Monier, A., Thrash, J.C., Temperton, B., Treusch, A.H., Kilpert, F., Worden, A.Z., and Giovannoni, S.J., 2013a. High-resolution SAR11 ecotype dymnamics at the Bermuda Atlantic Time-series Study site by phylogenetic placement of pyrosequences. *Nature, the ISME Journal*, **7**, 1322–1332.

Vergin, K.L., Done, B., Carlson, C.A., and Giovannoni, S.J., 2013b. Spatiotemporal distributions of rare bacterioplankton populations indicate adaptive strategies in the oligotrophic ocean. *Aquatic Microbial Ecology*, **71**, 1–13.

Vergin, K.L., Jhirad N., Dodge J., Carlson C.A., and Giovannoni S.J., 2017. Marine bacterioplankton consortia follow deterministic, non-neutral community assembly rules. *Aquatic Microbial Ecology*, **79**, 165–175.

Vila-Costa, M., Rinta-Kanto J.M., Poretsky R.S., Sun, S., Kiene, R.P., and Moran, M.A., 2014. Microbial controls on DMSP degradation and DMS formation in the Sargasso Sea. *Biogeochemistry* **120**, 295–305.

Wallhead, P.J., Garçon V.C., Casey J.R., Lomas M.W., 2014. Long-term variability of phytoplankton carbon biomass in the Sargasso Sea. *Global Biogeochemical Cycles,* **28**, 825–841.

Wolverton, M., 2016. Bottom-up and top-down controls on the microzooplankton community in the Sargasso Sea. Arizona State University.

Yumruktepe, V.Ç., Salihoğlu, B., and Neuer, S., 2020. Controls on carbon export in the subtropical North Atlantic. *Progress in Oceanography*, **187**, 102380.

CHAPTER 5

Biolochemical cycles and air-sea interactions in the Sargasso Sea

D.S. Grundle, N.R. Bates, S. Murdock and R.J. Johnson

5.1 Marine biogeochemical cycles in the Sargasso Sea

N.R. Bates

The global ocean is responding to environmental change that includes warming, changes in the water (or hydrological) cycle and ocean nutrient availability (e.g., Boyce *et al.*, 2010; Singh *et al.*, 2013) that controls the growth and accumulation of marine phytoplankton which in turn provide the support for the marine food web. The response of marine ecosystems and the biogeochemistry of essential elements such as carbon, oxygen, and nutrient compounds to environmental changes demands detailed observations and improvements in understanding the crucial physical, biological and chemical processes that control them.

Long-term ocean time series are a powerful tool for investigating ocean physics and biogeochemistry, effects on the global carbon cycle, and responses to ocean change. The original and continuing theme of the BATS program has been improving our scientific understanding of the *"time-varying" components of the ocean carbon cycle and related biogenic elements of interest (e.g., carbon, nitrogen, phosphorus, silica). This also includes identifying the relevant physical, chemical and ecosystem properties responsible for this variability.* Critical evaluation of seasonal, interannual and longer-scale dynamics of vertical mixing, control of ecosystem productivity by carbon and nutrient cycles, net exchange of carbon dioxide (CO_2) between the atmosphere and the ocean, and distribution of many biogenic elements within the sea requires long–term sustained observations (Michaels and Knap, 1996).

The Bermuda Atlantic Time-series Study (BATS) project was established in the late 1980s by NSF to support the monitoring of and experimental work on the physics, chemistry, and biology of the ocean at a location approximately 85 km to the southeast of the island of Bermuda in the North Atlantic Ocean (Michaels and Knap, 1996; Steinberg *et al.*, 2001; Lomas *et al.* 2013; Bates and Johnson, 2020, 2023). Since then, the BATS site has been sampled monthly to bimonthly during more than 480 cruises to date, with laboratories, research and logistical support, and ship support (R/V *Atlantic Explorer*) based at the Bermuda Institute of Ocean Sciences (BIOS; Bates and Johnson, 2023)

5.2 Ecosystem and biogeochemistry changes in the Sargasso Sea

N.R. Bates

In the late 1950s and early 1960s, Hydrostation S data were used to define seasonal cycles and interannual variations of basic hydrography and biology of the upper ocean (Be, 1960; Menzel and Ryther, 1960). Ocean productivity theories occurred during the 1960s, when pioneering work by Menzel and Ryther (1960) and Dugdale and Goering (1967) at Hydrostation S led to the formulation of the new production concept, allowing total primary productivity to be separated into a regenerated and 'new' component. Numerous studies have recently documented the dynamics of phytoplankton (e.g., Haidar and Thierstein, 2001; Lomas *et al.*, 2013; Wang and Malanotte-Rizzoli, 2014; Krumhardt *et al.*, 2016), zooplankton (Steinberg *et al.*, 2012) and even *Sargassum* weed (e.g., Laffoley *et al.*, 2011; Huffard *et al.*, 2014). Since the late 1960's, many studies have sought to elucidate seasonal oxygen cycling (e.g., Jenkins, 1982; Jenkins and Goldman, 1985; Cianca *et al.*, 2013), inorganic nutrient dynamics (e.g., Klein and Coste, 1984; Knap *et al.*, 1986; Jickells *et al.*, 1989; Michaels *et al.*, 1993; Lipschultz *et al.*, 2002; Bates and Hansell, 2004; Palter, 2005; Lozier *et al.*, 2011; Ren *et al.*, 2012; Singh *et al.*, 2013, Fawcett *et al.*, 2014, 2015, 2018) and new/export production rates (e.g., Lomas *et al.*, 2010). The marine genomic understanding of the Sargasso Sea, prompted by the paper of Venter *et al.* (2004), has expanded to genomic discovery of bacterioplankton, virus and *Archaea* at Hydrostation S (e.g., Morris *et al.*, 2004; Biers *et al.*, 2009; Ghai *et al.*, 2010; Tucker *et al.*, 2010; Thrash *et al.*, 2010; Thrash *et al.*, 2011; Sun *et al.*, 2011; Pathak *et al.*, 2012; Treusch *et al.*, 2012;

Nelson and Carlson, 2012; Davies *et al.*, 2012; Zhao *et al.*, 2013; Vergin *et al.*, 2013a,b; Mizuno *et al.*, 2014; Carini *et al.*, 2014).

From the 1980s to the early 2000s, chlorophyll a biomass and rates of *in situ* primary production observed offshore at BATS increased overall (Lomas *et al.*, 2010; Bates, 2017; D'Alelio *et al.*, 2020) with specific taxa such as coccolithophores (calcifying phytoplankton) growing at BATS (Krumhardt *et al.*, 2016). During this timeframe, rates of primary production have almost doubled, and chlorophyll biomass has increased by ~22% per decade at BATS (Lomas *et al.*, 2013), concurrent with significant increases in zooplankton biomass (Steinberg *et al.*, 2012; Ivory *et al.*, 2019). Furthermore, nitrate values in the mixed layer almost doubled over the past two and a half decades while suspended particulate organic matter (sPOM) and dissolved organic carbon increased by ~30% and 2% per decade, respectively, to the early 2010s (Bates, 2017).

However, from the early 2000s to the present, rates of primary production have decreased by >25% (Lomas *et al.*, 2022; D'Alelio *et al.*, 2020). A significant challenge will be understanding if primary production decreases in step with warming, increased stratification, and nutrient reduction or if its reduction is mitigated to some degree by changes in ecosystem community structure (larger cells to pico-nano eukaryotes) and new nitrogen/phosphorus controls. In the subtropical gyre region of the North Atlantic Ocean, warming, salinification, deoxygenation, ocean biology changes, and acidification have accelerated in their pace of change (e.g., Bates and Johnson, 2020; Lomas *et al.*, 2022). Oceanographic data collected provide critical information about ocean changes and what these changes might mean to the future of our oceans. From the late 1980s, surface and upper ocean subtropical waters of the North Atlantic Ocean have grown warmer (+1.2°C) and saltier (+0.11), lost oxygen (~8% over the past 40 years) but gained anthropogenic carbon dioxide (CO_2; 72% increase). Ocean biology and community structure have also changed, with primary production decreasing while organic carbon export has been maintained (Lomas *et al.*, 2022; Ivory *et al.*, 2019). In the recent decade, hydrographic changes have accelerated (Bates and Johnson, 2020, 2022). Fundamental questions and challenges remain about understanding present and future ocean function, prediction and modelling. Will these changes continue into the 2020s, and how will ocean ecology and biogeochemistry respond?

5.3 Ocean deoxygenation in the Sargasso Sea

N.R. Bates

The upper-ocean record of dissolved oxygen (DO) shows a decline of ~17.8 ± 2.4 µmoles kg^{-1} over the past 40 years at the Bermuda Atlantic Time-series Study (BATS) site (Bates and Johnson, 2020; Figure 11), with short-term year-to-year variability. The loss of oxygen in the surface and the euphotic zone is ~6.6% or ~1.5% per decade (Bates and Johnson, 2023). The decline of oxygen in the Sargasso Sea over the past forty years is similar to that shown for global ocean deoxygenation (ODO) of ~2.5 to 6 µmoles kg^{-1} $decade^{-1}$) in the thermocline (Bates and Johnson, 2023) and elsewhere across the North Atlantic Ocean (Stendardo and Gruber, 2012; Montes et al., 2016).

Bates and Johnson (2020) also report the apparent oxygen utilisation (AOU) rates in the Sargasso with AOU representing the difference between measured oxygen concentration and oxygen concentration at saturation in seawater with the same physical and chemical properties. AOU, as a calculated parameter, offers a few clues as it reflects changes in oxygen due to the combined effect of biological processes such as primary production and respiration, but also diffusion, circulation, and ventilation. Bates and Johnson (2020) assumed that the contribution of nitrification and denitrification to AOU is considered minor in surface waters. The trend in AOU in the upper 500m is about −0.54 µmoles kg^{-1} $year^{-1}$, which is slightly higher than the contemporaneous decrease in DO.

Such changes in dissolved oxygen in the Sargasso Sea are synergistic with ocean warming and ocean acidification (OA). And also connected to complex causes such solubility effects (Garcia and Gordon, 1992), ocean physics and stratification (Stramma *et al.*, 2010; Stramma and Schmidko, 2019), air-sea heat exchange, gas exchange, ocean primary production (Levin and LeBris, 2015), changes in microbial production and pathways (Lonberg *et al.*, 2016), zooplankton biomass changes (Bednarsk *et al.*, 2016), and expansion of the oxygen minimum zone (Rabalais *et al.*, 2014; Duarte *et al.*, 2016).

Tagklis *et al.* (2020) have suggested a modulation of North Atlantic Ocean deoxygenation over decadal time scales. The warming of the North Atlantic increases solubility, decreasing oxygen. However, this effect is partly counteracted by the reduction of primary production and weakening of carbon export from the surface/euphotic zone and its remineralization at depth (i.e., higher oxygen levels; Tagklis *et al.* (2020). Lomas *et al.* (2022)

have shown that the stratification of the upper ocean has increased in the Sargasso Sea. Furthermore, rates of primary production have declined over the last couple of decades. In addition, Leonelli *et al.* (2021) reported that the oligotrophic gyre of the North Atlantic Ocean has expanded its area over time and suggested lower nitrate supply in winter to the region. However, despite these changes, organic carbon export have maintained their rates at a similar magnitude over the last few decades due to "nutrient trapping" below the euphotic zone. This has been postulated to occur structure, leading to increases in the stoichiometric N:P and C:P ratios of particulate matter produced through photosynthesis (Lomas *et al.*, 2022)

5.4 Export of organic matter in the Sargasso Sea

L. Blanco-Bercial and N.R. Bates

The global carbon cycle in the ocean depends on the movement of particulate organic carbon (POC) from the surface to deep waters. Depending on the depth reached by the POC and hydrographic and biological processes, it can be again transformed into carbon dioxide (CO_2) in a layer with direct exchange with the atmosphere, or it can be stored in-depth for thousands of years to geological times in a process called carbon sequestration. Only a minimal portion of the carbon captured in the epipelagic gets transferred to the deep ocean as sinking particles or actively as migrating animals below the sequestration critical depth.

5.4.1 Concepts of export production in the Sargasso Sea. Although the standing stock of marine biota in the ocean is relatively small (i.e., 3 Pg C), the biological and biogeochemical processes that influence biota, ecosystems and growth are critical to the carbon cycling and exchanges between atmosphere and ocean of the active ocean carbon reservoirs, the most significant and rapid fluxes are those associated with photosynthetic production (primary production) on the land and in the ocean (Tanhua *et al.*, 2013; Sarmiento and Gruber, 2002). Marine phytoplankton are responsible for more than a third of the total gross global photosynthetic production (i.e., 50 Pg C $year^{-1}$). In the sea, photosynthesis is limited to the euphotic zone, the upper 100–150 m of the water column where light can penetrate. Net primary production (primary production in excess of respiration) converts CO_2 to organic matter that is stored as particulate organic carbon (POC; in living and detrital particles) and as dissolved organic carbon (DOC). In stratified regions of the ocean (lower latitudes), net primary production results in a drawdown of dissolved inorganic carbon (DIC) and partial pressure of CO_2 (pCO_2), which increases pH, allows for the influx of CO_2 from the atmosphere and an accumulation of organic matter as POC and DOC.

As living biomass is produced, some particles become senescent and form sinking aggregates, while other particles are consumed by herbivores and sinking faecal pellets (POC) are produced. These sinking aggregates and pellets remove carbon from the surface to be remineralized at depth via decomposition by bacteria or consumption by zooplankton and fish. In addition, DOC produced by phytoplankton or animal excretion in surface waters can also be transported downward by subduction or convective mixing of surface waters. Finally, vertically migrating zooplankton that feed in the surface waters at night and return to deep waters during the day actively transport dissolved and particulate material to depth, where a portion is metabolized (e.g., Fasham, 2003).

The portion of organic carbon produced in the surface ocean that can be exported and remineralized back to CO_2 in the deep ocean is the most crucial factor in the exchange of CO_2 between the atmosphere and the ocean. Although approximately 80% of the globally exported carbon is POC, DOC can represent 30%–50% of carbon export in the upper 500 m of the water column at specific ocean sites.

The biological pump of carbon refers to the processes that convert CO_2 (thereby drawing down DIC) to organic matter by photosynthesis and removing organic carbon to depth (where it is respired) via sinking, mixing, and active transport mechanisms. As shown in Fig. 8, the combined effect of the solubility and biological pump increases DIC and pCO_2 and decrease pH at depth in the Pacific Ocean. Once stored at intermediate and deep parts of the ocean, CO_2 is effectively removed from an exchange with the atmosphere for centuries to thousands of years, depending on global ocean circulation patterns.

The gross export of organic matter from the surface waters is estimated at approximately 11 Pg C $year^{-1}$. Of this, only about 2% of the organic matter exported from the surface waters reaches the seafloor and is stored in the abyssal sediment. In fact, most of the exported organic matter is remineralized back to DIC in the upper 500 m of the water column and released back to the atmosphere on timescales of months to years via upwelling, mixing, or ventilation of high density water at high latitudes. It is that the fraction of exported organic matter that reaches

the deep ocean (>1000 m) that becomes important for long-term atmospheric CO_2 regulation (e.g., Sarmiento and Gruber, 2006).

The primary factors that affect the efficiency of the biological pump include nutrient supply and plankton community structure. An efficient biological pump means that export mechanisms remove a significant fraction of the system's net production and, importantly, carbon from the surface waters. Net primary production is limited by the availability of other inorganic nutrients such as nitrogen, phosphorus, silicon and iron, as well as the physical stratification of surface waters. The complexity of nutrient cycling and its supply required to support primary production (i.e., for new and regenerated production) adds uncertainty to the current understanding of the dynamics of the biological pump (e.g., Fasham, 2003).

In the ocean, food web structure also plays an essential role in determining the size distribution of the organic particles produced and whether the organic carbon and associated nutrients are exported from or recycled within the surface waters. The production of large, rapidly settling cells, faecal pellets and particles typically makes the most significant contribution to the biological pump of carbon relative to the production of small, suspended particles. Factors such as the number of trophic links, the size of the primary producers (from larger cells to smaller picoplankton), the interaction between zooplankton and phytoplankton, the processes of aggregation and disaggregation of particles in the upper ocean, and the role of bacteria and viruses in processing organic matter. All these are important factors that determine the overall contribution of sinking particles to the biological pump of carbon (e.g., Sarmiento and Gruber, 2006).

5.4.2 Carbon export in the Sargasso Sea.

In the Sargasso Sea, the flux of POC is dominated by phytoplankton-derived (phytodetrital) particles, fecal pellets (from zooplankton and nekton), and fecal aggregates (more or less degraded fecal pellets, that have attracted other particles). Meanwhile, in the fall, phytodetrital aggregates dominate the POC flux to depth; in spring, despite the large production and phytoplankton biomass, the dominant flux at depth is dominated by faecal aggregates (Cruz *et al.*, 2021). Furthermore, most of the particles shared signatures of the zooplankton microbiome, suggesting that they had already been processed or altered by the resident zooplankton in their sinking processes. The aggregation processes, mediated by zooplankton activity in different ways (direct consumption, trapped in mucus webs, etc.) or attached to larger phytodetrital aggregates, would also facilitate the contribution of pico and nanoplankton to sinking particles (Amacher *et al.*, 2013; Lomas and Moran, 2011; Lomas *et al.*, 2022;), contributing to up to 10% of the POC in the Sargasso Sea. The small size of these plankton would have limited their contribution to carbon flux otherwise, although they are one of the main contributors to primary production in the Sargasso Sea. Another zooplankton contribution to the high vertical POC flux at depth is the active (i.e., not driven by gravity alone) flux linked to diel vertical migration. When the migrators travel to the deep layers and stay there during the daytime, many still carry in their digestive system contents of epipelagic origin. The continuous digestive activity then produces in-depth, below the 500 m layer, POC in the form of faecal pellets with contents derived from surface feeding (Tarrant *et al.*, 2021).

Although only reported for *Pleuromamma xiphias* (Tarrant *et al.*, 2021), other zooplankton, such as krill, travel even to deeper layers during the daytime (Niimi *et al.*, 2022). The quantitative contribution of this active flux to depth below the sequestration horizon, relative to the total POC, is something to be addressed in the future. The particles interact with the resident community once in the mesopelagic and below. This community participates in the disaggregation and repackaging the sinking particles, sometimes reducing the flux, but others create larger particles even at depth after feeding and producing faecal pellets. Often, intact faecal pellets can be detected at 1,500 m and 3,200 m depth (Shatova *et al.*, 2012), representing ~ 5% of the measured carbon flux. Those pellets were, however, likely originated by the resident community at depth, feeding on the passing flux instead of representing those formed by the surface community or even active migrators such as *Pleuromamma xiphias* (Shatova *et al.*, 2012).

Over the last three decades, despite the ongoing environmental changes, the POC flux to the deep ocean in the Sargasso Sea has been stable (Lomas *et al.*, 2022). Despite the changes in the nutrient stoichiometry, no changes are observed in the carbon flux at BATS. The possible explanation could include a shift in the phytoplankton community towards a higher proportion of cyanobacteria, which would balance the changes in nutrient availability and stabilize the carbon flux, but also the contribution to the accelerated flux of larger zooplankton or nekton, which would have been favoured by the increasing temperatures and stratification (Lomas *et al.*,

2022). Future research on the long-term trends in POC export to the deep ocean should also include the effect of events such as tropical storms and hurricanes. Such large storms cause the mixing of the surface oligotrophic waters with the cooler and nutrient-rich deeper waters. In the Sargasso Sea, hurricanes significantly affect the POC export to the deep ocean, detectable in the 1,500 m and 3,200 m layers. The increase of phytodetrital material and particles of zooplankton origin is also accompanied by a shift in the lipid composition of the falling particles and an increase of labile compounds in the deep ocean, reflecting the link between the surface and the meso- and bathypelagic zones (Pedrosa-Pàmies *et al.*, 2018, 2019). Although these events have been generally deemed rare and have limited impact on the long-term trends, the projected increase in the frequency and intensity of storms in the subtropical North Atlantic Ocean might significantly impact the export of carbon to the deep ocean.

5.4.3 *Chlorophyll and primary production changes in the Sargasso Sea.*

From the 1980s to the early 2000s, chlorophyll biomass and rates of *in situ* primary production observed offshore at BATS increased overall (Lomas *et al.*, 2010; Bates, 2017; D'Alelio *et al.*, 2020) with specific taxa such as coccolithophores (calcifying phytoplankton) growing at BATS

(Krumhardt *et al.*, 2016). During this timeframe, rates of primary production have almost doubled, and chlorophyll biomass has increased by ~22% per decade at BATS (Lomas *et al.*, 2013), concurrent with significant increases in zooplankton biomass (Steinberg *et al.*, 2012; Ivory *et al.*, 2019). Furthermore, nitrate values in the mixed layer almost doubled over the past two and a half decades while suspended particulate organic matter (sPOM) and dissolved organic carbon increased by ~30% and 2% per decade, respectively, to the early 2010s (Bates, 2017). However, from the early 2000s to the present, rates of primary production have decreased by >25% (Lomas *et al.*, 2022; D'Alelio *et al.*, 2020). A significant challenge will be understanding if primary production decreases in step with warming, increased stratification, and nutrient reduction or if its reduction is mitigated to some degree by changes in ecosystem community structure (larger cells to pico-nano eukaryotes) and new nitrogen/phosphorus controls.

5.4.4 *Export production changes.*

One of the significant advances made during the BATS program is a re-evaluation of the ocean's Biological Carbon Pump–the suite of biological processes that mediates carbon export to the deep ocean. Export pathways that were poorly quantified a decade ago–physical export of dissolved organic carbon (DOC), active carbon transport by diel migrant zooplankton, food web influences on the partitioning of primary production between POC and dissolved organic carbon (DOC), and changes in ecosystem-level nutrient use efficiency are ensconced as significant mechanisms of carbon export to the ocean interior (e.g., Carlson *et al.*, 1994; Steinberg *et al.*, 2000, 2001; Lomas *et al.*, 2002, 2013). Notably, over the past several decades, export production has remained steady while primary production has decreased (Lomas *et al.*, 2022) with significant changes in ecosystem community structure.

More recently, glider surveys around the BATS site indicate very short-lived and patchy pulses of chlorophyll and diel migrating zooplankton biomass associated with physical signatures infer nutrient inputs and ecosystem responses (R. Curry, unpublished glider data). The hypothesis that deep ocean nutrient ratios are controlled by the elemental requirements of sinking surface plankton, resulting in similar elemental ratios in both the surface plankton communities and deep-ocean dissolved nutrients, remains a central tenet in our understanding of ocean biogeochemistry (Redfield, 1934). The assumption of constancy in C:N:P Redfield ratio in plankton biomass is being challenged by regional field observations and laboratory studies (e.g., Weber and Deutsch, 2010; Martiny *et al.*, 2013; Teng *et al.*, 2014; Lomas *et al.*, 2021) providing some understanding of the controls on these cellular ratios. The observed global C:N:P ratio mean is ~140:20:1 in particulate matter but ranges from slightly less than Redfield at the poles (~120:13:1) to nearly twice Redfield (~200:32:1) in the subtropics. Furthermore, the N:P ratio in POM ranges from ~28 to 42 seasonally in the Sargasso Sea, with the lowest values in spring.

Understanding the connections between elemental ratios in surface plankton, the residual nutrient pool in the surface ocean, and the deep nutrient pools is essential to the ocean's biogeochemistry, including, but not limited to, future predictions of the future of the biological carbon pump.

5.5 References

Amacher, J., Neuer, S., and Lomas, M., 2013. DNA-based molecular fingerprinting of eukaryotic protists and cyanobacteria contributing to sinking particle flux at the Bermuda Atlantic time series study. *Deep Sea Research Part II: Topical Studies in Oceanography*, **93**, 71–83.

Bates, N.R., 2017. Twenty years of carbon cycle observations at Devils Hole, Bermuda provide insights in seasonal hypoxia, coral reef calcification and ocean acidification. *Frontiers in Marine Science*, **4** (Article 36); February 2017; doi: 10.3389/fmars.2017.00036.

Bates, N.R., and Hansell, D.A., 2004. Temporal variability of excess nitrate in the subtropical mode water of the North Atlantic Ocean. *Marine Chemistry*, **84** (3–4), 225–241, doi:10.1016/j.marchem.2003.08.003, Jan. 2004.

Bates, N.R., and Johnson, R.J. 2020. Acceleration of ocean warming, salinification, deoxygenation and acidification in the surface subtropical North Atlantic Ocean. *Nature Communications in Earth and Environment*, **1**, 33.

Bates, N.R., and Johnson, R.J., 2022. Ocean observing in the North Atlantic subtropical gyre. *Oceanography*, 34(4), 32–33.

Bates, N.R., and Johnson, R.J., 2023. Forty years of ocean acidification observations (1983–2023) in the Sargasso Sea at the Bermuda Atlantic Time-series Study (BATS) site. *Frontiers in Marine Science*.

Be, A.W.H., 1960. Ecology of recent planktonic foraminifera: Part 2-Bathymetric and seasonal distributions in the Sargasso Sea off Bermuda. *Micropalaentology*, **6**, 373–392.

Bednarsek, N., Harvey, C.J., Kaplan, I.C., Feely, R.A. and Mözma, J., 2016. Pteropods on the edge: Cumulative effects of ocean acidification, warming and deoxygenation. *Progress in Oceanography*, **145**, 1–24.

Boyce, D.G., Lewis, M.R., and Worm, B., 2010. Global phytoplankton decline over the past century. *Nature*, **466**, 591–596.

Carini, P., Campbell, E. O., Morré, J., Sañudo-Wilhelmy, S. A., Thrash, J. C., Bennett, S. E., and Giovannoni, S.J., 2014. Discovery of a SAR11 growth requirement for thiamin's pyrimidine precursor and its distribution in the Sargasso Sea. *The ISME journal*, **8**(8), 1727–1738.

Cianca, A., Santana, R., Hartman, S.E., Martin–Gonzalez, J.M., Gonzalez–Davila, M., Rueda, M.J., Llinas, O., and Neuer, S., 2013. Oxygen dynamics in the North Atlantic subtropical gyre. *Deep Sea Research*, **93**, 135–147.

Cruz, B.N., Brozak, S., and Neuer, S., 2021. Microscopy and DNA-based characterization of sinking particles at the Bermuda Atlantic Time-series Study station point to zooplankton mediation of particle flux. *Limnology and Oceanography*, **66**, 3697–3713.

D'Alelio, D., Rampone, S., Cusano, L.M., *et al.*, 2020. Machine learning identifies a strong association between warming and reduced primary productivity in an oligotrophic ocean gyre. *Scientific reports*, **10**, 3287.

Davies, N., Field, D., and The Genomic Observatories Network, 2012. Sequencing data: A genomic network to monitor Earth. *Nature*, **481**, 145, doi: 10.1038/481145a (11 January 2012).

Dugdale, R.C., Goering J.J. and Ryther R.H., 1967. High nitrogen fixation rates in the Sargasso Sea and Arabian Sea. *Limnol. Oceanogr.*, **9**, 507–510.

Duarte, C.N., Fulweiler, R.W., Lovelock, C.E., Martinetto, P., Saunders, M.I., Pandolfi, J.M., Gelcich, S., and Nixon, S.W., 2016. Reconsidering ocean calamities. *BioScience*, **65** (2), 130–139.

Fasham, M.J.R., 2003. *Ocean biogeochemistry: The role of the ocean carbon cycle in global change*. Berlin: Springer.

Fawcett, S.E., Lomas, M.W., Ward, B.E., and Sigman, D.M., 2014. The counterintuitive effect of summer –to-fall mixed layer deepening on eukaryotic new production in the Sargasso Sea. *Global Biogeochemical Cycles*, **28**, 86–102, doi:10.1002/2013GB004579.

Fawcett, S.E., Ward, B.B., Lomas, M.W., and Sigman, D.M., 2015. Vertical decoupling of nitrate assimilation and nitrification in the Sargasso Sea. *Deep Sea Research Part I: Oceanographic Research Papers* **103**, 64–72.

Fawcett, S.E., Johnson, K.S., Riser, S.C., Van Oostende, N., and Sigman, D.M., 2018. Low nutrient organic matter in the Sargasso Sea thermocline: A hypothesis for its role, identity and carbon cycle implications. *Marine Chemistry*, **207**, 108–133.

Garcia, H.E., and Gordon, L.I., 1992. Oxygen solubility in seawater: Better fitting equations. *Limnology and Oceanography*, **37** (6), 1307–1312.

Ghai, R., Martin-Cuadrado, Gonzaga, M., Heredia, I.G., Cabrera, R., Martin, J., Verdu, M., Deschamps, P., Moreira, D., Lopez-Garcia, P., Mira, A. and Rodriguez-Valera, F., 2010. Metagenome of the Mediterranean deep chlorophyll maximum studied and fosmid library 454 pyrosequencing. *International Society for Microbial Ecology*, **4**, 1154–1166.

Haidar, A.T., and Thierstein, H.R., 2001. Coccolithophore dynamics off Bermuda (N. Atlantic). *Deep-Sea Research II*, **48**, 1925–1956.

Helmke, P., Neuer, S., Lomas, M.W., Conte, M., and Freudenthal, T., 2010. Cross-basin differences in particulate organic carbon export and flux attenuation in the subtropical North Atlantic gyre. *Deep Sea Research Part I: Oceanographic Research Papers*, **57**, 213–227.

Huffard, C.L., von Thun, S., Sherman, A.D., Sealey, K., and Smith, Jr, K.L., 2014. Pelagic Sargassum community change over a 40-year period: temporal and spatial variability. *Marine Biology*, **161** (12), 2735–2751.

Ivory JA, Steinberg DK, Latour RJ (2019). Diel, seasonal, and interannual patterns in mesozooplankton abundance in the Sargasso Sea. *ICES Journal of Marine Science* **76**, 217–231.

Jenkins, W.R., 1982. On the climate of a subtropical ocean gyre: decade timescale variations in water mass renewal in the Sargasso Sea. *Journal Marine of Research Supplement*, **40**: 265–290.

Jenkins, W.R. and Goldman, J.C., 1985. Seasonal oxygen cycling and primary production in the Sargasso Sea. *Journal of Marine Research*. **43**:465–491.

Jickells, T.D., Knap, A.H., Sherriff-Dow, R. and Galloway, J.N., 1989. No ecosystem shift. *Nature*, **347**, 25–26.

Knap, A.H., Jickells, T.D., Pszenny, A. and Galloway, J.N., 1986. The significance of atmospheric derived fixed nitrogen on the productivity of the Sargasso Sea. *Nature*, **320**, 158–160.

Krumhardt, K.M., Lovenduski, N.S., Freeman, N.M., and Bates, N.R., 2016. Increasing coccolithophore abundance in the subtropical North Atlantic from 1994 to 2014. *Biogeosciences*, **13** (4) 1163–1177.

Laffoley, D. d'A., Roe, H.S.J., Angel, M.V., Ardron, J., Bates, N.R., Boyd, I.L., Brooke, S., Buck, K.N., Carlson, C.A., Causey, B., Conte, M.H., Christiansen, S., Cleary, J., Donnelly, J., Earle, S.A., Edwards, R., Gjerde, K.M., Giovannoni, S.J., Gulick, S., Gollock, M., Hallet, J., Halpin, P., Hanel, R., Hemphill, A., Johnson, R.J., Knap, A.H., Lomas, M.W., McKenna, S.A., Miller, M.J., Miller, P., Ming, F.W., Moffitt, R., Nelson, N.B., Parson, L., Peters, A.J., Pitt, J., Rouja, P., Roberts, J., Roberts, J., Seigel, D.A., Siuda, A., Steinberg, D.K., Stevenson, A., Sumaila, V.R., Swartz, W., Trott, T.M., and Vats. V., 2011. *The protection and management of the Sargasso Sea: The golden floating rainforest of the Atlantic Ocean: Summary Science and Supporting Evidence Case.* Sargasso Sea Alliance, 44 pp.

Leonelli, F.E., Bellicicco, M., Organelli, E., Buongiorno Nardelli, B., de Toma, V., Cammarota, C., Marullo, S., and Santoleri, R., 2021. Ultra-oligotrophic expansion in the North Atlantic subtropical gyre relvealed by 21 years of satellite observations. *Geophysical Research Letters*, **49**, 21, e2021GL096965.

Levin, L.A., and LeBris, N., 2015. The deep ocean under climate change. *Science*, **350**, 766–768.

Lipschultz, F.J., Bates, N.R., Carlson, C.A., and Hansell, D.A., 2002. New production in the Sargasso Sea: History and current status. *Global Biogeochemical Cycles*, **16** (1), 1001, doi:10.1029/2000GB001319, Mar. 2002.

Lomas, M.W., and Moran, S.B., 2011. Evidence for aggregation and export of cyanobacteria and nano-eukaryotes from the Sargasso Sea euphotic zone. *Biogeosciences*, **8**, 203–216.

Lomas, M., Bates, N.R., Knap, A.H., Karl, D.A., Lukas, R., Landry, M.R., Bidigare, R.R., Steinberg, D.K., and Carlson, C.A., 2002. Refining our understanding of ocean biogeochemistry and ecosystem functioning. *EOS*, November 2002.

Lomas, M.W., Steinberg, D.K., Dickey, T.D., Carlson, C.A., Nelson, N.B., Condon, R.H., and Bates, N.R., 2010. Increased ocean carbon export in the Sargasso Sea is countered by its enhanced mesopelagic attenuation. *Biogeosciences*, **7** (1), 57–70.

Lomas, M.W., Bates, N.R., Johnson, R.J., Knap, A.H, Steinberg, D.K., Carlson, C.A., 2013. Two decades and counting: 23–years of sustained open ocean biogeochemical measurements in the Sargasso Sea. *Deep–Sea Research II*, 93, 16–32, doi: 10.1016/j.dsr2.2013.01.008. Lomas *et al.*, 2021

Lomas, M.W., Bates, N.R., Johnson, R.J., Steinberg, D.K., Tanioka, T., 2022. Adaptive carbon export response to warming in the Sargasso Sea. *Nature Communications*, **13**, 1211.

Lønborg, C., Cuevas, L.A., Reinthaler, T., Herndl, G.J., Gasol, J., Alvarez–Salgado, X., and Bates, N.R., 2016. Temperature dependence of prokaryotic production. *Frontiers in Marine Science*, **3** (131), doi: 10.3389/fmars.2016.00090.

Lozier, M.S., Dave, A.C., Palter, J.B., Gerber, L.M. and Barber, R.T., 2011. On the relationship between stratification and primary productivity in the North Atlantic. *Geophysical Research Letters*, **38**, LI8609, doi:10.1029/2011GL049414.

Martiny, A.C., Vrugt, J.A., Primeau, F.W., and Lomas, M.W., 2013. Regional variation in the particulate organic carbon to nitrogen ration in the surface ocean. *Global Biogeochemical Cycles*, **27** (3), 723–731.

Menzel, D.W. and Ryther, J.H., 1960. The annual cycle of primary production in the Sargasso Sea off Bermuda. *Deep Sea Res.*, **6**, 351–367.

Michaels, A. F., Siegel, D.A., Johnson, R.J., Knap, A.H. and Galloway, J.N., 1993. Episodic inputs of atmospheric nitrogen to the Sargasso Sea: Contributions to new production and phytoplankton blooms. *Global Biogeochem. Cycles*, **7**, 339–351.

Michaels, A.F and Knap, A.H., 1996. Overview of the US JGOFS Bermuda Atlantic Time-series Study and the Hydrostation S program. *Deep-Sea Research Part II-Topical Studies in Oceanography*, **43**, 157–198.

Mizuno, C.M., Ghai, R., and Rodriguez-Valera, F., 2014. Evidence for metaviromic islands in marine phages. *Frontiers in Microbiology*, **5**, doi:10.3389/fmicb.2014.00027.

Montes, E., Muller-Karger, F.E., Cianca, A., Lomas, M.W., Lorenzoni, L., and Habtes, S., 2016. Decadal variability in the oxygen inventory of North Atlantic subtropical underwater captured by sustained, long-term oceanographic time series observations. *Global Biogeochemical Cycles*, **30** (3), 460–478.

Morris, R.M., M.S. Rappe, E. Urbach, S.A. Connon, and Giovannoni, S.J., 2004. Prevalence of the Chloroflexi-related SAR202 bacterioplankton cluster throughout the mesopelagic zone and deep ocean. *Applied and Environmental Microbiology* **70**, 2836–2842.

Nelson, C.E. and Carlson, C.A., 2012. Tracking differential incorporation of dissolved organic carbon types among diverse lineages of Sargasso Sea bacterioplankton. *Environmental Microbiology*, **14** (6), doi: 10.1111/j.1462-920.2012.02738.x

Niimi, Y., Blanco-Bercial, L., Maas, A.E., *et al.*, 2022. Merging integrative taxonomy and the biogeochemical contributions of the Euphausiids in the Sargasso Sea. In: *2022 Ocean Sciences Meeting*, Hawaii.

Palter J.B., Lozier M.S. and Barber R.T., 2005. The effect of advection on the nutrient reservoir in the North Atlantic subtropical gyre. *Nature*, **437**, 687–692.

Pathak, G.P., Losi, A. and Gartner, W., 2012. Metagenome-based screening reveals worldwide distribution of LOV-domain proteins. *Photochemistry and Photobiology*, **88**, 107-118.

Pedrosa-Pàmies, R., Conte, M.H., Weber, J.C., Johnson R., 2018. Carbon cycling in the Sargasso Sea water column: Insights from lipid biomarkers in suspended particles. *Progress in Oceanography*, **168**, 248–278.

Pedrosa-Pàmies, R, Conte, M.H., Weber, J.C., and Johnson, R., 2019. Hurricanes enhance labile carbon export to the deep ocean. *Geophysical Research Letters*, **46**, 10484–10494.

Rabalais, N.N., Cai, W.-J., Carstensen, J., Conley, D.J., Fry, B., Hu, X., Quiñones-Rivera, Z., Rosenberg, R., Slomp, C.P., Turner, E.R., Voss, M., Wissel, B., and Zhang, J., 2014. Eutrophication-driven deoxygenation in the coastal ocean. *Oceanography*, **27**, 172-182.

Redfield, A.C., 1934. On the proportions of organic derivatives in seawater and their relation to the composition of plankton. *James Johnstone memorial volume*, 176–192.

Ren, H., Sigman, D.M., Thunell, R.C., and Prokopenko, M.G., 2012. Nitrogen isotopic composition of planktonic foraminifera from the modern ocean and recent sediments. *Limnol. Oceanogr.*, **57**(4), 1011–1024, doi:10.4319/lo.2012.57.4.1011.

Singh, A., Lomas, M.W., and Bates, N.R., 2013. Revisiting N_2 fixation in the North Atlantic Ocean: Significance of Redfield ratio and climate variability. *Deep-Sea Research II*, **93**, 148–158, doi: 10.1016/j.dsr2.2013.04.008.

Shatova, O., Koweek, D., Conte, M.H., and Weber, J.C., 2012. Contribution of zooplankton fecal pellets to deep ocean particle flux in the Sargasso Sea assessed using quantitative image analysis. *Journal of Plankton Research*, **34**, 905–921.

Steinberg, D.K., Carlson, C.A., Bates, N.R., Goldthwait, S.A., Madin, L.P., and Michaels, A.F., 2000. Zooplankton vertical migration and the active transport of dissolved organic and inorganic carbon in the Sargasso Sea. *Deep–Sea Research I*, **47**, 137–158, doi:10.1016/S0967–0637(99)00052–7, Jan. 2000.

Steinberg, D.K, Carlson, C.A., Bates, N.R., Johnson, R.J., Michaels, A.F., and Knap, A.H., 2001. Overview of the US JGOFS Bermuda Atlantic Time–series Study (BATS): a decade–scale look at ocean biology and biogeochemistry. *Deep–Sea Research II*, **48** (8–9), 1405–1447, doi:10.1016/S0967–0645(00)00148–X.

Steinberg, D.K., Lomas, M.W., and Cope, J.S., 2012. Long-term increase in mesozooplankton biomass in the Sargasso Sea: Linkage to climate and implications for food web dynamics and biogeochemical cycling. *Global Biogeochemical Cycles*, **26**, GB1004.

Stendardo, I., and Gruber, N., 2012. Oxygen trends over five decades in the North Atlantic. *Journal of Geophysical Research*, **117**, C111.

Stone J.P., and Steinberg D.K, 2014. Long-term time-series study of salp population dynamics in the Sargasso Sea. Marine Ecology Progress Series, **510**, 111–127.

Stone J.P., and Steinberg D.K., 2016. Salp contributions to vertical carbon flux in the Sargasso Sea. *Deep Sea Research Part I: Oceanographic Research Papers*, 113, 90-100.

Stramma, L., Schmidtko, S., Levin, L.A. and Johnson, G.C., 2010. Ocean oxygen minima expansions and their biological impacts. *Deep Sea Res. Part I*, 57, 587–595.

Stramma, L., and Schmidtko, S., 2019. Global evidence of deoxygenation. in *Ocean Deoxygenation: Everyone's Problem*. (editors Laffoley, D., and Baxter, J. M.) 25–36, (IUCN).

Sun, J., Steindler, L., Thrash, J.C., Halsey, K.H., and Smith, D.P., 2011. One carbon metabolism in SAR11 pelagic marine bacteria. *PLoS ONE 6*(8), e23973, doi:10.1371/journal.pone.0023973.

Tagklis, F., Ito, T., and Bracco, A., 2020. Modulation of the North Atlantic deoxygenation by the slowdown of the nutrient stream. *Biogeosciences*, **17**, 231.

Tanhua, T., Bates, N.R., and Kortzinger, A., 2013. The marine carbon cycle and ocean anthropogenic CO_2 inventories. In: *Ocean Circulation and Climate* (J. Church *et al.*), **103**, http://dx.doi.org/10.1016/B978-0-12-391851-2.00030-1, Elsevier Press.

Tarrant, A.M., McNamara-Bordewick, N., Blanco-Bercial, L., Miccoli, A., and Maas, A.E., 2021. Diel metabolic patterns in a migratory oceanic copepod. *Journal of Experimental Marine Biology and Ecology*, **545**, 151643.

Teng, Y.C., Primeau, F.W., Moore, J.K., Lomas, M.W., and Martiny, A.C., 2014. Global-scale variations of the ratio of carbon to phosphorus in exported marine organic matter. *Nature Geoscience*, **7**, 895–898.

Thrash, C.J., Stingl, U., Cho, J-C., Ferriera, S., Johnson, J., Vergin, K.L. and Giovannoni, S.J., 2010. Genome sequence of the novel marine member of the *Gammaproteobaacteria* strain HTCC5015. *Journal of Bacteriology*, July 2010, 3838–3839.

Thrash, C.J., Cho, J-C., Bertabnolli, A.D., Ferriera, S., Johnson, J., Vergin, K.L. and Giovannoni, S., 2011. Genome sequence of the marine Janibacter Sp. Strain HTCC2649. *Journal of bacteriology*, January 2011, 584–585.

Treusch, A.H., Demir-Hilton, E., Vergin, K.L., *et al.* 2012. Phytoplankton distribution patterns in the northwestern Sargasso Sea revealed by small subunit rRNA genes from plastids. *The ISME Journal*, **6**, 481–492.

Tucker, K.P., Parsons, R., Symonds, E.M. and Breitbart, M., 2010. Diversity and distribution of single-stranded DNA phages in the North Atlantic Ocean. *International Society of Microbial Ecology*, December 2010, doi:10.1038/ismej.2010.188.

Venter, J.C., Remington, K, Heidelberg, J.F, A.L.Halpern, Rusch, D., Eisen, J.A., Wu, D., Paulsen, I., Nelson, K., Nelson, W., Fouts, D.E., Levy, S., Knap, A.H., Lomas, M.W., Nealson, K., White, O., Peterson, J., Hoffman, J., Parsons, R., Baden-Tillson, H., Pfannkock, C., Rogers, Y. and Smith, H.O., 2004. Environmental genome shotgun sequencing of the Sargasso Sea. *Science*, **304**, 5667, 66–74.

Vergin, K.L., Beszteri, B., Monier, A., Thrash, J.C., Temperton, B., Treusch, A.H., Kilpert, F., Worden, A.Z., and Giovannoni, S.J., 2013. High-resolution SAR11 ecotype dymnamics at the Bermuda Atlantic Time-series Study site by phylogenetic placement of pyrosequences. *Nature, the ISME Journal*, **7**, 1322–1332.

Vergin, K.L., Done, B., Carlson, C.A., and Giovannoni, S.J., 2013. Spatiotemporal distributions of rare bacterioplankton populations indicate adaptive strategies in the oligotrophic ocean. *Aquatic Microbial Ecology*, **71**, 1–13.

Wang, C., and Malanotte-Rizzoli, P., 2014. Diagnosis of physical and biological control over phytoplankton in the Gulf of Maine-Georges Bank region using an adjoint assimilation approach. *Journal of Ocean University China*, **13**, 356–368.

Weber, T.S., and Deutsch, C., 2010. Ocean nutrient ratios governed by plankton biogeography. *Nature*, **467**, 550–554.

Zhao, Y., Tempertin, B., Thrash, J.C., Schwalbach, M.S., Vergin, K., Landry, Z.C., Ellisman, M., Deerinck, T., Sullivan, M.B and Giovannoni, S.J., 2013. Abundant SAR11 viruses in the ocean. *Nature*, **494** (7437), doi:10.1038/nature11921.

CHAPTER 6

The marine carbon cycle and ocean acidification

N.R. Bates

6.1 Introduction

N.R. Bates

The question of why carbon is an essential and critical element is relevant to understanding the Sargasso Sea marine carbon cycle and the global carbon cycle (e.g., Schlesinger, 1997; Fasham, 2003). As an element and constituent of numerous types of chemical forms, carbon has several unique properties that make it a necessary component of life, energy flow, chemical equilibria and regulation of aqueous and marine systems and climate regulation.

Carbon is found in the Earth system in many different inorganic and organic forms. Importantly, it forms complex, stable carbon compounds, such as proteins and carbohydrates, which are the fundamental building blocks of life. Photosynthesis provides marine plants (phytoplankton) with the ability to transform energy from sunlight and transform carbon dioxide (CO_2) into organic matter. In the ocean, photosynthesis by pelagic phytoplankton primarily converts inorganic carbon and nutrients into complex organic carbon materials and influences the CO_2-carbonate chemical system (e.g., Zeebe and Wolf-Gladrow, 2003; Dickson *et al.*, 2007; Millero, 2013), the pH of seawater and uptake of anthropogenic CO_2 (e.g., Sabine *et al.*, 2004; DeVries *et al.*, 2019; Gruber *et al.*, 2019), and exchange of CO_2 (and other gases) at the air-sea interface (e.g., Wanninkhof, 1999; Takahashi *et al.*, 2009; Liss and Johnson, 2014; Bakker *et al.*, 2016). All organisms, including autotrophs and heterotrophs, then catabolize these organic compounds to their inorganic constituents via respiration, yielding energy for their metabolic requirements. As discussed in Chapter Four, the evolution of molecular biology/genomic tools and "big data" synthesis have produced new insights into the microbial ecology of the global ocean, including the Sargasso Sea (Moran *et al.*, 2022). Production, consumption, flow and transformation of these organic materials provide energy and resources for all trophic states of the ocean ecosystem, including higher trophic levels of juvenile fish to marine mammals.

Carbon in its inorganic gaseous phases such as carbon dioxide (CO_2), carbon monoxide (CO), and methane (CH_4). Each of these gases has important greenhouse properties that influence the climate system. Such greenhouse gases, including water vapour in the atmosphere, alter the balance of energy inputs and outputs in the Earth system. As a result of the natural occurrence of greenhouse gases, the lower part of the Earth's atmosphere warms, critical for maintaining liquid water and life on Earth. In the last century, human activities have caused a rapid increase in greenhouse gas concentrations in the atmosphere, thereby impacting the world's climate through the effects of global warming and its myriad impacts (e.g., global water cycle changes, sea level rise, reduction of sea ice and the cryosphere glacial ice mass; e.g., Schlesinger, 1997; Fasham, 2003; Mackenzie and Lerman, 2010). As discussed earlier in chapter three, changes in the climate system have also contributed to the warming of the global ocean and +1.2°C warming of the Sargasso Sea (Bates and Johnson, 2020), salinification, and deoxygenation of the subtropical gyre.

Carbon dioxide also has a profound impact on seawater chemistry, with impacts already reported for the Sargasso Sea. Anthropogenic carbon uptake by the ocean has also changed ocean chemistry by absorbing CO_2 in a gradual process termed ocean acidification (e.g., Caldeira and Wickett, 2003; Doney *et al.*, 2009). In the past few decades, international research efforts have substantially improved scientific understanding of the global carbon cycle, and in particular, the functioning and dynamics of the global ocean carbon cycle and the impact and effects of ocean acidification (Riebesall *et al.*, 2010; Gattuso and Hansson, 2011).

In the marine environment, biological and chemical processes react to global environmental change and influence climate by helping to regulate the concentration of CO_2 in the atmosphere (e.g., Mackenzie and Lerman, 2010; Figure 6.1). The following topics are discussed, including (1) the critical importance of the ocean to the global carbon cycle (Sarmiento and Gruber, 2002, 2006; Bates, 2019; Bakker *et al.*, 2016; Friedlingstein *et al.*, 2020, 2022; 2023); (2) the ocean carbon cycle, the chemistry

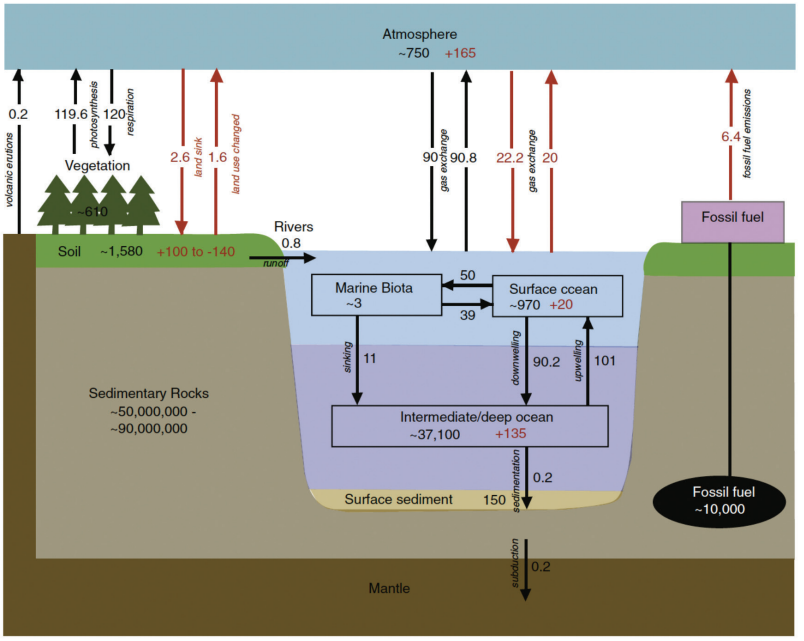

FIGURE 6.1. **Reservoirs and fluxes of carbon in the earth system. The values and arrows denote size of reservoir and fluxes of the natural carbon cycle are denoted in black. The values and arrows denote size of reservoir and fluxes of the perturbed carbon cycle are denoted in red. Figure prepared by N.R. Bates and modified from various sources (e.g., Sarmiento, J. L. and Gruber, N. (2002). Sinks for anthropogenic carbon. Physics Today 55 (8), 30, https://doi.org/10.1063/1.1510279; Mackenzie, F.T. and Lerman, A. (2010). Carbon in the geobiosphere: Earth's outer shell. Dordrecht: Springer, pp. 402; Tanhua, T., Bates, N.R., and Kortzinger, A. (2013). The marine carbon cycle and ocean anthropogenic CO_2 inventories, In: Ocean circulation and climate, J. Church et al. (eds). Elsevier Press: Amsterdam, pp. 103.**

of carbon dioxide in seawater and ocean acidification; (3) the mechanisms of carbon exchange between the ocean and atmosphere; (4) recent perturbations in the marine carbon cycle of the Sargasso Sea and, (5) the roles of the "solubility," "biological," and "carbonate" pumps in the ocean carbon cycle.

6.2 The global carbon cycle

N.R. Bates

There are complex transformations and fluxes of inorganic and organic carbon between the major components of the Earth system. Carbon, in its various forms, is stored in four primary Earth system reservoirs (or pools), including the atmosphere, lithosphere, biosphere, and hydrosphere (Mackenzie and Lerman, 2010; Williams and Follows, 2011). Each carbon reservoir contains various organic and inorganic carbon compounds ranging in size and mobility within the sediment-atmosphere-terrestrial biosphere-ocean system. The exchange and storage times for each carbon reservoir can vary from hours (in the case of ocean production of organic matter and its remineralization by bacteria, Moran *et al.*, 2022) to millions of years (in the case of many sediments and rocks).

The lithosphere contains the most substantial amount of carbon (10^{23} g C), which is primarily buried in the form of calcium carbonate ($CaCO_3$) minerals (e.g., $CaCO_3$, $CaMgCO_3$, and $FeCO_3$) found in siliciclastic and limestone sediments (Figure 6.1). It also contains organic compounds such as oil, natural gas, and coal (fossil fuels), which have been mobilized in the age of the Anthropocene. Carbon in the lithosphere is generally transformed into other carbon reservoirs. This occurs on timescales of millions of years and through slow geological processes such as chemical weathering (e.g., predominantly siliciclastic rocks such as igneous and metamorphic, and carbonate rocks such as limestones), sedimentation, subduction, and volcanic eruptions (i.e., smaller fluxes each year; Figure 6.1). The lithosphere is considered a relatively inactive component of the global carbon cycle (although fossil fuels have been added to the active reservoirs at high rates during the last century) and not contributing to societally relevant climate and environmental changes in the Anthropocene.

The Earth's active carbon reservoirs contain approximately ~41,000 Pg of carbon (1 Pg = 1015 g C), which is partitioned between the atmosphere (~750 Pg C), the terrestrial biosphere (~2,200 Pg C), and the ocean (~38,070 Pg C; Figure 6.1). The absolute sum of carbon found in the active reservoirs of carbon is in near steady state by slow geological processes. But rapid biogeochemical processes over societally relevant time-scales are driving the redistribution of carbon among the active reservoirs.

Human activities over the past century, such as the use of fossil fuels, cement manufacture, deforestation and terrestrial habitat changes, have substantially increased the total amount of carbon stored in the atmosphere.

Furthermore, perturbed the exchanges of carbon between the atmosphere, the terrestrial biosphere, and the ocean (Figure 6.1; Mackenzie and Lerman, 2010; Williams and Follows, 2011). In particular, the release of CO_2 from fossil fuel use, cement manufacture, and deforestation since the beinning of the industrial age (nineteenth century) has increased the partial pressure of atmospheric CO_2 from 280 ppm to present-day values of 400 ppm, an increase of ~30% in the last century (Figure 6.1; Sabine *et al.*, 2004; Gruber et al., 2019).

In the era of the Anthropocene, human activities currently cause the release of approximately 6–8 Pg of "anthropogenic" carbon into the atmosphere every year. About half of the anthropogenic CO_2 remains in the atmosphere, while the residual carbon is transferred to the ocean and the terrestrial biosphere. Those carbon reservoirs that remove and sequester CO_2 from the atmosphere are called active carbon "sinks" on societally relevant timescales (Figure 6.1; Mackenzie and Lerman, 2010). The partitioning of anthropogenic carbon dioxide between the functional oceanic and terrestrial sinks is challenging to quantify yearly.

Quantifying controls on the partitioning is necessary for understanding the dynamics and complexities of the global carbon cycle. Oceanographers estimate that 70% of the anthropogenic CO_2 is absorbed by the ocean each year, based on current understanding of ocean circulation and ecosystem processes, and the remainder by the terrestrial biosphere. The best estimate of the ocean's present amount of anthropogenic carbon is ~155 Pg C in 2010, representing only about 45% of the cumulative fossil fuel emissions of 350 Pg C in 2009 (Sabine *et al.*, 2004; Sarmiento and Gruber, 2006). From our knowledge of seawater CO_2 chemistry and the timescale of ocean ventilation, it can be predicted that millennia from now, in a future steady state, the ocean will account for the storage of approximately 80% of all cumulative emissions of anthropogenic CO_2. This fraction will be further enhanced toward 95% when equilibration with carbonate sediments is also considered (e.g., Mackenzie and Lerman, 2010). The marine carbon cycle is a critical elemental cycle of the ocean and, due to its interaction with the atmospheric CO_2 concentration, is of fundamental importance for the Earth's climate. Quantifying the magnitude of the oceanic sink for anthropogenic CO_2 is dependent on understanding the interplay of various chemical, physical, and biological factors influencing the global ocean. Future improvement of knowledge about ocean carbon cycle dynamics, in turn, helps constrain knowledge about the uptake of anthropogenic carbon into the terrestrial biosphere.

6.3 The ocean carbon cycle and carbon dioxide chemistry

N.R. Bates

If we ignore the comparatively inert (on timescales relevant to the Anthropocene) lithospheric carbon pools, the ocean is the largest carbon reservoir of the atmosphere–terrestrial biosphere– ocean system. Ocean carbon occurs in different inorganic and organic forms, including dissolved CO_2, bicarbonate (HCO_3^-), carbonate (CO_3^{2-}) and organic carbon compounds. The preindustrial ocean contained more than 60 times as much inorganic carbon as the atmosphere. This large reservoir and its complicated internal ocean dynamics are the primary influence on the atmospheric CO_2 content over time scales of centuries and millennia. Therefore, even small changes in the natural components of the marine carbon cycle may be expected under the evolving anthropogenic forcing through changes known as ocean warming, ocean eutrophication, ocean acidification, and ocean deoxygenation, bear the potential to significant feedback to the Earth's climate system. The large size of the marine carbon reservoir relative to the atmosphere and the fact that CO_2 is one of the most soluble of the major gases in seawater results in the global ocean having a substantial capacity to absorb CO_2 and buffer changes in the atmospheric CO_2 content, including anthropogenic CO_2 (e.g., Mackenzie and Lerman, 2010; Sarmiento and Gruber, 2006; Williams and Follows, 2011; Bates, 2019).

The chemistry of carbon dioxide in seawater gives rise to a rather complex chemical system, often called the seawater CO_2-carbonate system (or marine CO_2 system or marine carbonate system). The seawater CO_2-carbonate system is responsible for ~95% of the acid-base buffering capacity of seawater. This equilibria chemistry essentially controls the pH of seawater (e.g., Zeebe and Wolf-Gladrow, 2001; Millero, 2013). As a basis for understanding the seawater CO_2.carbonate system in the Sargasso Sea and its changes over the last few decades, it is essential to understand the basic concepts of the chemical equilibria of CO_2 in seawater. For example, relatively small changes in the proportion of bicarbonate (HCO_3^-) and carbonate (CO_3^{2-}) have a substantial impact on pH, the activity of hydrogen ions and calcium carbonate ($CaCO_3$) mineral saturation states. And, in turn, on direct and indirect influence on ocean biology and ecosystems.

The chemical basis of the seawater CO_2-carbonate system is the hydration reaction of CO_2 with water to form carbonic acid (H_2CO_3) and subsequent dissociation chemical reactions. This hydration reaction is slow, and most of the CO_2 in seawater remains in a physically dissolved state rather than in the combined form of carbonic acid. The marine carbonate system thus encompasses four inorganic carbon species, CO_2, H_2CO_3, HCO_3^-, and carbonate CO_3^{2-}, which are connected through chemical equilibria that have been thermodynamically characterized to a high degree of accuracy. The concentration of dissolved CO_2 in seawater is relatively minor because CO_2 reacts with water to form a weak acid, carbonic acid (H_2CO_3). As a diprotic acid, H_2CO_3 rapidly dissociates (within milliseconds) in two steps, which leads to the formation of two ionic species, bicarbonate (HCO_3^-) and carbonate (CO_3^{2-}). The speciation within this acid-base system is a function of pH. These reactions provide a chemical buffer, maintain the pH of the ocean within a small range, and constrain the amount of atmospheric CO_2 that can be taken up by the ocean (e.g., Zeebe and Wolf-Gladrow, 2001; Dickson *et al.*, 2007).

In simple terms, for every 20 molecules of CO_2 absorbed by the ocean, 19 molecules are rapidly converted to HCO_3^- and CO_3^{2-}. Over the relatively narrow pH range of seawater (approximately 7.8 to 8.2), most inorganic carbon is found in the form of HCO_3^- (~90%), followed by CO_3^{2-} (~10%) and finally CO_2/H_2CO_3 (<1%). The concentration of inorganic carbon species and other chemical species of interest (e.g., H^+, OH^-, BO_4) are expressed in the form of $[CO_2]$, $[H_2CO_3]$, $[HCO_3^-]$, $[CO_32-]$ and $[H^+]$ with the brackets denoting chemical concentration (e.g., Zeebe and Wolf-Gladrow, 2001; Millero, 2013).

The amount of dissolved CO_2 in seawater (i.e., $[CO_2]$ cannot be directly determined analytically (Dickson *et al.*, 2007). However, the chemical characterization of the seawater CO_2-carbonate system is achieved through a knowledge of acid-base equilibrium and kinetics and measurement of two of four commonly observable carbonate parameters, such as (1) dissolved inorganic carbon (DIC); (2) total alkalinity (TA); (3) pH (i.e., $-\log_{10} H^+$); and, (4) partial pressure or fugacity of CO_2 (i.e., pCO_2 or fCO_2), and temperature, salinity, and pressure data (with relevance to the Sargasso Sea, please see Bates *et al.*, 1996 a,b; Bates *et al.*, 2014; Bates and Johnson, 2020).

Seawater DIC refers to the total amount of CO_2, HCO_3^- and CO_3^{2-} in seawater. The alkalinity of seawater (i.e., TA) is a measure of the bases present in seawater, consisting mainly of HCO_3^-, and CO_3^{2-} (e.g., TA is ~$[HCO_3^-]$ + 2$[CO_3^{2-}]$, plus minor constituents such as borate (BO_4) and hydrogen ions (H^+). The pCO_2 or fCO_2 of seawater measures the contribution of CO_2 to total gas pressure. Of the four measurable parameters, pCO_2 or fCO_2, and pH are highly influenced by temperature and pressure changes in the ocean, while DIC and TA are independent of such environmental changes (e.g., Zeebe and Wolf-Gladrow, 2001; Dickson *et al.*, 2007).

The amount and proportions of inorganic carbon species in seawater are controlled not only by the chemical reactions outlined above but also by various physical and biological processes, including (1) the exchange of CO_2 between ocean and atmosphere, (2) the solubility of CO_2, (3) photosynthesis and respiration, and, (4) the formation and dissolution of calcium carbonate

($CaCO_3$) (e.g., Williams and Follows, 2011; Millero, 2013). Changes in DIC and TA concentrations influence the solubility of CO_2 in seawater (i.e., the ability of seawater to absorb CO_2). With the addition of acid (i.e., H^+), the chemical reactions shift toward a higher concentration of CO_2 in seawater, and pH decreases (seawater becomes less alkaline). If a base is added to seawater, or CO_2 taken up by marine phytoplankton through photosynthesis, for example, then pH will rise (seawater becomes more alkaline). Uptake of anthropogenic CO_2 into the global ocean causes shifts in the seawater CO_2-carbonate system which affects all species and all but one measurable parameter, such that CO_2, HCO_3^-, H^+, DIC and pCO_2 increase, CO_3^{2-} and pH decrease while TA remains unchanged. The uptake, accumulation and storage of anthropogenic CO_2 in the global ocean results in a change in ocean chemistry and a decrease in pH, termed ocean acidification (OA; Caldeira and Wickett, 2003; Riebesell *et al.* 2010; Gattuso and Hansson, 2011; Millero, 2013; Gruber *et al.*, 2019).

6.4 The marine carbon cycle and its perturbation

N.R. Bates

The current understanding of the state of the marine carbon cycle (Figure 15) is reasonably well constrained. Physically, the ocean can be thought of as two concentric spheres, the surface ocean and the deep ocean, separated by a density discontinuity called the pycnocline (e.g., Schlesinger, 1997; Sarmiento and Gruber, 2002, 2006). The surface ocean occupies the upper few hundred meters of the water column and contains approximately 970 Pg C as DIC (Figure 10) of which a small percentage is living biota and dead detritus. The absorption of CO_2

by the ocean through gas exchange occurs in the mixed layer which is in direct contact with the atmosphere. The uptake of anthropogenic CO_2 from the atmosphere results in increases in partial pressure of CO_2 (pCO_2) across the global ocean (e.g., Takahashi *et al.*, 1999, 2009; Bates *et al.*, 2014; Bakker *et al.*, 2016; Friedlingstein *et al.*, 2019, 2021, 2022, 2023). The surface ocean typically reaches equilibrium with the atmosphere within 1 year. The partial pressure of CO_2 in the surface ocean is slightly less than or higher than that of the atmosphere. This depends on the controlling physical and biological variables of the ocean as described above, and the uptake of CO_2 thus changes temporally and spatially with changing environmental conditions. The deep ocean represents the largest ocean volume and is supersaturated with CO_2, with a DIC stock of 37,100 Pg C (Fig. 10), or 50 times the DIC contained in the atmosphere (Schlesinger, 1997; Sarmiento and Gruber, 2006; Mackenzie and Lerman, 2010; Bates, 2019).

The marine carbon reservoir receives carbon in various forms from the terrestrial system through river runoff as particulate and dissolved organic and inorganic carbon, which in turn are exported into shelf and deep-sea sediments. The estimated input/output balance of 0.6 Pg C $year^{-1}$ is assumed to drive a natural sea-to-air flux of CO_2, both in the preindustrial and current ocean, which is similar to the riverine flux of carbon entering the ocean each year. The anthropogenic CO_2 uptake in the global ocean of currently about 2.2 Pg C $year^{-1}$, and in the opposite direction to the natural sea-to-air flux. The resulting net air-to-sea flux of CO_2 of 1.6+/- 0.9 Pg C $year^{-1}$ is in good agreement with an independent flux estimate based on a global surface ocean pCO_2 climatology that includes more than 5 million pCO_2 measurements from the past four decades compiled into data repositories such as the Surface Ocean Carbon Atlas (SOCAT; Bakker *et al.*, 2016). The observational constraints on the air–sea flux of both natural and anthropogenic CO_2 uptake by the global ocean provide additional constraint for estimating the land sink of CO_2 and land use changes over time (e.g., Sabine *et al.*, 2004; Khatiwala *et al.*, 2013; Gruber *et al.*, 2019).

6.5 Marine carbon cycle and ocean acidification trends in the Sargasso Sea

N.R. Bates

6.5.1 *Ocean time-series.*

Although quite a few open-ocean and coastal ocean CO2 time-series have been initiated, only six open-ocean time-series sites are of sufficient length to evaluate longer-term interannual trends globally. These are: (1) BATS (Bermuda Atlantic Time-series Study), located near Bermuda (31°40'N, 64°10'W) in the NW Atlantic Ocean; (2) Hydrostation S, (32°10'N, 64°30'W) located near Bermuda in the NW Atlantic Ocean, (3) ALOHA (A Long-term Oligotrophic Habitat Assessment) or HOT site, located near Hawaii (22°45'N, 158°W) in the North Pacific Ocean; and; (4) ESTOC (European Station for Time-series in the Ocean Canary Islands (ESTOC), located near Gran Canaria in the NE Atlantic Ocean; (5) Irminger and, (6) Icelandic Seas (Bates *et al.*, 2014; Lange *et al.*, 2023).

Such long-term observations at time series show upward trends of dissolved inorganic carbon (DIC) and seawater pCO_2 due to the uptake of anthropogenic CO_2 (e.g., Bates *et al.*, 2014). The anticipated rate of change in surface ocean CO_2 due to the accumulation of anthropogenic CO_2 in the atmosphere and the surface ocean buffer factor (assuming that near-surface waters in the subtropical gyres have residence times long enough to equilibrate entirely with the anthropogenic perturbation in atmospheric CO_2) can be theoretically calculated. An equilibrium rate of dissolved inorganic carbon (DIC) increases due to anthropogenic CO_2 of +0.9 µmoles kg-1 yr^{-1} was calculated for the subtropical gyres including the Sargasso Sea (Bates *et al.*, 2002; 2014; Gruber and Sarmiento, 2002; Bates and Johnson, 2020, 2022). Any assessment of long-term trends in oceanic CO_2 is complicated by sizeable seasonal variability of the inorganic carbon cycle due to processes such as seasonal temperature, salinity, and density changes, vertical and horizontal mixing, biological production, diurnal warming/cooling, and storm events (e.g., Bates *et al.*, 2002; Gruber *et al.*, 2002; Dore *et al.*, 2003; Keeling *et al.*, 2004; Brix *et al.*, 2004; Bates, 2012; Bates *et al.*, 2012; Bates and Johnson, 2020). Interpretation of oceanic CO_2 time-series data is further complicated by variability imparted by spatial heterogeneity in the ocean as a result of mesoscale and sub-mesoscale phenomena (e.g., chapter 2.5) and meridional and zonal physical gradients.

6.5.2 *Marine carbon cycle changes in the surface waters of the Sargasso Sea.*

The Sargasso Sea has also absorbed human-produced carbon dioxide (anthropogenic CO_2) from the atmosphere, with anthropogenic CO_2 concentrations almost doubling from the 1980s to the 2010s (Bates and Johnson, 2020). Both BATS and Hydrostation S data have contributed to broader views of global ocean carbon cycling and

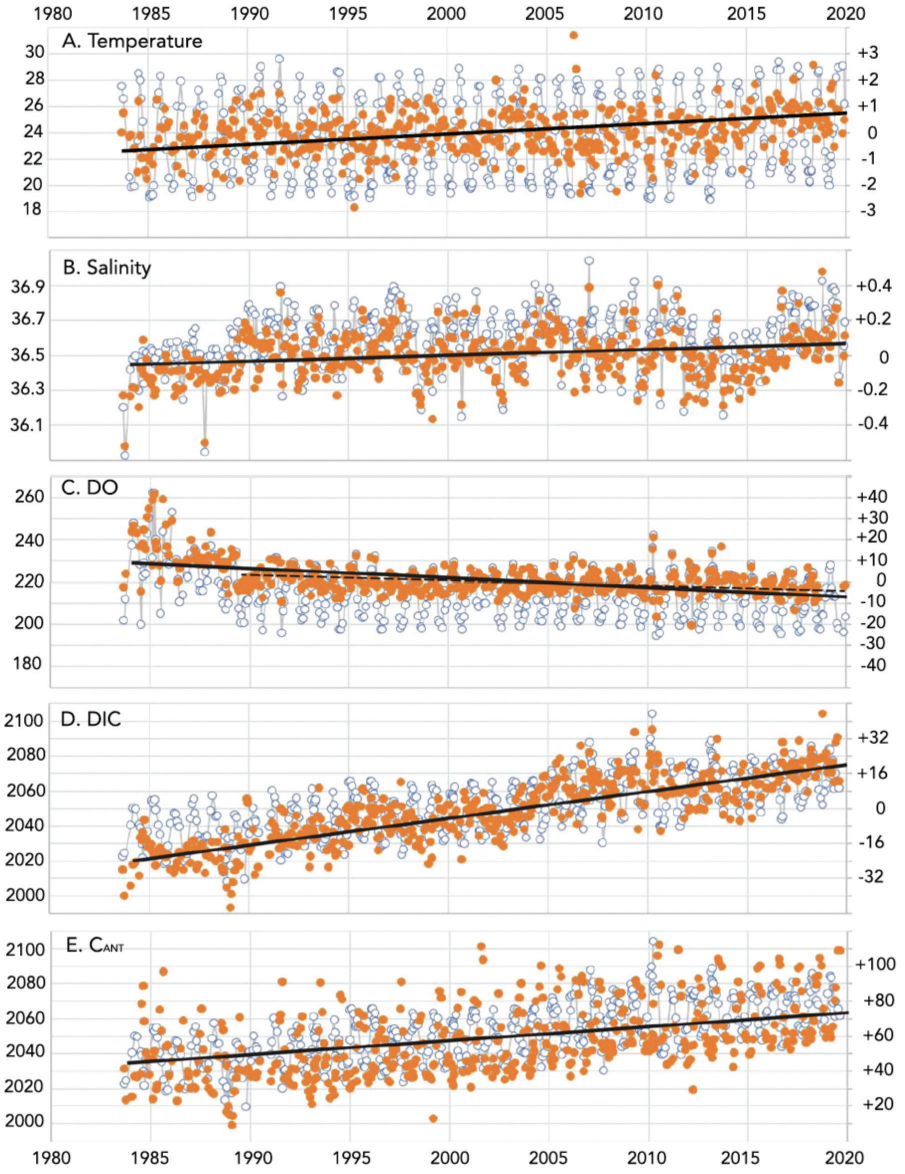

FIGURE 6.2. Hydrographic and seawater CO_2–carbonate properties at the BATS site (1988–present) with earlier data (1983–1988) from Hydrostation S. Observed data (left vertical axis; open blue symbols) and anomalies (right vertical axis; orange symbols) are shown. Regression lines are from anomaly data plotted in the right vertical axis. a Surface temperature and anomalies (°C). b Surface salinity and anomalies. c Surface dissolved oxygen (DO) and DO anomalies (µmoles kg−1); the dashed line shows the trend from 1990. d Surface DIC and salinity normalised DIC (nDIC; µmoles kg^{-1}). e nDIC and C_{ANT} values (µmoles kg^{-1}). Credit. Bates and Johnson, 2020.

trends (Dore *et al.*, 2009; Pelejero et al., 2010; Schuster et al., 2013; Bakker *et al.*, 2014; Bates et al., 2014; Bates and Johnson, 2020, 2022), anthropogenic CO_2 storage (Tanhua et al., 2013), ocean acidification trends (e.g., Bates, 2007; Bates *et al.*, 2012; 2014), and even contributed to better understanding of calcification on the Bermuda reef (Bates, 2002; Bates *et al.*, 2010; Andersson *et al.*, 2014; Yeakel *et al.* 2015; Bates, 2017; Smith and Warren, 2019; Griffin et al., 2022).

Over the past forty years, the surface ocean CO_2 concentrations have increased at a similar rate to the increase of atmospheric CO_2, and these data constitute the longest record of ocean CO_2 changes in the global ocean (Bates *et al.*, 2014; Bates and Johnson, 2020; Figure 6.2 shows temperature). Rates of uptake of CO_2 by the ocean determined by observations at BATS and Hydrostation S in the Sargasso Sea is an essential component for understanding the global ocean carbon cycle and climate change (Bindoff *et al.*, 2007; Rhein *et al.*, 2013; Bakker *et al.*, 2016; Friedlingstein et al., 2019, 2022, 2023). In addition to air-sea CO_2 gas exchange insights gained at BATS and Hydrostation S, oceanographic data have played an essential role in helping the scientific community understand dynamics of another important climate-relevant gas in the upper ocean with its sampling programs for DMS (e.g., Cropp *et al.*, 2004; Le Clainche *et al.*, 2004; Toole and Siegel, 2004; Bailey, 2008; Belviso, 2009; Le Clainche *et al.*, 2010; Polimene *et al.*, 2012; Belviso *et al.*,

2012; Amrani *et al.*, 2013; Vila-Costa *et al.*, 2014; Levine *et al.*, 2015; Masotti *et al.*, 2015).

6.5.3 *Inorganic carbon changes in the surface waters of the Sargasso Sea.*

The observations near Bermuda provide the longest record of seawater CO_2–carbonate chemistry in the global open ocean and Sargasso Sea (Bates and Johnson, 2020). Surface TA shows similar seasonal patterns to salinity (see Chapter Two). As a result of salinification in the Sargasso Sea over time, a slight increase in alkalinity has been evident over the past forty years The change in alkalinity in the Sargasso Sea over time is due to the change in the balance of evaporation and precipitation, and ocean circulation change in the North Atlantic as salinity normalised alkalinity (nTA) shows statistically insignificant changes over time (Bates and Johnson, 2020, 2023).

In the Sargasso Sea, surface ocean DIC exhibits typical summer to wintertime seasonality of ~30–40 µmoles kg^{-1} (salinity normalised DIC also shows a similar pattern but with reduced seasonality; Figure 6.3; Bates and Johnson, 2020, 2023). Such seasonality was evident in the 1980s through to the present time (e.g., Bates *et al.*, 1996a,b; Bates, 2001, 2007; Bates *et al.*, 2012; Bates, 2012) but with DIC changing over time due to the uptake of anthropogenic CO_2 from the atmosphere. Surface DIC and nDIC have significantly increased at 1.26 ± 0.04 and 1.07 ± 0.03 µmoles kg^{-1} $year^{-1}$, respectively, over the past 40 years. The difference between DIC and nDIC trends indicates that salinity changes contributed about 20% of the changes in DIC.

Earlier studies at BATS, elsewhere off Hawaii and the Canary Islands (e.g., Bates, 2001; Bates *et al.*, 2002; Bates, 2007; Dore *et al.*, 2009; Gonzalez-Davila *et al.*, 2010; Bates *et al.*, 2012, 2014), have previously attributed the increase in DIC to the oceanic uptake of anthropogenic CO_2 from the atmosphere (Khatiwala *et al.*, 2013; Bates *et al.*, 2014; Gruber *et al.*, 2019). Bates and Johnson (2020) used the TrOCA method (Touratier and Goyet, 2004; Touratier *et al.*, 2007; Yool *et al.*, 2010; Bates, 2018) to determine whether the remaining 80% of the observed DIC increase is due to oceanic anthropogenic CO_2 uptake. The TrOCA method has limitations in use for anthropogenic CO_2 quantification. Nevertheless, the TrOCA method provides a valuable tracer of ocean chemical changes over time (Figure 6.4). TrOCA anthropogenic carbon concentration (CANT) surface values in the Sargasso Sea exhibit seasonal ranges of ~30–40 µmoles kg^{-1}. Notably, C_{ANT} has increased by ~38 µmoles kg^{-1} (+72%) over the past forty years, and anthropogenic CO_2 concentration has almost doubled in the upper ocean. The rate of increase of CANT and nDIC are nearly identical (1.03 ± 0.05 vs.

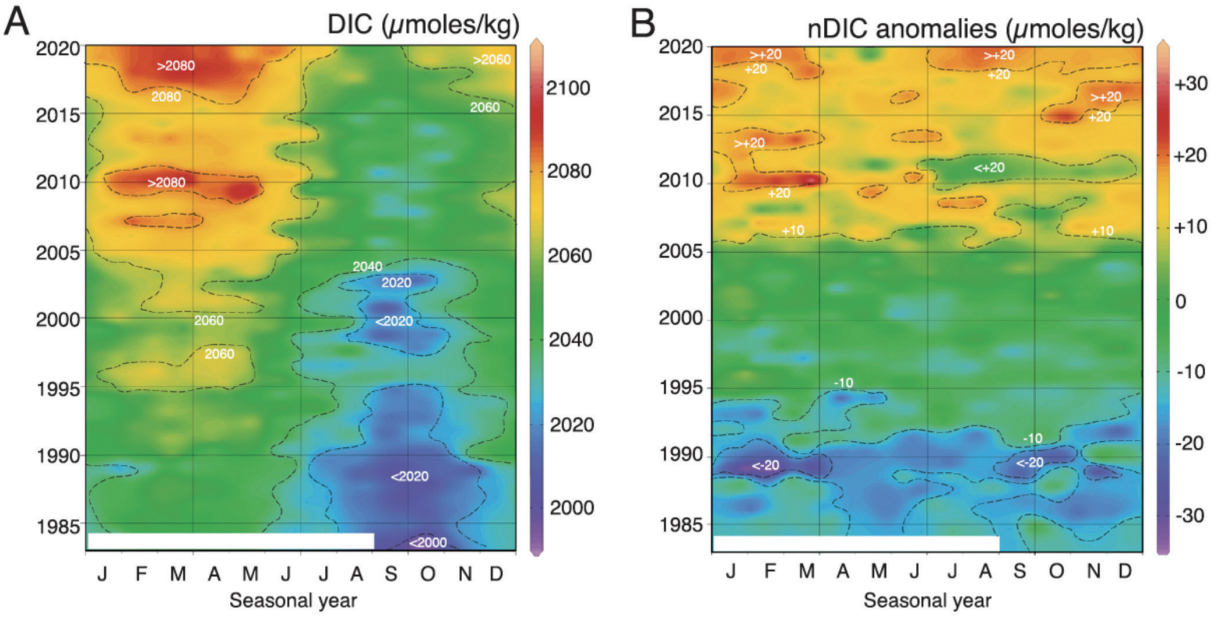

FIGURE 6.3. **Seawater CO_2–carbonate properties at BATS (1988–present) with earlier data (1983–1988) from Hydrostation S. a Scatter plot of DIC (µmoles kg^{-1}). b Scatter plot of nDIC anomalies (µmoles kg^{-1}). Credit: Bates and Johnson, 2023.**

1.07 ± 0.03 µmoles kg^{-1} $year^{-1}$). This indicates that ocean uptake of anthropogenic CO_2 has significantly changed ocean carbon chemistry over the past four decades at least.

6.5.3 *Ocean acidification.*

The BATS and Hydrostation S ocean data allow direct detection of the signal of ocean acidification in North Atlantic Ocean surface waters. As noted earlier, CO_2 dissolved into seawater creates carbonic acid, which, in turn, rapidly dissociates into bicarbonate [HCO_3^-] and then carbonate [CO_3^{2-}]. Chemical equilibria reactions keep the average contributions of [HCO_3^-], [CO_3^{2-}] and [CO_2]aq to DIC about 88%, 11% and 1%, respectively. Furthermore, pH and [CO_3^{2-}] decrease as seawater absorbs CO_2, a process termed ocean acidification (OA). This change in ocean chemistry is potentially impactful for those organisms that secrete calcium carbonate shells, skeletons, and tests. And for marine ecosystems where calcification and pH controls on biogeochemical processes are essential factors.

Data collected at Hydrostation S and BATS indicate that ocean pH decreased substantially over the past forty years, such that the seasonal chemical conditions observed in 2020 are now outside the range seen only a few decades before (Bates and Johnson, 2020). Ocean acidity has increased by about 30% from the 1980s to 2010s, with chemical conditions in the Sargasso Sea clearly different to past states for at least a few million years. The chemical conditions suitable for pelagic calcifiers in the open ocean have also reduced over time.

Over the past 40 years, the Sargasso Sea has also absorbed human-produced carbon dioxide (CO_2) from the atmosphere, almost doubling the amount of CO_2 in the upper waters (Bates *et al.*, 2012, 2014; Bates and Johnson, 2020). Due to the increase in DIC, there has been a 72% increase in anthropogenic CO_2 content (C_{ANT}) (Figure 6.4).

In the Sargasso Sea, the typical pH of surface waters in the 1980s ranged from higher winter values of ~8.2 to summertime lows of ~8.08–8.10 (Figure 19). Notably, the ocean remains mildly alkaline in this century (~7.98–8.05). Concurrently with the ocean surface changes in DIC, C_{ANT}, fCO_2 and ß values, pH has also declined by approximately 0.07 from 1983 to 2020 (Figure 6.5; Bates and Johnson, 2020, 2023). The mean rate of pH change is ~0.0019 ± 0.0001 $year^{-1}$ over the past forty years (Bates and Johnson, 2023). This is a more negative rate than previously reported, representing a ~40% increase in hydrogen ion concentration since 1983.

Ocean pH has decreased by 0.1, and ocean acidity has increased by nearly 30%, with present-day ocean

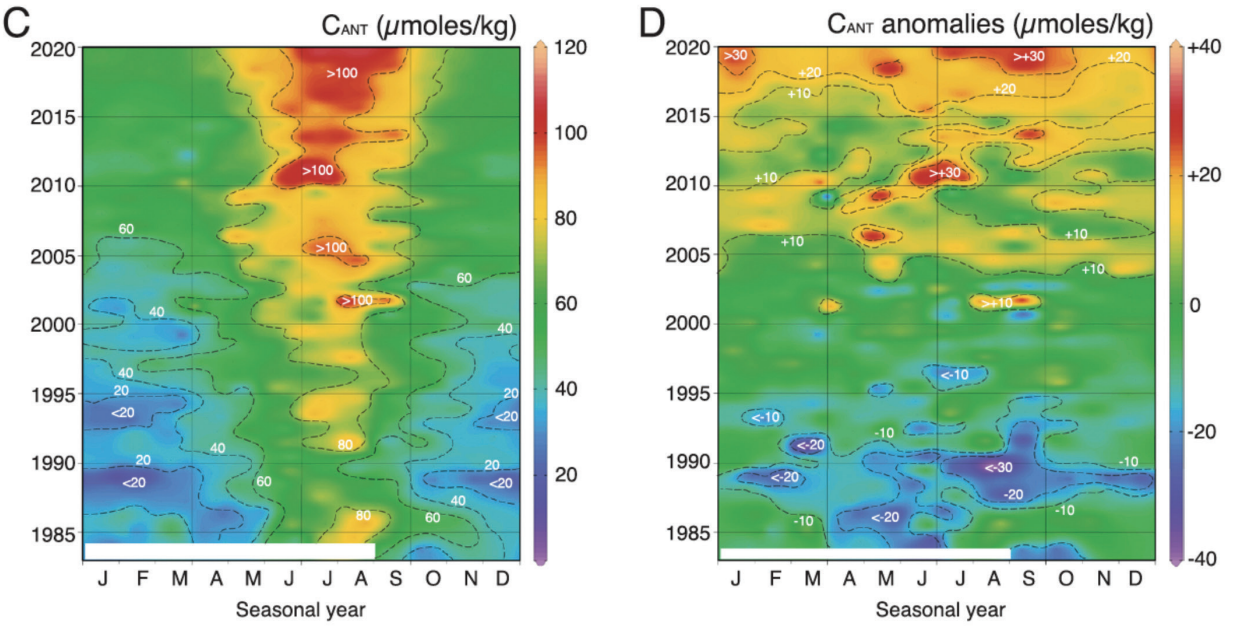

FIGURE 6.4. **c Scatter plot of C_{ANT} (µmoles kg^{-1}). d Scatter plot of of C_{ANT} anomalies (µmoles kg^{-1}). e Surface fCO_2 (µatm). f Surface fCO_2 anomalies (µatm). Dashed lines for contours are included.**

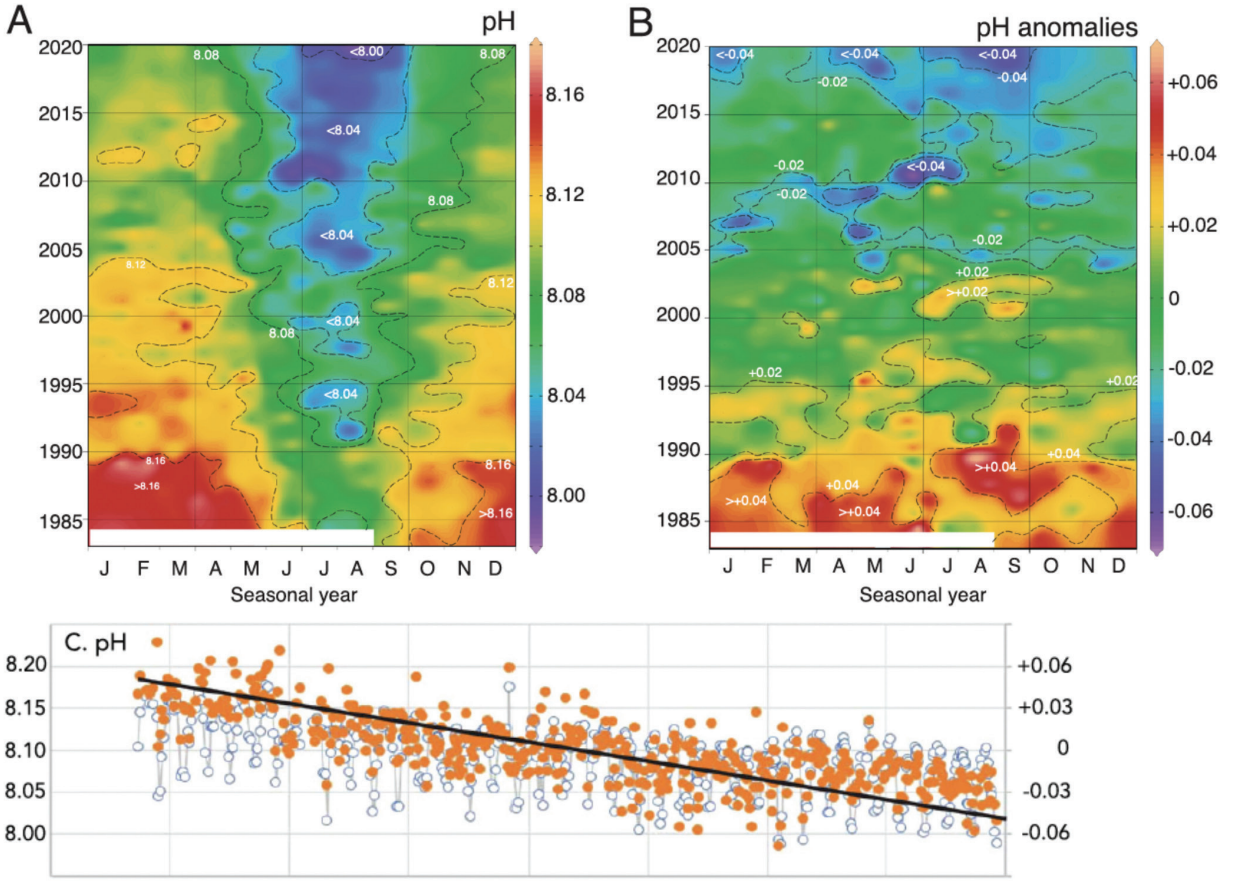

FIGURE 6.5. Seawater CO2–carbonate properties at BATS (1988–present) with earlier data (1983–1988) from Hydrostation S. a Surface pH. b Surface pH anomalies; c. pH changes over time. Credit. Bates and Johnson, 2020, 2023.

chemistry less favourable for the formation of calcium carbonate by coccolithophores and shelled pteropods. Over a few decades, the CO_2 and pH chemical conditions have reached numbers outside of the seasonal ranges observed in the 1980s and beforehand. The combined BATS/Hydrostation "S" CO_2 time-series (from 1983) is globally the longest continuous record of open ocean carbonate chemistry that shows significant impacts due to the uptake of anthropogenic CO_2, increase in ocean CO_2 inventories and chemical changes due to ocean acidification (OA; Bates *et al.*, 2012, 2014; Bates and Johnson, 2020), and data to challenge the assumptions of inorganic carbon dynamics and controls in the North Atlantic Ocean (Friedlingstein *et al.*, 2020, 2022). The changes in seawater pH over the past forty years or so are also reflected in changes in the boron content of Bermuda coral calcium carbonate (Goodkin *et al.*, 2015). Such changes in the CO_2-carbonate equilibria and pH have direct and indirect impacts on ocean ecology and function in the Sargasso Sea (Lomas *et al.*, 2013).

6.5.4 *Marine carbon cycle changes in deeper waters of the Sargasso Sea.*

In deeper subtropical mode waters (STMW), the mean rate of change of nDIC (1988-2001) was significantly higher than surface waters, increasing at a rate of 2.2 +/- 0.26 µmoles kg^{-1} $year^{-1}$ (Bates *et al.*, 2002; Bates, 2012). The STMW of the North Atlantic Ocean is formed each winter by cooling and convective mixing of surface waters at the northern edges of the subtropical gyre and south of the Gulf Stream (Klein and Hogg, 1996; Hazeleger and Drijfhout, 1998). The shallow depths of the subtropical gyre (~250-400 m deep) are ventilated during STMW formation, and the STMW layer is found throughout the subtropical gyre. This water mass is classically defined by temperatures ranging from 17.8° to 18.4°C, by a salinity of ~36.5 ± 0.05, and by a minimum in the vertical gradients of potential density (or isopycnic potential vorticity) (e.g., Klein and Hogg, 1996; Jenkins, 1998; Hanawa and Talley, 2001; Alfutis and Cornillon, 2001; Maze and Marshall, 2011). The non-conservative increase of CO_2 does not

result from remineralization of organic matter or density variability, but rather, weak wintertime mixing and lack of STMW ventilation, which appear associated with an NAO positive phase (Bates et al., 2002; Gruber *et al.*, 2002). Since 1988, ~0.6-2.8 Pg (1015g) of CO_2 has accumulated within the gyre STMW, representing a long-term oceanic sink of CO_2 (>10 years). The accumulation of CO_2 in STMW should continue until winters with more vigorous mixing (associated with an NAO negative phase) entrain STMW CO_2 into surface waters, ultimately releasing CO_2 into the atmosphere. Interannual variability in the uptake of CO_2 into STMW thus provides another factor and feedback controlling the global ocean uptake of CO_2.

In the last decade, the rate of formation of STMW has slowed down and, in some years, stopped entirely (Stevens *et al.*, 2020). This change in the subtropical gyre suggests that uptake and storage of inorganic carbon has also reduced over the last decade (2010s) compared to the 2000s (Bates, 2012).

6.6 Ocean calcium carbonate and trends in the Sargasso Sea

N.R. Bates

6.6.1 *Introduction*

Precipitation or calcification (i.e., the formation of calcium carbonate or $CaCO_3$ in shells, tests, or skeletons of organisms) and dissolution of $CaCO_3$ are defined by the production of calcium carbonate using dissolved calcium, $[HCO_3^-]$, $[CO_3^{2-}]$ and CO_2 (Zeebe and Wolf-Gladrow, 2003). In these chemical reactions, calcification/$CaCO_3$ precipitation reduces TA, and dissolution increases TA. The saturation states for common $CaCO_3$ minerals such as calcite ($Q_{calcite}$) and aragonite ($Q_{aragonite}$) can be computed from any two of measured seawater CO_2-carbonate parameters (i.e., DIC, TA, pCO_2 and pH; e.g., Zeebe and Wolf-Gladrow, 2003; Dickson *et al.*, 2007; Williams and Follows, 2011).

The saturation states for calcite ($Q_{calcite}$) and aragonite ($Q_{aragonite}$) are defined by the solubility product of calcite and aragonite, respectively. The value of W indicates whether $CaCO_3$ minerals are likely to form in seawater (Q > 1) or dissolve in seawater (Q < 1). In general terms, calcification (i.e., $CaCO_3$ precipitation) produces CO_2, which can increase pCO_2 and decrease pH. Dissolution of $CaCO_3$ generates $[HCO_3^-]$ and $[CO_3^{2-}]$ with the uptake of CO_2 (e.g., Zeebe and Wolf-Gladrow, 2001).

Production of calcium carbonate ($CaCO_3$) by calcifying marine phytoplankton such as coccolithophores, pteropods and foraminifera also contributes substantively to carbon export to the deep ocean. Extensive coccolithophore blooms in other regions of the global ocean (e.g., Bering Sea, Gulf of Maine, off Iceland) can significantly impact the ocean carbon cycle (e.g., Robertson *et al.*, 1994; Bates *et al.*, 1996a; Murata and Takizawa, 2002; Murata, 2006; Harley *et al.*, 2010; Balch *et al.*, 2022). In the Sargasso Sea, episodic coccolithophore blooms have been observed, accompanied by significant decreases in ocean alkalinity observed (Bates *et al.*, 1996b). Unlike other taxonomic classes of marine phytoplankton, coccolithophores can increase seawater pCO_2 content and thus contribute to a negative coccolithophore-CO_2 feedback (Riebesall *et al.*, 2000; Ridgewell *et al.*, 2007) that has important implications for the role of the global ocean in the uptake of anthropogenic CO_2, modulation of atmospheric CO_2 and climate responses over the next few centuries (Gattuso and Hansson, 2012).

An additional process considered part of the biological pump (depending on how it is defined) is the formation and sinking of $CaCO_3$ by calcifying organisms. This includes calcareous skeletal material produced by specific marine phytoplankton taxa (e.g., coccolithophores) and pelagic animals (e.g., pteropods and foraminifera). Calcification is a biogeochemical process by which marine organisms combine calcium and carbonate ions to form shells, tests and other calcium carbonate structures. The resulting $CaCO_3$ from biological processes tends to be dense and, therefore, sinks out of the surface water as particles as a contribution to export production (Figure 6.1). The global $CaCO_3$ flux is about 1.9 Pg C $year^{-1}$ or about 20% of organic carbon export. However, unlike organic matter, $CaCO_3$ is not remineralized as it sinks; instead, it only begins to dissolve, especially in intermediate and deep waters, which are undersaturated with respect to CaCO3 (Ω <1). However, recent studies indicate that a substantial portion of exported calcium carbonate begins to dissolve in relatively shallow waters that are oversaturated (Ω > 1). Complete dissolution of $CaCO_3$ minerals (typically calcite) typically occurs at depths of approximately 1–4 km (in the North Pacific Ocean) to 5 km (in the North Atlantic Ocean). This depth zone is known as the carbonate compensation depth. $CaCO_3$ is typically found in sediments shallower than the carbonate compensation depth. Globally, the CO_2 sink in sedimentary rock is four times greater than carbon in organic sediments (e.g., Mackenzie and Lerman, 2010).

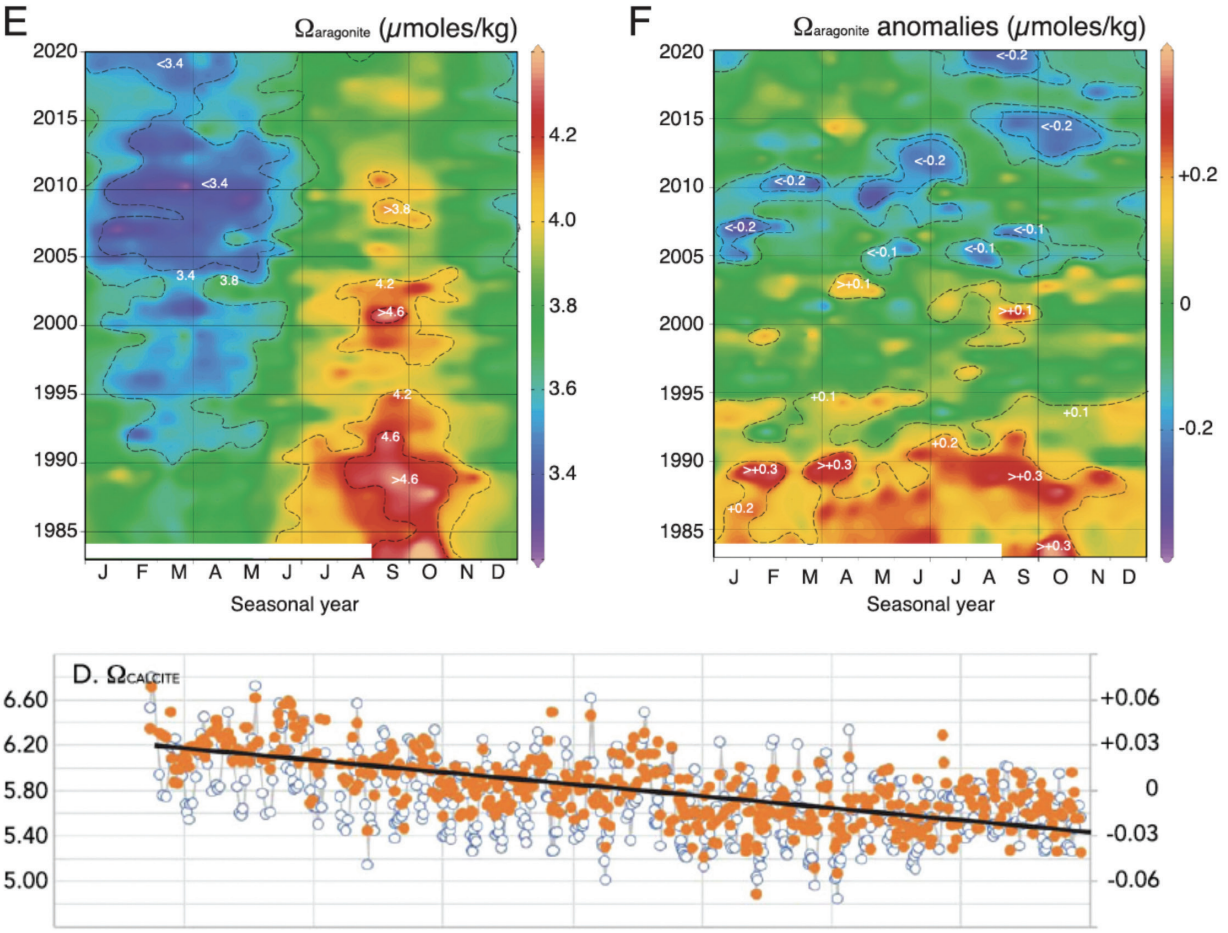

FIGURE 6.6. **Seawater CO_2-carbonate properties at BATS (1988–present) with earlier data (1983–1988) from Hydrostation S. e Surface Ωaragonite. f Surface Ωaragonite anomalies. c. Ωaragonite anomalies changes over time. Credit. Bates and Johnson, 2020.**

6.6.2 *Sargasso Sea trends*

In the Sargasso Sea, the rate of pH change is ~0.0019 +/- 0.0001 year^{-1} (Bates and Johnson, 2020). Both Qcalcite and Qaragonite exhibit seasonal changes of ~0.3 to 0.5 (Figure 6.6), while Qcalcite and Qaragonite have decreased by 0.52 and 0.35 in the past forty years at rates of 0.014±0.001 year^{-1} and 0.009±0.001 year^{-1}, respectively (Bates and Johnson, 2020, 2023).

6.6.3 *Insights into coral reef status and other ecological components in the North Atlantic Ocean.*

The observations at Hydrostation S and BATS also provide a critically important context for understanding the present status of calcification and dissolution of the Bermuda coral reef system. While Bermuda's coral reefs remain relatively healthy, the reef system now experiences seasonal net dissolution for several months due to ocean uptake of anthropogenic CO_2 (e.g., Yeakel *et al.*, 2015; Bates, 2017; Courtney *et al.*, 2017; Smith and Warren, 2019; Griffin *et al.*, 2022). Similar seasonal net dissolution of reef systems has also been observed in the Florida reef tract. Comparison of Hydrostation S data with paleo-proxies such as Sr/Ca ratios in Bermuda corals have extended time-series records back over centennial scales to the Little Ice Age (Goodkin *et al.*, 2005; 2008) with recent analysis of boron isotopes in corals, a paleo–proxy for ocean pH, extending our observational record of pH (e.g., Bates *et al.*, 2014) back in time (Goodkin *et al.*, 2015).

In the Sargasso Sea, there are other records of calcium carbonate production, particularly coccolithophores, at the same time as a reduction in primary production (Gao *et al.*, 2012; Lomas *et al.*, 2022). Recent studies report declines in coccolithophore production (Krumhardt *et*

al., 2016; Lv *et al.*, 2017). Other records of carbonate production in the Sargasso Sea also show decreases over time, especially in the last couple of decades (Conte and Weber, 2014; Smart *et al.*, 2014; Salmon *et al.*, 2015; Conte *et al.*, 2019). There is also a decoupling of organic and inorganic carbon production in the Sargasso Sea (Estapa *et al.*, 2015) with as-yet-determined influences for bacteria and microbial ecology (Lomas *et al.*, 2012; Moran *et al.*, 2022). The unknown impact of Sargassum weed in the North Atlantic subtropical gyre (e.g., Koch *et al.*, 2013; Hodgkins *et al.*, 2017; Xu *et al.*, 2017; Fidai *et al.*, 2020) was one the primary focus of the Laloffey et al., (2011) scientific case for the protection of the Sargasso Sea.

6.7 Climate variability influences on the Sargasso Sea

N.R. Bates

Variability in the marine carbon cycle and ocean carbon sources and sinks has been studied most thoroughly in the tropical Pacific Ocean in connection with the El Niño Southern Oscillation (ENSO). El Niño-La Niña changes have profound impacts on weather and climate globally. By contrast, little is known about the contribution of the subtropical and subpolar gyres to atmospheric CO2 variations, even though these gyres cover more than half of the world's oceans. Natural modes of climate variability, such as the North Atlantic Oscillation (NAO), El Niño-Southern Oscillation, and Arctic Oscillation (AO), also have regional (particularly in Europe) and global impacts on weather and climate.

The dominant mode of atmospheric and climate variability in the North Atlantic Ocean region is the NAO, which is a dipole meridional oscillation in atmospheric pressure between the Iceland Low and Açores High (Hurrell, 1995; Hurrell and Van Loon, 1997; Hurrell *et al.*, 2002; Bates, 2012). The NAO is linked to the Arctic Oscillation (AO), a tripolar oscillation between the North Pacific and North Atlantic, centred over the Arctic region (Visbeck *et al.*, 2001). The NAO has significant effects on climate and atmospheric variability. Strong eastward airflow between the Iceland Low and Açores High carries storms towards western Europe from North America. If the NAO index is negative, storm tracks are thought to shift southward, cooling surface waters, enhancing 18°C mode water formation and deepening winter mixed layers (Rodwell et al., 1999). In western Europe, for example, there is an increase in winter storms and precipitation during these periods. During positive NAO winters, westerlies weaken that usually prevail between Florida and Cape Hatteras (west of the Azores High). The reduction of wind stress and heat exchange lead to the development of warm water surface anomalies in the subtropical gyres (e.g., Cayan, 1992a,b) with a magnitude of ~0.2 to 0.4°C (e.g., Davies *et al.*, 1997; Kapala *et al.*, 1998; Stevens *et al.*, 2020).

Although the NAO is the dominant mode of mid-latitude atmospheric variation, dynamical relations between El Ninõ and the Atlantic climate have long been documented (e.g., Enfield and Mayer, 1997; see references in Penland and Matrosova, 1998). For example, the Gulf Stream position shifts northwards after El Niño events and during NAO-positive phases with a lag of ~2 years (e.g., Taylor *et al.*, 1998; Taylor and Stephens, 1998). Within 4-12 months of El Niño warming in the Pacific Ocean, warming is observed in the tropical North Atlantic, Caribbean Sea and the SE subtropical gyre (e.g., Penland and Matrosova, 1998). The mechanism for this apparently relates to a reduction in cloud cover in the drier, more stable Atlantic atmosphere (e.g., Davies *et al.*, 1997; Jones and Thorncroft, 1998). The ocean carbon cycle of the Sargasso Sea is influenced by NAO and ENSO (e.g., Gruber et al., 2002; Bates, 2002; Bates, 2012)

6.8 Air-sea gas exchange

N.R. Bates

6.8.1 *Solubility of gases, including CO_2.*

As background for understanding the changes in air-sea CO_2 gas exchange in the Sargasso Sea, the basic concept of solubility and chemical buffering of seawater (i.e., Revelle factor) is given here. The solubility of CO_2 in seawater is an essential factor in controlling gas exchange between the ocean and the atmosphere. Thermodynamics and Henry's law equations determine the relationship between solubility and seawater properties (e.g., Zeebe and Wolf-Gladrow, 2003). In simplest terms, S is the solubility of the gas in a liquid, k is the solubility constant (k is a function primarily of temperature), and P is the overlying pressure of the gas in the atmosphere, such that $S = kP$.

Seawater properties such as temperature, salinity, and partial pressure of CO_2 determine the solubility of CO_2. For example, at 0°C in seawater, the solubility of CO_2 is double that in seawater at 20°C. Thus, importantly, colder water will tend to absorb more CO_2 than warmer water. Henry's law also describes the relationship between the pCO_2 or fCO_2 in solution and its concentration (i.e., $[CO_2]$). Colder waters tend to have lower

pCO_2 or fCO_2 than warmer waters. In simple terms, for every 1°C temperature increase, seawater pCO_2 or fCO_2 increases by about 4.0%–4.2%. Seawater pCO_2 (and fCO_2) is also influenced by complicated thermodynamic relationships between the different inorganic carbon species (see above). For example, a decrease in seawater DIC or temperature acts to decrease pCO_2, while a decrease in alkalinity acts to increase pCO_2 (Zeebe and Wolf-Gladrow, 2001).

6.8.2 *Chemical buffering of CO_2 in seawater*

The chemical buffering of CO_2 in the global ocean is an important carbon sink. As CO_2 is absorbed by seawater, it is scavenged by ocean chemistry and converts to HCO_3^{2-} and CO_3^{2-}. In simple terms, the amount of CO_2 added to seawater is much greater than the increase in seawater dissolved CO_2 due to the chemical equilibria and transformation to more prevalent carbonate species (i.e., HCO_3^{2-} and CO_3^{2-}). The capacity of seawater to absorb atmospheric CO_2 (due to a perturbation or uptake of anthropogenic CO_2) is known as the Revelle factor (or buffer factor, b, which relates the change in pCO_2 (or fCO_2) to DIC after chemical equilibration of the seawater CO_2-carbonate system to its new state. The Revelle factor of surface waters is highly variable, ranging from ~8–10 in the tropics to ~12–15 in the polar and subpolar regions (e.g., Sabine *et al.*, 2004).

6.8.3 *Gas exchange at the ocean-atmosphere interface*

Carbon dioxide is transferred across the air-sea interface by molecular diffusion and turbulence at the ocean surface. The flux (F) of CO_2 between the atmosphere and ocean is driven by the concentration difference between the reservoirs and expressed as $F = Dp\ CO_2 Kw$. $Dp\ CO_2$ is the concentration difference between the ocean and atmosphere, and Kw is the transfer coefficient across the air–sea interface, termed the piston velocity or gas transfer velocity. The physical and biological process impacting the gas exchange of CO_2 and other gases are complicated and involves processes such as diffusion, turbulent mixing, waves breaking and entrainment of air bubbles, and biological processes that influence the distribution of organic matter and surfactants in the air–sea interface (e.g., Wanninkhof, 1999; Liss and Johnson, 2014).

In simple terms, the rate of transfer of CO_2 between the ocean and atmosphere is driven by the concentration difference between the ocean and atmosphere, and turbulence at the ocean surface is typically a function of wind speed. The gas transfer velocity of CO_2 is related to solubility and the strength of the wind blowing on the sea surface. As wind speed increases, the rate of air–sea CO_2 exchange) or oxygen and other gases) also increases. The turbulence in surface waters caused by breaking waves also contributes to gas exchange. This occurs as air bubbles dissolve, following entrainment into the mixed layer of the ocean. The detailed process underlying gas exchange is the subject of scientific research (e.g., Wanninkhof, 1992; Liss and Johnson, 2014).

In cold waters, seawater pCO_2 tends to be lower than atmospheric pCO_2, thus driving the direction of CO_2 gas exchange from the atmosphere to the ocean (Takahashi *et al.*, 2009). In warmer waters, seawater pCO_2 tends to be higher than atmospheric pCO_2, and CO_2 gas exchange occurs in the opposite direction, from the ocean to the atmosphere. Although tropical waters tend to be sources of CO_2 to the atmosphere, factors (QQQ values of 8–10) and have the largest capacity to absorb CO_2 from the atmosphere (if the tropical water has high pCO_2 due to ocean warming and upwelling of CO_2 rich water did not counteract this process; for example, Sabine *et al.*, 2004).

6.8.4 *The atmosphere-ocean exchanges of CO_2 in the Sargasso Sea*

The Sargasso Sea is an essential region for uptake of CO_2 from the atmosphere with distinct seasonal variability in uptake and release of CO_2 (Bates *et al.*, 1996; Bates, 2001, 2002; Bates, 2007; Takahashi *et al.*, 2009; Bates *et al.*, 2012; Bates *et al.*, 2014; Bates and Johnson, 2020, 2022). The annual net ocean uptake of CO_2 in the subtropical gyre of the North Atlantic off Bermuda appears to be increasing in contrast to other parts of the North Atlantic Ocean (especially in the subpolar gyre; Watson *et al.*, 2009; Schuster *et al.*, 2009; and the global ocean Friedlingstein *et al.*, 2019, 2021, 2022, 2023).

6.8.5 *Ocean CO_2 and buffering in the Sargasso Sea*

Bates and Johnson (2020) have shown that surface seawater fCO_2 exhibits substantial seasonality with typical ranges of ~40-60 µatm (Figure 6.7). Such changes seasonally reflect the underlying variability of temperature and DIC (similar patterns are observed for pCO_2).

The uptake of anthropogenic CO_2 by surface waters results in an increase in DIC, and surface seawater fCO_2 exhibited significant gain over the forty years. The rate of change of fCO_2 is 1.9 +0.08 µatm $year^{-1}$ (Bates and Johnson, 2020, 2023). This represents an increase of nearly 25% from 1980 to 2023. Thus, the winter and summer fCO_2 values in the 2020s are outside the range

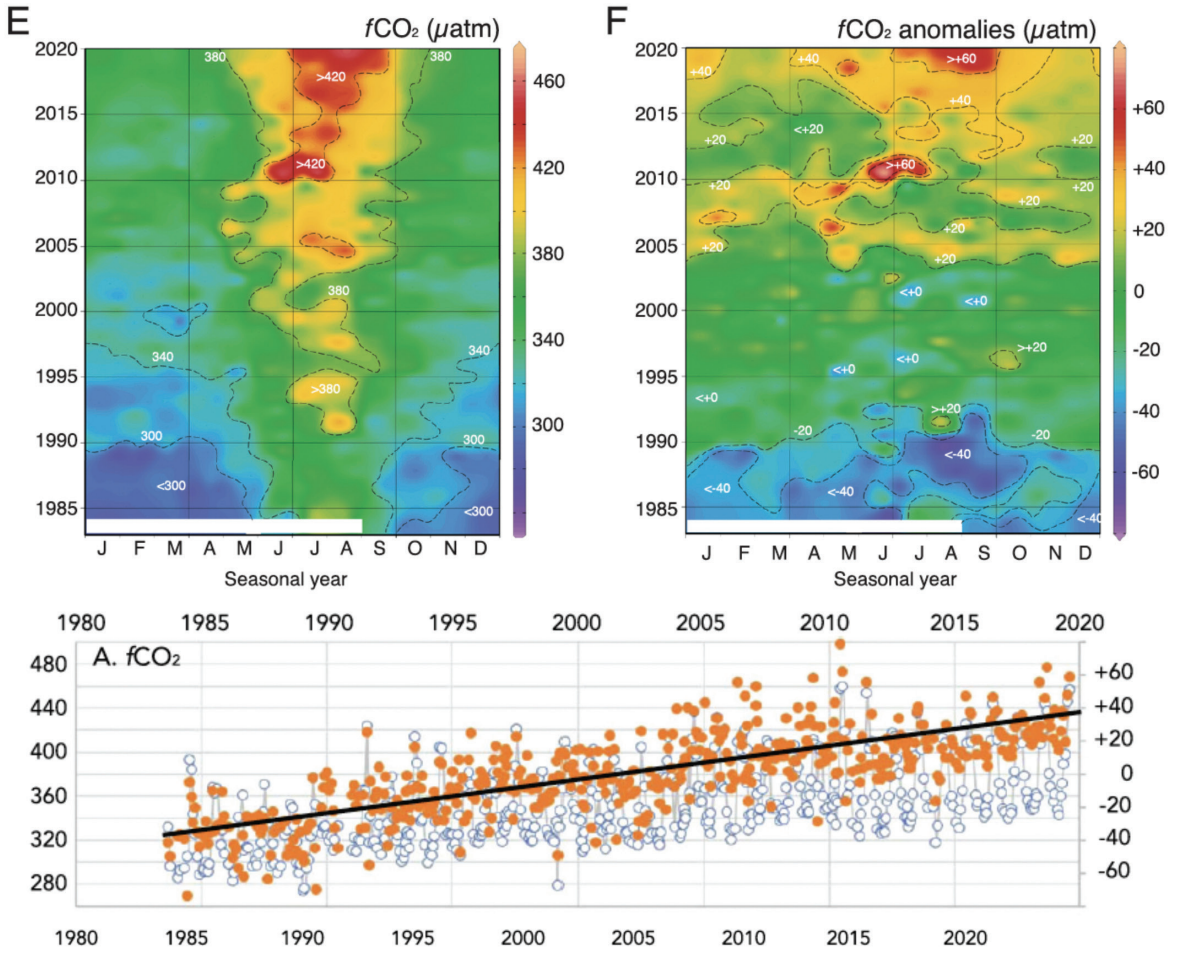

FIGURE 6.7. **Seawater CO_2–carbonate properties at BATS (1988–present) with earlier data (1983–1988) from Hydrostation S. e Surface fCO_2. f Surface fCO_2 anomalies. a. Surface fCO_2 changes over time. Credit. Bates and Johnson, 2020.**

observed in the 1980s (Bates and Johnson, 2023).

The increasing trend of seawater fCO_2 observed in the Sargasso Sea is similar to observed changes in atmospheric fCO_2. Over shorter time scales, similar trends in surface seawater fCO_2 have been reported elsewhere (Bates et al. 2014). Given that surface and atmospheric fCO_2 increases have tracked each other over time, this suggests that air-sea CO_2 gas exchange has not changed significantly. The implication is that the ocean CO_2 sink in the subtropical gyre remained unchanged over the past forty years. Earlier studies have concluded that the increases in fCO_2 largely reflect the uptake of anthropogenic CO_2 and increasing DIC. There are minor influences due to the small changes in temperature, salinity and alkalinity over time (Bates et al., 2014; Bates and Johnson, 2020).

The Revelle factor (QQQ) reflects the underlying chemical state that can facilitate air-sea CO_2 exchange. The ocean's ability to absorb CO_2 from the atmosphere decreases with higher b values, and the chemical buffering capacity reduces. In the Sargasso Sea, the seasonality of QQQ is ~0.4. Wintertime values are higher than summertime values. Lower b conditions reflect the underlying capacity for seawater to absorb CO_2, yet the lowest fCO_2 occurs in winter and coincides with seasonally higher QQQ values (Bates and Johnson, 2020). Notably, the Revelle factor, b, is increasing over time (~0.54±0.04; Figure 6.8). Such changes in ocean chemistry illustrate that the ocean's capacity to absorb CO_2 from the atmosphere is gradually declining (~6% since 1980). This provides additional future feedback when assessing the fate of anthropogenic CO_2 in the atmosphere. This also includes its transfer to the ocean.

Recently, Landschutzer et al. (2017) reported that winter to summer fCO_2 difference has grown from the

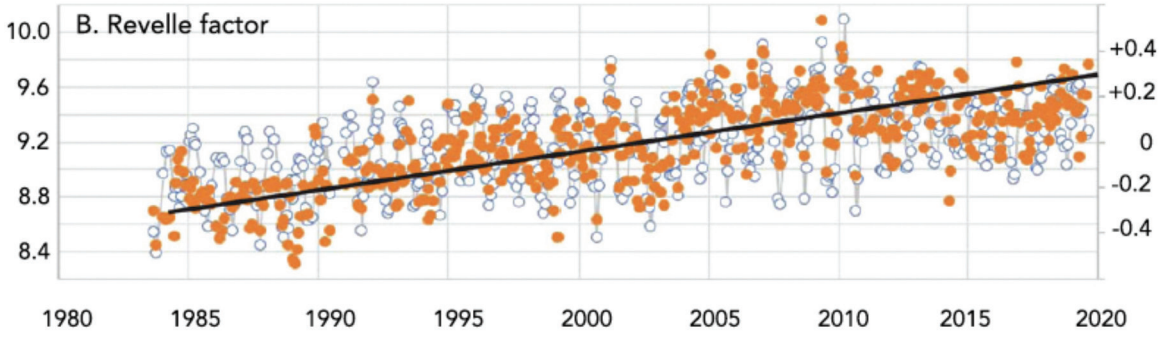

FIGURE 6.8. **Seawater CO_2–carbonate properties at BATS (1988–present) with earlier data (1983–1988) from Hydrostation S. a. Surface *Revelle factor* changes over time. Credit. Bates and Johnson, 2020.**

1980s to the 2010s. The rates were +1.5 to +3.8 µatm per decade, with the BATS site in the Sargasso Sea (+1.5 µatm per decade) and the Hawaii Ocean Time Series (+3.8 µatm per decade) in the North Pacific Ocean. These changes have been attributed to the long-term increase in CO_2, $[CO_2]_{aq}$ in the surface ocean and the increase in the Revelle factor.

At the BATS-Hydrostation S site, the mean winter-to-summer fCO_2 difference increases from the 1980s to the 2010s simultaneously with increasing $[CO_2]_{aq}$ and Revelle factor. The increase in mean winter-to-summer fCO_2 difference is 4.1 µatm per decade.

The diverging winter and summer fCO_2 conditions are associated with the reduction in winter length (i.e., the season with water less than 22°C has decreased from 157.7±10.8 days in the 1980s to 124.7±24.7 days in the 2010s; Bates and Johnson, 2020). The increase in summer length and higher rate of warming (the season with water higher than 25°C) has increased from 121.0±23.4 days in the 1980s to 140.3±11.3 days in the 2010s; Bates and Johnson, 2020). The BATS-Hydrostation S winter-to-summer fCO_2 difference also substantially increased by ~10 µatm in the 2010s (due to summertime warming and higher fCO_2).

6.8.6 *Dimethylsulphide (DMS) summer paradox and the Sargasso Sea*

Dimethylsulphide (DMS) is produced through biogeochemical processes in the surface ocean food web. DMS is the primary source of natural sulfur to the atmosphere, where the gas is oxidized to sulphate and methane sulfonate aerosols (Shaw, 1983), which act as cloud condensation nuclei. Variability in oceanic DMS production and ventilation to the atmosphere has the potential to alter aerosol abundance, cloud coverage, and cloud properties, which in turn affects the atmospheric radiative balance and climate (i.e., Charlson *et al.*, 1987).

There is a need to quantitatively understand biogenic sulfur dynamics in the oceans and the role of DMS in structuring past, as well as future, global climates. To accomplish this, a better understanding of the fates of the DMS and dimethylsulfoniopropionate (dissolved and particulate DMSP) pools in the ocean is required. The task is difficult because the biological and chemical processes involved in the cycling of biogenic sulphur are broad and complex. Short-term (UV inhibition, nutrient pulses) and long-term (light regime, nutrient regime, temperature) stressors impact the biogeochemical cycling processes of the oceanic sulphur pool. Because the oceans account for > 50% of the global source of reduced sulfur to the atmosphere, it is critical to understand the various reservoirs and cycling processes. In the Sargasso Sea, early measurements of oceanic DMS and DMSP have provided the only long-term time series for DMS in the deep ocean (Dacey *et al.*, 1998; Toole et al., 2008). The observed decoupling of DMS concentration from any measure of its precursors (i.e., DSMP) embodies the 'DMS summer paradox' hypothesis (Simó and Pedrós-Alió, 1999; Belviso *et al.*, 2012; Polimene *et al.*, 2012; Vila-Costa *et al.*, 2014; Levine *et al.*, 2015; Masotti *et al.*, 2015). The DMS' summer paradox' is a reoccurring phenomenon in the Sargasso Sea.

The continuing development of more precise and accurate measurement techniques is also imperative, as demonstrated by the significant reduction in DMSPd concentrations. Time-series data such as these are essential for understanding present global ocean dynamics and modelling and predicting future fluctuations in physical, chemical, and biological processes.

6.9 References

Alfutis., M.A., and Cornillon P., 2001. Annual and interannual changes in the North Atlantic STMW layer properties. *Journal of Physical Oceanography*, **31**, 2066–2086.

Amrani, A., Said–Ahmed, W., Shaked, Y., and Kiene, R.P., 2013. Sulfur isotope homogeneity of oceanic DMSP and DMS. PNAS, **110**, 46, 18413-18418, doi: 10.1073/pnas.1312956110.

Andersson, A.J., Yeakel, K.L., Bates, N.R., and de Putron, S., 2014. Future changes in reef metabolism oppose anthropogenic ocean acidification on coral reefs. *Nature Climate Change*, 4, 56–61, doi:10.1038/nclimate2050.

Bailey, K.E., Toole, D.A., Blomquist, B., Najjar, R.G., Huebert, B., Kieber, D.J., Kiene, R.P., Matrai, P., Westby, G.R. and Valle, D.A., 2008. Dimethylsulfide production in Sargasso Sea eddies. *Deep-Sea Res., II*, **55**, 1491–1504.

Bakker, D.C.E, Pfeil, B., Smith, K., Hankin, S., Olsen, A, Alin, S.R., Cosca, C., Hales, B., Harasawa, S., Kozyr, A., Nojiri, Y., O'Brien, K.M., Schuster, U., Telszewski, M., Tilbrook, B., Wada, C., Akl, J., Barbero, L., Bates, N.R., Boutin, J., Cai, W–J., Castle, R.D., Chavez, F.P., Chen, L., Chierici, M., Currie, K., de Baar H.J.W., Evans, W., Feely, R.A., Fransson, A., Gao, Z., Hardman-Mountford, N., Hoppema, M., Huang, W-J., Hunt, C.W., Huss, B., Ichikawa, T., Jacobson, A., Johannessen, T., Jones, E.M., Jones, S.D., Jutterstrøm, S., Kitidis, V., Körtzinger, A., Landschützer, P., Lauvset, S.K., Lefèvre N., Manke A.B., Mathis J.T., Merlivat, L., Metzl, N., Monteiro, P., Murata, A., Newberger, T., Ono, T., Park, G-H., Paterson, K., Pierrot D., Ríos, A.F., Sabine, C.L., Saito, S., Salisbury, J., Sarma, V.V.S.S., Schlitzer, R., Sieger, R., Skjelvan, I., Steinhoff, T, Sullivan, K, Sutherland, S.C., Suzuki, T., Sutton, A.J., Sweeney, C., Takahashi, T., Tjiputra, J., Tsurushima, N., van Heuven, S.M.A.C., Vandemark, D.,Vlahos, P., Wallace, D.W.R., Wanninkhof R., and Watson A.J., 2014. An update to the surface ocean carbon atlas (SOCAT version 2). *Earth System Science Data*, **6**, 69–90.

Bakker, D.C.E., Pfeil, B., Landa, C.S., Metzl, N., O'Brien, K.M., Olsen, A., Smith, K., Cosca, C., Harasawa, S., Jones, S.D., Nakaoka, S.-I., Nojiri, Y., Schuster, U., Steinhoff, T., Sweeney, C., Takahashi, T., Tilbrook, B., Wada, C., Wanninkhof, R., Alin, S.R., Balestrini, C.F., Barbero, L., Bates, N.R., Bianchi, A.A., Bonou, F., Boutin, J., Bozec, Y., Burger, E., Cai, W.–J., Castle, R.D., Chen, L., Chierici, M., Currie, K., Evans, W., Featherstone, C., Feely, R.A., Fransson, A., Goyet, C., Greenwood, N., Gregor, L., Hankin, S., Hardman–Mountford, N.J., Harlay, J., Hauck, J., Hoppema, M., Humphreys, M.P., Hunt, C.W., Huss, B., J. Severino, J., Ibánhez, P., Johannessen, T., Keeling, R., Kitidis, V., Körtzinger, A., Kozyr, A., Krasakopolou, E., Kuwata, A., Landschützer, P., Lauvset, S.K., Lefèvre, N., LoMonaco, C., Manke, A., Mathis, J.T., Merlivat, L., Millero, F.J., Monteiro, P.M.S., Munro, D.R., Murata, A., Newberger, T., Omar, A.M., Ono, T., Paterson, K., Pearce, D., Pierrot, D., Robbins, L.L., Saito, S., Salisbury, J., Schlitzer, R., Schneider, B., Schweitzer, R., Sieger, R., Skjelvan, I., Sullivan, K.F., Sutherland, S.C., Sutton, A.J., Tadokoro, K., Telszewski, M., Tuma, M., van Heuven, S.M.A.C., Vandemark, D., Ward,, B., Watson, A.J., and Xu, S., 2016. A multi–decade record of high quality *f*CO2 data in version 3 of the Surface Ocean CO2 Atlas (SOCAT). *Earth System Science Data.*

Balch, W.M., Drapeau, D.T., Bowler, B.C., Record, N.R., Bates, N.R., Pinkham, S., Garley, R., and Mitchell, C., 2022. Changing hydrographic, biogeochemical, and acidification properties in the Gulf of Maine as measured by the Gulf of Maine North Atlantic Time-series, GNATS, between 1998 and 2018. *Journal of Geophysical Research, Biogeosciences*, **127** (6), e2022JG006790.

Bates, N.R., 2001. Interannual variability of oceanic CO2 and biogeochemical properties in the Western North Atlantic subtropical gyre. *Deep Sea Research II*, **48**, 1507–1528.

Bates, N.R., 2002. Seasonal variability of the effect of coral reefs on seawater CO2 and air-sea CO2 exchange. *Limnology and Oceanography*, **47** (1), 43-52, Jan. 2002.

Bates, N.R., 2007. Interannual variability of the oceanic CO2 sink in the subtropical gyre of the North Atlantic Ocean over the last two decades. *Journal of Geophysical Research (Oceans)*, **112** (C9), C09013, doi: 10.1029/2006JC003759, May 4, 2007.

Bates, N.R. 2012. Multi-decadal uptake of carbon dioxide into subtropical mode waters of the North Atlantic Ocean. *Biogeosciences*, bg-2011-478, 8 (6), 12451–12476.

Bates, N.R., 2017. Twenty years of marine carbon cycle observations at Devils Hole Bermuda provide insights into seasonal hypoxia, coral reef calcification and ocean acidification. *Frontiers in Marine Science*, **4**, https://doi.org/10.3389/fmars.2017.00036.

Bates, N.R., 2018. Seawater carbonate chemistry distributions across the Eastern South Pacific Ocean sampled as part of the GEOTRACES project and changes in marine carbonate chemistry over the past twenty years. *Frontiers in Marine Science*, **5**, 1–18.

Bates, N.R., 2019. Ocean Carbon Cycle. *Encyclopaedia of Marine Science.*

Bates, N.R., and Johnson, R.J., 2020. Acceleration of ocean warming, salinification, deoxygenation, and acidification in the surface subtropical North Atlantic Ocean. *Nature Communications in Earth and Environment*, **1**, 1–12.

Bates, N.R., and Johnson, R.J., 2022. Ocean observing in the North Atlantic subtropical gyre. *Oceanography*, **34**(4), 32–33.

Bates, N.R., and Johnson, R.J., 2023. Forty years of ocean acidification observations (1983-2023) in the Sargasso Sea at the Bermuda Atlantic Time-series Study (BATS) site. *Frontiers in Marine Science.*

Bates, N.R., Michaels, A.F. and Knap, A.H., 1996. Seasonal and interannual variability of oceanic carbon dioxide species at the US JGOFS Bermuda Atlantic Time-series Study (BATS) site. *Deep Sea Research II*, **43**, 347–383.

Bates, N.R., Michaels, A.F. and Knap, A.H., 1996. Alkalinity changes in the Sargasso Sea: geochemical evidence of calcification? *Marine Chemistry*, **51**, 347–358.

Bates, N.R., Pequignet, A. C., Johnson, R. J. and Gruber, N., 2002. A short–term sink for atmospheric CO2 in subtropical mode water of the North Atlantic Ocean. *Nature*, **420**, 489–493.

Bates, N.R., Best, M.H., Neely, K., Garley, R., Dickson, A.G., and Johnson, R.J., 2012. Indicators of anthropogenic carbon dioxide uptake and ocean acidification in the North Atlantic Ocean. *Biogeosciences*, **9**, 2509–2522, doi: 10.10.5194/bg–9–2509–2012.

Bates, N.R., Astor, Y.M., Church, M.J., Currie, K., Dore, J.E., Gonzalez–Davila, M., Lorenzoni, L., Muller–Karger, F.E., Olafsson, J., and Santana–Casiano, J.M., 2014. Changing ocean chemistry: A time–series view of ocean uptake of anthropogenic CO2 and ocean acidification. *Oceanography*, **27**(1), 121–141, http://dx.doi.org/10.5670/oceanog.2014.03.

Belviso, S., and Caniaux, G., 2009. A new assessment in North Atlantic waters of the relationship between DMS concentration and the upper mixed layer solar radiation dose. *Global Biogeochemical Cycles*, **23**, GB1014.

Belviso, S., Masotti, I., Tagliabue, A., Bopp, L., Brockman, P., Fichot, C., Caniaux, G., Prieur, L., Ras, J., and Uitz, J., 2012. DMS dynamics in the most oligotrophic subtropical zones of the global ocean. *Biogeochemistry*, doi: 10.1007/s10533-011-9648-1.

Bindoff, N.L., Willebrand, J., Artale, V., Cazenave, A., Gregory, J., Gulev, S., Hanawa, K., Le Quéré, C., Levitus, S., Nojiri, Y., Shum, C.K., Talley, L.D., and Unnikrishnan, A., 2007. *Observations: Oceanic Climate Change and Sea Level. In: Climate Change 2007: The Physical Science Basis.* Contribution of Working Group I to the Fourth Assessment Report of the Intergovernmental Panel on Climate Change [Solomon, S., D. Qin, M. Manning, Z. Chen, M. Marquis, K.B. Averyt, M. Tignor and H.L. Miller (eds.)]. Cambridge University Press, Cambridge, United Kingdom and New York, NY, USA.

Brix, H., Gruber, N. and Keeling, C.D., 2004. Interannual variability of the upper carbon cycle atstation ALOHA near Hawaii. *Global Biogeochemical Cycles*, **18**, GB4019.

Caldeira, K., and Wickett M.E., 2003. Anthropogenic carbon and ocean pH. *Nature*, **425**, 365. https://doi.org/10.1038/425365a.

Cayan, D.R., 1992a. Latent and sensible heat flux anomalies over the Northern Oceans: the connection to monthly atmospheric circulation. *Journal of Climate*, **5**, 354–369.

Cayan, D.R., 1992b. Latent and sensible heat flux anomalies over the Northern Oceans: driving the sea surface temperature. *Journal of Physical Oceanography*, **22**, 859–881.

Charlson, R.J., Lovelock, J.E., Andreae M.O., and Warren S.G., 1987. Oceanic phytoplankton, atmospheric sulfur, cloud albedo and climate. *Nature*, **326**, 655–661.

Conte, M.H., and Weber, J.C., 2014. Particle flux in the deep Sargasso Sea. *Oceanography*, **27** (1), 142–147.

Conte, M.H., Carter, A.M., Koweek, D.A., Huang, S., and Weber, J.C., 2019. The elemental composition of the deep particle flux in the Sargasso Sea. *Chemical Geology*, **511**, 279–313.

Courtney, T.A., Lebrato, M., Bates, N.R., Collins, A., de Putron, S.J., Garley, R., Johnson, R.J., Molinero, J.C., Noyes, T.J., Sabine, C.L., and Andersson, A.J. 2017. Environmental controls on modern coral and reef-scale calcification. *Science Advances*, **3**(11), 317011356

Cropp, R.A., Norbury, J., Gabric, A.J., and Braddock, R.D. 2004. Modeling dimethylsulphide production in the upper ocean. *Global Biogeochemical Cycles*, 18.

Dacey, J.W., Howse, F.A., Michaels, A.F., and Wakeham, S.G., 1998. Temporal variability of dimethylsulfide and dimethylsulfoniopropionate in the Sargasso Sea. *Deep-Sea Research I*, **45**, 2085–2099.

Davies, J.R., Rowell, D.P., and Folland, C.K., 1997. North Atlantic and European seasonal predictability using an ensemble of multidecadal atmospheric GCM simulations. *International Journal of Climate*, **17**, 1263–1284.

DeVries, T., Le Quéré, C., Andrews, O., and Seferian, R., 2019. Decadal trends in the ocean carbon sink. *Proc. Natl Acad. Sci. USA*, 116, 11646–11651.

Dickson, A.G., Sabine, C.L., and Christian, J.R., 2007. *Guide to Best Practices for Ocean CO2 Measurements.* North Pacific Marine Science Organization, Sidney, British Columbia, 2007) PICES Special Publication 3.

Doney, S.C., Fabry, V.J., Feely, R.A., and Kleypas, J.A., 2009. Ocean acidification: The other CO2 problem. *Annual Review of Marine Science*, **1**, 169–192.

Dore, J.E., Lukas, R., Sadler, D.W., and Karl, D.M., 2003. Climate-driven changes to the atmospheric CO2 sink in the subtropical North Pacific Ocean. *Nature*, **424**, 754–757.

Dore, J.E., Lukas, R., Sadler, D.W., Church, M.J. and Karl, D.M., 2009. Physical and biogeochemical modulation of ocean acidification in the central North Pacific. *Proceedings of the National Academy of Science, USA*, **106**, 12235–12240.

Enfield, D.B., and Mayer, D.A., 1997. Tropical Atlantic sea surface temperature variability and its relation to El Niño-Southern Oscillation. *Journal of Geophysical Research*, **102**, 929–945.

Estapa, M.L., Siegel, D.A., Buesseler, K.O., Stanley, R.H.R., Lomas, M.W., and Nelson, N.B., 2015. Decoupling of net community and export production on submesoscales in the Sargasso Sea. *Global Biogeochemical Cycles*, **29** (80), 1266–1288.

Fasham, M.J.R., 2003. Ocean biogeochemistry: The role of the ocean carbon cycle in global change. Berlin: Springer 297.

Fidai, Y.A., Dash, J., Tompkins, E.L., and Tonon, T., 2020. A systematic review of floating and beach landing records of Sargassum beyond the Sargasso Sea. *Environmental Research Communications*, **2** (12), 122001.

Friedlingstein, P., et al., 2019. Global carbon budget, 2019. *Earth System Science Data*, **11**, 1783–1838

Friedlingstein, P., O'Sullivan, M., Jones, M. W., Andrew, R. M., Hauck, J., Olsen, A., Peters, G.P., Peters, W., Pongratz, J., Sitch, S., Le Qu r , C., Canadell, J. G., Ciais, P., Jackson, R. B., Alin, S., Arag o, L. E. O. C., Arneth, A., Arora, V., Bates,

N. R., Becker, M., Benoit-Cattin, A., Bittig, H. C., Bopp, L., Bultan, S., Chandra, N., Chevallier, F., Chini, L. P., Evans, W., Florentie, L., Forster, P. M., Gasser, T., Gehlen, M., Gilfillan, D., Gkritzalis, T., Gregor, L., Gruber, N., Harris, I., Hartung, K., Haverd, V., Houghton, R. A., Ilyina, T., Jain, A. K., Joetzjer, E., Kadono, K., Kato, E., Kitidis, V., Korsbakken, J. I., Landschützer, P., Lefèvre, N., Lenton, A., Lienert, S., Liu, Z., Lombardozzi, D., Marland, G., Metzl, N., Munro, D. R., Nabel, J. E. M. S., Nakaoka, S.-I., Niwa, Y., O'Brien, K., Ono, T., Palmer, P. I., Pierrot, D., Poulter, B., Resplandy, L., Robertson, E., Rödenbeck, C., Schwinger, J., Séférian, R., Skjelvan, I., Smith, A. J. P., Sutton, A. J., Tanhua, T., Tans, P. P., Tian, H., Tilbrook, B., van der Werf, G., Vuichard, N., Walker, A. P., Wanninkhof, R., Watson, A. J., Willis, D., Wiltshire, A. J., Yuan, W., Yue, X., and Zaehle, S.: Global Carbon Budget 2020, Earth Syst. Sci. Data, 12, 3269–3340, 2020.

Friedlingstein, P., *et al.*, 2022. Global Carbon Budget 2022. *Earth Syst. Sci. Data*, 14(11), 4811–4900.

Friedlingstein, P., *et al.*, 2022. Global Carbon Budget 2021. *Earth Syst. Sci. Data*, 14(4), 1917-2005.

Friedlingstein, P., *et al.*, 2023. Global Carbon Budget 2022. *Earth System Science Data*.

Gao, K., Helbling, E.W., H der, D.-P., and Hutchins, D.A., 2012. Responses of marine primary producers to interactions between ocean acidification, solar radiation and warming. *Marine Ecology Progress Series*, **470**, 167–189.

Gattuso, J-P., and Hansson, L. (eds.) 2011. *Ocean acidification*, Oxford University Press, 326 pp.

Glover D.M., Jenkins WJ, and Doney S.C., 2011. Modeling methods in marine science. Cambridge: Cambridge University Press p. 571.

González-Dávila, M., Santana-Casiano, J.M., Rueda, M.J., and Llinas, O., 2010. The water column distribution of carbonate system variables at the ESTOC site from 1995 to 2004. *Biogeosciences*, **7**, 3067–3081.

Goodkin, N.F., Hughen, K.A., Cohen A.L. and Smith S.R., 2005. Record of little ice age sea surface temperatures at Bermuda using a growth-dependent calibration of coral Sr/Ca. *Paleoceanography*, **20**, PA4016.

Goodkin, N.F., Hughen, K.A., Curry, W.B., Doney, S.C. and Ostermann, D.R. 2008. Sea surface temperature and salinity variability at Bermuda during the end of the Little Ice Age. *Paleooceanography* **23**: 10.1029/2007PA001532.

Goodkin, N.F., Wang, B.–S., You, C.–F., Hughen, K.A., Grumet–Prouty, N., Bates, N.R., and Doney, S.C., 2015. Ocean circulation and biogeochemistry moderate interannual and decadal surface water pH changes in the Sargasso Sea. *Geophysical Research Letters*, 42(12), 4931–4939.

Griffin, A.J., Anderson, J., Ballard, J., Bates, N.R., Garley, R., Johnson, R., Martz, T., Pacheco, F., Takeshita, Y., and Andersson, A.J., 2022. Seasonal changes in seawater calcium and alkalinity in the Sargasso Sea and across the Bermuda carbonate platform. *Marine chemistry*, 238, 104064.

Gruber, N., and Sarmiento, J.L., 2002. *Biogeochemical Physical Interactions in Elemental Cycles, in The Sea: Biological-Physical Interactions in the Ocean*, edited by A. R. Robinson, J. J. McCarthy, and B.J. Rothschild, John Wiley and Sons, New York, Volume **12**, 337-399.

Gruber, N., Bates, N.R. and Keeling, C.D., 2002. Interannual variability in the North Atlantic Ocean carbon sink. *Science*, **298**, 2374–2378.

Gruber, N., Clement, N., Carter, B.R., Feely, R.A., Van Heuven, S., Hoppema, M., Ishii, M., Key, R.M., Kozyr, A., Lauvset, S.K., Lo Monaco, C., Mathis, C.T., Murata, A., Perez, F.F., Sabine, C.L., Tanhua, T., and Wanninkhof, R., 2019. The oceanic sink for anthropogenic CO2 from 1994 to 2007. *Science*, **363**, 1193–1199.

Hanawa, K., and Talley, L.D., 2001. Mode waters. In Ocean Circulation and Climate (G. Siedler, J. Church and J. Gould, Editors), Academic Press, San Diego, International Geophysics Series, volume 77, pp. 373–386.

Harley, J., Borges, A.V., Van Der Zee, C., Delille, B., Godi, R.H.M., Schiettecatte, L.-S., Roevros, N., Aerts, K., Plapernat, P.-E., Rebreanu, L., Groom, S., Daro, M.-H., Van Grieken, R., and Chou, L., 2010. Biogeochemical study of coccolithophore bloom in the northern Bay of Biscay (NE Atlantic Ocean) in June 2004. *Progress in Oceanography*, **86**, 317–336.

Hazeleger, W., and Drifjhout, S.S., 1998. Mode water variability in a model of the subtropical gyre: response to atmospheric forcing. *Journal of Physical Oceanography*, **28**, 266–288.

Hodgkins, H., Matthews, T., Morris, D., Boswell, J., Brumfield, A., George, R.Y., and Hayden, L., 2017. *et al.*, 2017.

Hurrell, J.W., 1995. Decadal trends in the North Atlantic Oscillation: regional temperatures and precipitation. *Science*, **269**, 676–679.

Hurrell, J.W., and Van Loon, H., 1997. Decadal variations in climate associated with the North Atlantic Oscillation. *Climatic Change*, **36**, 301–326.

Hurrell, J.W., Kushnir, Y., and Visbeck, M., 2002. The North Atlantic Oscillation. *Science*, **291**, 603–606.

Jenkins, W.F. 1998. Studying subtropical thermocline ventilation and circulation using tritium and He-3. *Journal of Geophysical Research, Oceans*, **103**, 15817–15831.

Jones, C.G., and Thorncroft, C.D., 1998. The role of El Niño in Atlantic tropical cyclone activity. Weather, **53**, 324–336.

Kapala, A., Maechel, H., and Flohn, H., 1998. Behaviour of the centres of action above the Atlantic since 1881. Part II Associations with regional climate anomalies. *International Journal of Climatology*, **18**, 23–36.

Keeling, C.D., Brix, H., and Gruber, N., 2004. Seasonal and long-term dynamics of the upper ocean carbon cycle at Station ALOHA near Hawaii. *Global Biogeochemical Cycles*, **18**.

Khatiwala, S., Tanhua, T., Mikaloff-Fletcher, S., Gerber, M., Doney, S.C., Graven, H.D., Gruber, N., McKinley,

G.A., Murata, A, Rios, A., and Sabine, C.L., 2013. Global ocean storage of anthropogenic carbon. *Biogeosciences*, **10**, 2169–2191.

Klein, B., and Hogg N., 1996. On the interannual variability of 18 Degree Water formation as observed from moored instruments at 55°W. *Deep-Sea Research*, **43**, 1777–1806.

Koch, M., Bowes, G., Ross, C., and Zhang, X.-H., 2013. Climate change and ocean acidification effects on seagrasses and marine macroalgae. *Global Change Biology*, **19** (1), 103–132.

Krumhardt, K.M., Lovenduski, N. S., Freeman, N.M. and Bates, N.R., 2016. Increasing coccolithophore abundance in the subtropical North Atlantic from 1994 to 2014. *Biogeosciences*, **13**, 1163–1177.

Landschützer, P., Gruber, N., Bakker, D.C.E., Stemmler, I. and Six, K.D., 2018. Strengthening seasonal marine CO2 variations due to increasing atmospheric CO2. Nat. Clim. Change 8, 146–150.

Laffoley, D. d'A., Roe, H.S.J., Angel, M.V., Ardron, J., Bates, N.R., Boyd, I.L., Brooke, S., Buck, K.N., Carlson, C.A., Causey, B., Conte, M.H., Christiansen, S., Cleary, J., Donnelly, J., Earle, S.A., Edwards, R., Gjerde, K.M., Giovannoni, S.J., Gulick, S., Gollock, M., Hallet, J., Halpin, P., Hanel, R., Hemphill, A., Johnson, R.J., Knap, A.H., Lomas, M.W., McKenna, S.A., Miller, M.J., Miller, P., Ming, F.W., Moffitt, R., Nelson, N.B., Parson, L., Peters, A.J4., Pitt, J., Rouja, P., Roberts, J., Roberts, J., Seigel, D.A., Siuda, A., Steinberg, D.K., Stevenson, A., Sumaila, V.R., Swartz, W., Trott, T.M., and Vats. V., 2011. *The protection and management of the Sargasso Sea: The golden floating rainforest of the Atlantic Ocean. Summary Science Case.* Sargasso Sea Alliance, 53pp.

Landschützer, P., Gruber, N., Bakker, D. C. E., Stemmler, I. and Six, K.D., 2018. Strengthening seasonal marine CO2 variations due to increasing atmospheric CO2. *Nature Climate Change*, **8**, 146–150.

Lange, N., Fiedler, B., Ivarez, M., Benoit-Cattin, A., Benway, H., Buttigieg, P.L., Coppola, L., Currie, K., Flecha, S., Honda, M., Huertas, E., Lauvset, S.K., Muller-Karger, F., Körtzinger, A., O'Brien, K.M., Ólafsdóttir, S.R., Pacheco, F.C., Rueda-Roa, D., Skjelvan, I., Wakita, M., White, A., and Tanhua, T., 2023. Synthesis product for Ocean Time-series (SPOTS)–A ship-based biogeochemical pilot. *Earth System Science Data*; https://doi.org/10.5194/essd-2023-238.

Le Clainche, Y., Levasseur, M., Venzina, A., Dacey, J.W.H. and Saucier, F.J., 2004. Behavior of the ocean DMS(P) pools in the Sargasso Sea viewed in a coupled physical-biogeochemical ocean model. *Canadian Journal of Fisheries and Aquatic Sciences* **61**:788–803.

Le Clainche, Y., Vezina, A., Levasseur, M., Cropp, R.A., Gunson, J.R., Vallina, S.M., Vogt, M., Lancelot, C., Allen, J.I., Archer, S.D., Bopp, L., Deal, C., Elliot, S., Jin, M., Malin, G., Schomann, V., Simo, R., Six, K.D. and Stefels, J., 2010. A first appraisal of prognostic ocean DMS models and prospects for their use in climate models. *Global Biogeochem. Cycles*, **24**, GB3021.

Levine, N.M, Toole, D., Neeley, A., Bates, N.R., Doney, S., and Dacey, J., 2015. Revising upper-ocean sulfur dynamics near Bermuda: New lessons from three years of concentration and rate measurements. *Environmental Chemistry*. MS EN15045, http://dx.doi.org/10.1071/EN15045.

Liss P.S., and Johnson M.T., 2014. Ocean-atmosphere interactions of gases and particles. Heidelberg: Springer Open p. 315.

Lomas, M.W., Bates, N.R., Buck, K.R., and Knap, A.H., 2011. Oceanography of the Sargasso Sea Overview of Scientific Studies. Sargasso Sea Commission, 94 pp.

Lomas, M.W., Bates, N.R., Johnson, R.J., Knap, A.H, Steinberg, D.K., Carlson, C.A., 2013. Two decades and counting: 23–years of sustained open ocean biogeochemical measurements in the Sargasso Sea. *Deep–Sea Research II*, 93, 16–32, doi: 10.1016/j.dsr2.2013.01.008.

Lomas, M.W., Bates, N.R., Johnson, R.J., Steinberg, D.K., and Tanioka, T., 2022. Adaptive carbon response to warming in the Sargasso Sea. *Nature Communications*, **13** (1), 1211.

Lv, J., Kuang, Y., and Zhang, H., 2017. Patterns of coccolithophore pigment change under global acidification conditions based on in-situ observations at BATS site between July 1990-Dec 2008. *Frontiers of Earth Science*, 11, 297–307.

Mackenzie, F.T., and Lerman, A., 2010. Carbon in the geobiosphere: Earth's outer shell. Dordrecht: Springer p. 402.

Masotti, I., Belviso, S., Bopp, L., Tagliabue, A., and Bucciarelli, E., 2015. Effects of light and phosphorus on summer DMS dynamics in subtropical waters using a global ocean biogeochemical model. *Environmental Chemistry*, **13** (2), 379–389.

Maze, G., and Marshall, J., 2011. Diagnosing the observed seasonal cycle of Atlantic subtropical mode water using potential vorticity and its attendant theorems. *Journal of Physical Oceanography*, **41**, 1986–1999.

Millero, F.J., 2013. Chemical Oceanography, Fourth Edition. 552, CRC Press p. 552.

Moran, M.-A., Kujawinski, E.B., Schroer, W.F., Amin, S.F., Bates, N.R., Bertrand, E.M., Braakman, R., Brown, C.T., Covert, M.W., Doney, S.C., Dyrhman, S.T., Edison, A.S., Eran, AS.M., Levine, N.M., Li, L., Ross, A.C., Saito, M.C., Santoro, A.E., Segre, D., Shade, A., Sullivan, M.B., and Varwdi, A., 2022. Microbial metabolites in the marine carbon cycle. *Nature Microbiology*, 7, 508–523.

Murata A, 2006. Increased surface seawater pCO_2 in the eastern Bering Sea shelf: an effect of blooms of coccolithophorid Emiliania huxleyi. *Global Biogeochemical Cycles*, GB4006, doi: 10.1029/2005GB002615.

Murata A, and Takizawa T., 2002. Impact of a coccolithophorid bloom on the CO2 system in surface waters of the eastern Bering Sea shelf. *Geophysical Research Letters*, **29** (11), Art. No. 1547.

Pelejero, C., Calvo, E. and Hoegh-Guldberg, O., 2010. Paleo-perspectives on ocean acidification. *Trends in Ecology and Evolution*, **25**, 332–344.

Penland, C., and Matrosova, L., 1998. SST anomaly in the El Nino region is a strong 6 month predictor of SST anomaly in the north Tropical Atlantic. *Journal of Climate*, **11**, 483–490.

Polimene, L., Archer, S.D., Butenschon, M. and Allen, J.I., 2012. A mechanistic explanation of the Sargasso Sea DMS "summer paradox". *Biogeochemistry*, **110**, doi:10.1007/s10533-011-9674-z.

Rhein, M., S.R. Rintoul, S. Aoki, E. Campos, D. Chambers, R.A. Feely, S. Gulev, G.C. Johnson, S.A. Josey, A. Kostianoy, C. Mauritzen, D. Roemmich, L.D. Talley and F. Wang, 2013. Observations: Ocean. In: *Climate Change 2013: The Physical Science Basis*. Contribution of Working Group I to the Fifth Assessment Report of the Intergovernmental Panel on Climate Change [Stocker, T.F., D. Qin, G.-K. Plattner, M. Tignor, S.K. Allen, J. Boschung, A. Nauels, Y. Xia, V. Bex and P.M. Midgley (eds.)]. Cambridge University Press, Cambridge, United Kingdom and New York, NY, USA.

Riebesell, U., I. Zondervan, B. Rost, P.D. Tortell, P.D., Zeebe, R.E., and Morel, F.M.M., 2000. Reduced calcification of marine plankton in response to increased atmospheric CO_2. *Nature*, **407**, 364–367.

Riebesell, U., Fabry, F.J., Hansson, L., and Gattuso, J.-P., 2010. Guide to best practices for ocean acidification research and data reporting. Brussels: European Commission p. 258.

Ridgwell, A., Zondervan, I, Hargreaves, J.C., Bijma, J., and Lenton, T.M., 2007. Assessing the potential long-term increase of oceanic fossil fuel CO2 uptake due to CO2-calcification feedback. *Biogeosciences*, **4** (4), 481–492.

Robertson, J.E., Robinson, C., Turner, D.R., Holligan, P., Watson, A.J., Boyd, P., Fernandez, E., and Finch, M., 1994. The impact of a coccolithophore bloom on oceanic carbon uptake in the northeast Atlantic during summer 1991. *Deep-Sea Research I*, **41** (2), 297–314.

Rodwell, M.J., Rowell, D.P., and Folland, C.K., 1999. Oceanic forcing of the wintertime North Atlantic Oscillation and European climate. *Nature*, **398**, 320–323.

Sabine, C.L., Feely, R.A., Gruber, N., Key, R.M., Lee, K., Bullister, J.L., Wanninkhof, R., Wong, C.S., Wallace, D.W.R., Tilbrook, B., Millero, F.J., Peng, T.-H., Kozyr, A., Ono, T., and Rios, A.F., 2004. The oceanic sink for anthropogenic CO_2, *Science*, **305**, 367–371.

Salmon, K.H., Anand, P., Sexton, P.F., and Conte, M.H., 2015. Upper ocean mixing controls the seasonality of planktonic foraminifer fluxes and associated strength of carbonate pump in the oligotrophic North Atlantic. *Biogeosciences*, **12** (1), 223–235.

Sarmiento, J.L., and Gruber, N., 2002. Sinks for anthropogenic carbon. Physics Today 55(8): 30. https://doi.org/10.1063/1.1510279.

Sarmiento, J.L., and Gruber, N., 2006. *Ocean biogeochemical dynamics*. Princeton: Princeton University Press p. 499.

Schlesinger W.H., 1997. *Biogeochemistry: An analysis of global change*. New York: Academic Press p. 443.

Schuster, U., Watson, A.J., Bates, N.R., Corbiere, A., Gonzalez-Davila, M., Metzl, N., Pierrot, D., and Santana-Casiano, M., 2009. Trends in North Atlantic sea-surface fCO_2 from 1990 to 2006. *Deep-Sea Research II*, **56**, 620–629.

Schuster, U., McKinley, G., Bates, N.R., Chevallier, F., Doney, S., Fay, A., Gonzaléz-Dávila, M., Gruber, N., Jones, S., Landschützer, P., Lefévre, N., Manizza, M., Mathis, J., Metzl, M., Olsen, A., Rios, A., and Santana-Casiano, J.M., 2013. Atlantic and Arctic air-sea CO_2 fluxes, 1990–2009. *Biogeosciences*, **10**, 1, 607–627; doi: 10.5194/bg-10-607-2013.

Shaw, G.E., 1983. Bio-controlled thermostasis involving the sulfur cycle. *Climatic Change*, **5**, 297–303.

Simo, R., and Pedros-Alio, C., 1999. Short-term variability in the open ocean dimethylsulphide. *Global Biogeochemical Cycles*, **13**, 1173–1181.

Smart, S.M., ren, H., Fawcett, S.E., Schiebel, R., Conte, M.H., Rafter, P.A., Ellis, K.K., Weigand, M.A., Oleynik, S., Haug, G.H., and Sigman, D.M., 2014. Ground-truthing the planktic foraminifer-bound nitrogen isotope paleo-proxy in the Sargasso Sea. *Geochimica et Cosmochimica Acta*, **235**, 463–482.

Smith, S.R., and Warren, T., 2019. Chapter 22 – Bermuda and the Sargasso Sea. In. *World Seas: An Environmental Evaluation.* Volume 1: Europe, the Americas and West Africa, 531–547, Academic Press.

Stevens, S.W., Johnson, R.J., Maze, G., and Bates, N.R. 2020. A recent decline in North Atlantic subtropical mode water formation. *Nature Climate Change*, **10** (4), 335–341.

Takahashi, T., Wanninkhof, R.H., Feely, R.A., Weiss, R.F., Chipman, D.W., Bates, N.R., Olafsson, J., Sabine, C.L., and Sutherland, S.G., 1999. Net sea–air CO2 flux over the global oceans: An improved estimate based on the sea–air pCO_2 difference. *Proceedings of the Second International CO_2 in the Oceans Meeting*, Tsukuba, Japan, January 1999, CGER– I037–99, 9–15.

Takahashi, T., Sutherland, S.C., Wanninkhof, R., Sweeney, C., Feely, R.A., Chipman, D.W., Hales, B., Friederich, G., Chavez, F., Watson, A., Bakker, D.C.E., Schuster, U., Metzl, N., Yoshikawa–Inoue, H., Ishii, M., Midorikawa, Nojiri, Y., Kortzinger, A., Steinhoff, T., Hoppema, M., Olafsson, J., Arnarson, T.S., Tilbrook, B., Johannessen, T., Olsen, A., Bellerby, R., Wong, C.S., Delille, B., Bates, N.R., and de Baar, H.J.W., 2009. Climatological mean and decadal change in surface ocean pCO_2, and net sea–air CO2 flux over the global oceans. *Deep–Sea Research II*, 56 (8–10), 554–577, doi: 10.1016/j.dsr2.2008.12.009.

Tanhua, T., Bates, N.R., and Kortzinger, A., 2013. The marine carbon cycle and ocean anthropogenic CO2 inventories. In: Church J, *et al.* (ed.) *Ocean circulation and climate*, p. 103. Amsterdam: Elsevier Press.

Taylor, A.H., and Stephens, J.A., 1998. The North Atlantic Oscillation and the latitude of the Gulf Stream. *Tellus*, 50A, 134–142.

Taylor, A.H., Jordan, M.B., and Stephens, J.A., 1998. Gulf Stream shifts following ENSO events. *Nature*, **393**, 638.

Toole, D.A. and Seigel, D.A., 2004. Light-driven cycling of dimethylsulfide (DMS) in the Sargasso Sea: Closing the loop. Geophys. Res. Lett., **31**.

Toole, D.A., Siegel, D.A., and Doney, S.C., 2008. A light-driven, one-dimensional dimethylsulfide biogeochemical cycling model for the Sargasso Sea. *Journal of Geophysical Research-Biogeosciences*, **113**, G02009.

Touratier, F., and Goyet, C., 2004. Applying the new TrOCA approach to assess the distribution of anthropogenic CO_2 in the Atlantic Ocean. J. *Mar. Syst.*, **46**, 181–197.

Touratier, F., and Goyet, C., 2004. Definition, properties, and Atlantic distribution of the new tracer TrOCA. J. *Mar. Syst.*, **46**, 169–179.

Touratier, F., Azouzi, L., and Goyet, C., 2007. CFC-11, QQQ^{14}C and ^{3}He tracers as a means to assess anthropogenic CO2 concentrations in the ocean. *Tellus*, **59B**, 318–325.

Vila-Costa, M., Rinta-Kanto, J.M., Poretsky, R.S., Sun, S., Kiene, R.P., and Moran, M.A., 2014. Microbial controls on DMSP degradation and DMS formation in the Sargasso Sea. *Biogeochemistry* **120**, 295–305.

Visbeck, M., Hurrell, J.W., Polvani, L., and Cullen, H.M., 2001. The North Atlantic Oscillation: Past, present, and future. *Proceedings National Academy of Sciences*, **98**, 12876–12877.

Wanninkhof, R., 1992. Relationship between wind speed and gas exchange over the ocean. *Journal of Geophysical Research*, **97** (C5), 7373–7382.

Watson, A.J, Schuster, U., Bakker, D.C.E., Bates, N.R., Corbiere, A., Gonzalez–Davila, M., Friedrich, T., Hauck, J., Heinze, C., Johannessen, T., K rtzinger, A., Metzl, N., Olafsson, J., Olsen, A., Oschlies, A., Padin, X.A., Pfiel, B., Santana–Casiano, M., Steinhoff, T., Telszewski, M., Rios, A.F., Wallace, D.W.R., and Wanninkhof, R., 2009. Accurately tracking the variation in the North Atlantic sink for atmospheric CO_2. *Science*, **326**, 1391–1393, doi: 10.1126/science.1177394, Dec. 9, 2009.

Williams, R.G., and Follows, M.J., 2011. *Ocean dynamics and the carbon cycle.* Cambridge: Cambridge University Press, 404 pp.

Xu, Z., Gao, G., Xu, J., and Wu, H., 2017. Physiological response of a golden tide alga (Sargassum muticum) to the interaction of ocean acidification and phosphorus enrichment. *Biogeosciences*, **14** (3), 671–681.

Yeakel, K.L., Andersson A.J., Bates, N.R., Noyes, T.J., Collins A., and Garley, R., 2015. Shifts in coral reef biogeochemistry and resulting acidification linked to offshore productivity. *Proceedings of the National Academy of Sciences*, **112**, 14512–14517.

Yool, A., Oschlies, A., Nurser, A. J. G. and Gruber, N., 2010. A model-based assessment of the TrOCA approach for estimating anthropogenic carbon in the ocean. *Biogeosciences*, **7**, 723– 751.

Zeebe, R.E., and Wolf-Gladrow, D., 2001. *CO_2 in seawater: Equilibrium, kinetics, isotopes.* Amsterdam: Elsevier Science p. 346.


SARGADOM

MARVIVA

SARGASSO SEA
COMMISSION

UBO
Université de Bretagne Occidentale

OFB
OFFICE FRANÇAIS DE LA BIODIVERSITÉ

FONDS FRANÇAIS POUR
L'ENVIRONNEMENT MONDIAL

unesco

UNDP

gef

Food and Agriculture
Organization of the
United Nations

COMMON
OCEANS
PROGRAM

JP Rouja

gef

FFEM FONDS FRANÇAIS POUR L'ENVIRONNEMENT MONDIAL